Aus dem Institut für Muskuloskelettale Medizin
Klinik der Universität München – MUM
Direktion:
Prof. Dr. Wolfgang Böcker
Prof. Dr. Boris Holzapfel

The potential of Integrin α10β1-selected mesenchymal stem cells for therapy of post-traumatic osteoarthritis in a mouse model

Dissertation

zum Erwerb des Doktorgrades der Medizin

an der Medizinischen Fakultät der

Ludwig-Maximilians-Universität zu München

vorgelegt von

Jelena Juliane Schwarz

aus

Sindelfingen

2023

Mit Genehmigung der Medizinischen Fakultät

der Universität München

Berichterstatter:	PD Dr. Attila Aszódi
Mitberichterstatter:	Prof. Dr. Marcus Schmitt-Sody Prof. Dr. Matthias Pietschmann
Mitbetreuung durch den promovierten Mitarbeiter:	Dr. Paolo Alberton
Dekan:	Prof. Dr. med. Thomas Gudermann
Tag der mündlichen Prüfung:	05.10.2023

Meiner Familie

TABLE OF CONTENT

LIST OF FIGURES

LIST OF TABLES

SUMMARY

Osteoarthritis is the most common musculoskeletal disorder leading to disability, particularly in the elderly, and is responsible for an enormous socio-economic burden worldwide. Due to its avascular and aneural nature and the quiescent state of its resident cells, articular cartilage has a poor capacity for self-repair. Current treatments for OA are unsatisfactory and to date, neither disease modifying drugs nor curative treatments have been developed. Mesenchymal stem cells are easy to harvest, possess high cell renewal and regeneration capabilities due to secretion of factors, good differentiation potential, as well as low immunogenic properties, making them an attractive tool for the treatment of degenerating conditions. In order to improve the tissue-specific regenerative potential of MSCs, so called 'priming' strategies have been extensively investigated in the recent years. In the cartilage field, it has been found that the expression of the transmembrane receptor integrin α10 can be modulated in human mesenchymal stem cells (MSCs), and its expression directly correlates with improved chondrogenic differentiation potential *in vitro*.

In the present study human bone marrow-derived mesenchymal stem cells, expanded in media containing human platelet lysate and sorted for integrin α10 ($\alpha10^{high}$), were tested for the treatment of post-traumatic osteoarthritis (PT-OA) in a mouse model. Unsorted cells from the same donor were used as control.

First, this study shows that the sorted cells retain the trilineage differentiation potential typical for adult mesenchymal stem cells (MSCs). Second, the study demonstrates that platelet lysate treatment results in chondrogenic commitment of MSCs and furthermore a better chondrogenic differentiation of sorted $\alpha10^{high}$ MSCs in pellet culture experiments compared to unsorted cells. Third, commercial hydrogels were tested and the Artiss® fibrin gel was identified as suitable hydrogel in this study, which enables *in vitro* remodeling and supports cell survival. In addition, an *in vivo* preliminary study shows that MSCs persisted in the gel at least one day after injection into the mouse knee joint, suggesting that Artiss® is an appropriate carrier for therapeutic, *in vivo* delivery of MSCs. Fourth, the ability of the $\alpha10^{high}$ MSCs to ameliorate the onset and progression of OA in a PT-OA mouse model induced by surgical destabilization of the medial meniscus (DMM) was tested. For this purpose, unsorted and $\alpha10^{high}$ MSCs were encapsulated into Artiss® fibrin gel and injected into the knee joint cavity immediately after the DMM operation. Histological analyses of the knee joints to monitor articular cartilage degradation were performed eight weeks after post-operation. The histopathological scoring analysis reveals that articular cartilage erosion is significantly attenuated in the group that received $\alpha10^{high}$

MSCs compared to mice injected with unsorted MSCs or the cell-free vehicle. In support of the protective role of $\alpha10^{high}$ MSCs in PT-OA, the circulating levels of the neo-epitope CTX-II as a marker of collagen type II degradation were determined, and it turned out that significantly reduced CTX-II levels in the blood of mice receiving $\alpha10^{high}$ MSCs were found compared to mice injected with unsorted MSCs. Finally, it was not possible to detect human cells in the joint cavity of MSC injected mice eight weeks post-operation, using human a *CMT1A*-specific PCR on genomic DNA templates isolated from mouse knee tissue sections. This would rather suggest a paracrine mode of action of the $\alpha10^{high}$ MSCs in the early phase post injury, yet the eventual direct participation of the injected MSCs in the regeneration of damaged cartilage cannot be excluded.

In conclusion, this study shows that $\alpha10^{high}$ MSCs represent a promising therapeutic tool that is safe in a pre-clinical mouse model and has protective potential against PT-OA.

ZUSAMMENFASSUNG

Osteoarthrose ist die häufigste muskuloskelettale Erkrankung, die zu Beeinträchtigungen insbesondere bei älteren Personen führt und die eine enorme sozio-ökonomischen Belastung weltweit darstellt. Auf Grund der mangelnden Vaskularisation und Innervierung sowie der ruhenden Gewebszellen verfügt Gelenkknorpel nur über ein geringfügiges Selbsterneuerungspotential. Die derzeitigen Therapiemöglichkeiten sind unbefriedigend und bis heute gibt es weder Medikamente noch Behandlungsmöglichkeiten, die den Krankheitsverlauf verändern oder heilen können. Mesenchymale Stammzellen sind leicht zu gewinnen und verfügen über eine hohe Zellerneuerungsfähigkeit ebenso wie ein ausgeprägtes Differenzierungspotential, wodurch sie ein attraktives Instrument für die Behandlung degenerativer Prozesse darstellen. Um das gewebespezifische Regenerationspotential von mesenchymalen Stammzellen zu verbessern, wurden in den letzten Jahren vermehrt sogenannte "Priming"- Strategien untersucht. Im Bereich der Knorpelforschung stellte sich heraus, dass die Expression des Transmembranrezeptors Integrin α10 beeinflusst werden kann und dass dessen Expression direkt mit einem verbesserten chondrogenen Differenzierungspotential *in vitro* korreliert.

In der vorliegenden Studie wurden humane Knochenmarksstammzellen für die Behandlung einer post-traumatischen Arthrose in einem Mausmodell verwendet. Hierfür wurden die Stammzellen vorab in einem mit Thrombozytenlysat angereicherten Medium kultiviert und anschließend nach Integrin α10 sortiert. Die unsortierten Zellen desselben Spenders wurden als Kontrolle verwendet.

Als erstes zeigt diese Studie, dass die sortierten Zellen weiterhin ihr Differenzierungspotential in die drei typischen Zelllinien adulter mesenchymaler Stammzellen beibehielten. Zweitens wird gezeigt, dass die Anreicherung mit Thrombozytenlysat in einer chondrogenen Festlegung der Stammzellen resultierte. Zudem wiesen die nach Integrin α10 sortierten Stammzellen ein wesentlich höheres chondrogenes Differenzierungspotential in Pellet-Zellkultur Experimenten auf als unsortierte Zellen. Drittens erfolgte die Testung der kommerziellen Hydrogele, von denen insbesondere das Artiss® Fibringel *in vitro* Umbauprozesse sowie das Überleben der Zellen unterstützte. Darüber hinaus konnte eine vorläufige *in vivo* Studie zeigen, dass mesenchymale Stammzellen im Fibringel mindestens einen Tag nach der Injektion im mäuslichen Kniegelenk nachweisbar waren, sodass das Artiss® Fibringel als ein geeignetes Transportmedium für therapeutische *in vivo* Verabreichungen von Stammzellen erachtet werden kann. Viertens wurde die Fähigkeit der nach Integrin α10 sortierten Stammzellen

getestet, das Auftreten und das Fortschreiten von Arthrose zu verlangsamen beziehungsweise abzumildern. Hierfür wurde ein posttraumatisches Osteoarthrose-Modell genutzt, welches durch eine chirurgische Destabilisierung des medialen Meniskus in Mäusen Osteoarthrose induziert. Die unsortierten und die nach Integrin α10 sortierten Zellen wurden mit dem Artiss® Fibringel vermengt und unmittelbar nach der Destabilisierungs-Operation in die Kniegelenkshöhle injiziert. Die histologischen Analysen der Kniegelenke zur Evaluierung des Gelenkknorpelabbaus wurden acht Wochen nach der Operation durchgeführt. Die histopathologische Auswertung zeigte, dass die Gelenkknorpelerosion in den Kniegelenken der Mäuse, die nach Integrin α10 sortierte Stammzellen erhalten haben, signifikant geringer war im Vergleich zu den Mäusen, die unsortierte Stammzellen erhalten haben, beziehungsweise die nur das zellfreie Fibringel erhalten haben. Um die These der protektiven Rolle von Integrin α10 sortierten Zellen in posttraumatischer Arthrose zu untermauern, wurde zusätzlich das zirkulierende Neo-Epitop CTX-II als Marker für den Abbau von Kollagen Typ II bestimmt. Hier zeigten sich deutlich erniedrigte CTX-II Konzentrationen im Blut der Mäuse, die nach Integrin α10 sortierte Zellen erhielten im Vergleich zu den Mäusen, die unsortierte Stammzellen injiziert bekommen haben. Letztlich gelang es nicht humane Zellen acht Wochen postoperativ in den Mäuseknien nachzuweisen. Hierfür wurde eine *CMT1A*-spezifische PCR an genomischen DNA-Proben durchgeführt, die aus Gewebeschnitten der Mäuseknie isoliert worden waren. Dies deutet daher eher auf eine parakrine Wirkung der nach Integrin α10 sortierten Stammzellen in der frühen posttraumatischen Phase hin, wobei eine direkte Beteiligung der injizierten Stammzellen an der Regeneration des geschädigten Knorpels nicht ausgeschlossen werden kann.

Zusammenfassend zeigt diese Studie, dass nach Integrin α10 sortierte Stammzellen ein vielversprechendes therapeutisches Instrument darstellen, welche in einem präklinischen Mausmodell sicher anzuwenden sind und ein protektives Potential bezüglich posttraumatischer Arthrose aufweisen.

1 INTRODUCTION

1.1 OSTEOARTHRITIS – CLINICAL RELEVANCE

Osteoarthritis (OA) is one of the most common degenerative joint disease affecting approximately 250 million people in the world[1,2]. OA is described by progressive degeneration of the articular cartilage (AC) with damage that may extend until the underlying subchondral bone, as well as the inflammation of the surrounding soft tissue such as ligaments and synovia. Every joint in the human body is susceptible to OA, nevertheless hip and knee, the main weight bearing joints, are the most affected anatomical sites. In early stages of OA, appearance of symptoms is rare, but with its progression patients suffer from pain, joint swelling and impaired physical function until a possible complete loss of mobility of the joint[3]. In this respect, physical disability and chronic pain are the main reasons why OA represents an enormous economic burden on the healthcare systems worldwide. The prolonged and expensive conservative treatments required for OA are mostly unsatisfactory, and patients often end up needing arthroplastic surgery. Clinical operations represent the most obvious direct costs, but important to keep in consideration are the associated socio-economical drawbacks like reduced quality of life, inefficient productivity, decrease of working days, as well as the increased use of healthcare resources[4,5], which altogether constitute a significant indirect cost of OA. In the year 2013, the prevalence of OA in Germany was 22,3% for women and 18,1% for men[6]. According to *Salmon et al*., the total annual average costs per patient for hip and knee OA worldwide were around 11100 € (2013), with rising tendency due to increased life expectancy[5].

1.1.1 DIAGNOSIS OF OA

For the diagnosis of OA, clinical as well as radiological criteria must be considered. The American College of Rheumatology (ACR) classification includes clinical criteria such as people older than 50 years as well as crepitus or stiffness for more than 30 minutes[7]. For the assessment of radiological findings, the classification implemented by Kellgren and Lawrence is widely used and accepted. These criteria are oriented towards structural changes, such as joint space narrowing, occurrence of osteophytes, subchondral sclerosis and cysts[8]. If those criteria are applied together, the sensitivity of the Kellgren and Lawrence system to detect OA increases. Nevertheless, early stages of OA are more difficult to detect, therefore, additional examinations such as magnetic resonance imaging (MRI) scans or diagnostic arthroscopy are often needed[9]. However, arthroscopy is an invasive procedure, which is not used for primary diagnostic. On the other hand, arthroscopy offers the possibility to remove demolished cartilage

or meniscus, as well as the examination of the cartilage such as the consistence with the help of specific instruments. However, *Moseley et al*. could not find evidence for a better outcome of patients receiving arthroscopy for diagnosis compared to non-invasive diagnostic methods[10]. Another desirable method to identify patients with OA is the usage of diagnostic biomarkers. Inflammatory markers in the blood such as the C-reactive protein (CRP) or interleukin-6 (IL-6) have been found to be increased in OA-patients, but these markers remain not completely specific for OA, because they are related also to other pathologies. Promising more specific biomarker candidates are structural protein byproducts generated by degradation processes during OA. For example, cleavage products (C2C) or neoepitopes (CTX-II, C2M) of degraded collagen type II as well as cartilage oligomeric matrix protein (COMP) can be detected at elevated levels in the blood or urine of OA patients[11]. However, according to the current guideline of the DGOU (Deutsche Gesellschaft für Orthopädie und Unfallchirurgie), no valid biomarkers for the diagnosis of OA are currently available[12], and the lack of reproducibility and validation of these emphasizes the need for further investigations[12].

1.1.2 ETIOLOGY OF OA

During the development of OA, the cartilage and its surrounding joint tissues are exposed to multifactorial and complex interactions of metabolites, which are not yet completely understood. In this regard, a deeper understanding of the pathophysiological pathways and causes of OA may help to identify potential therapeutic targets. Aging, trauma, abnormal biomechanics, genetic predispositions, metabolic syndromes including obesity and diabetes as well as comorbidities such as cardiovascular disease, possibly contribute to the development of OA. The consensus main risk factors for OA are mechanical distress, genetics and age-related degeneration.

Mechanical distress is typically caused by abnormal anatomy, chronic overweight condition or combination of both. Anomalous anatomy comprises congenital or acquired malformations, like misalignment of the limb axis or malformation of the tibial or patella-femoral joint surfaces[13]. The other most important mechanically-driven cause of OA is direct injury. Misuse and instability of joints cause a shift towards rarely loaded regions followed by cartilage breakdown as shown by *Andriacchi et al.*[14,15]. Additionally, the presence of inflammatory proteins combined with mechanical overload results in increased upregulation of catabolic pathways leading to a stronger cartilage degradation[16,17]. Furthermore, degradation fragments of collagen type II and fibronectin in the synovial fluid stimulate chondrocytes into a vicious cycle to produce matrix-degrading proteinases leading to accelerated matrix degradation[18,19].

However, age-related OA remains one of the most common forms of OA. The accumulation of several risk factors during aging processes together with reduced regenerative capacities bears high risk for the development of OA. Although OA is not a necessary condition of aging[3], the rarity of OA in young people (age below 30 years) implies the impact of age on articular cartilage degeneration and OA[20]. In the United States the median age of patients suffering from knee OA is 55 years[21]. Moreover, OA is a chronic disease, where decades are necessary for the development of the condition. During aging, the intensification of inflammatory processes and the accumulation of fat tissue increase the levels of circulating inflammatory cytokines (e.g. Interleukin-6)[22]. Additionally, leptin, adiponectin and resistin, members of the adipokine-family expressed in fat tissue, play important roles in inflammatory processes during the development of OA[23]. This pro-inflammatory state together with the excessive loading provoke cell senescence in tissues like cartilage and the related joint structures. Exposure of senescent chondrocytes to chronic stress or mechanical stimulation results in DNA damage and telomere-shortening. Further, the secretory phenotype of these cells is changing towards higher expression levels of matrix metalloproteinases (MMPs), such as the collagen-degrading MMP-13. The lost ability to maintain homeostasis in senescent chondrocytes goes along with a decreased production of the extracellular matrix (ECM). Additionally, a reduced anabolic response and decreased proliferation rate is observed, despite stimulation with growth factors[24,20]. Altogether these are typical features of the aging process[25]. A similar scenario can be observed in obese people. Overweight implies abnormal joint overload and accelerated release of inflammatory mediators as well as adipokines. As the increase of fat tissue is not only an independent disease, but also an age-dependent side-effect, a clear separation of these two etiologies is difficult[26].

Besides the environmental risk factors, genetics can also have a high impact on the development of OA, although just a few OA-associated genes have been identified to date[27]. A genome-wide association study funded by the Arthritis Research UK Osteoarthritis Genetics (arcOGEN) Consortium could identify eleven loci associated with OA[28]. For example, GDF5 (Growth/differentiation factor 5), a signaling molecule belonging to the TGF-beta superfamily, displays a significant and reproducible down-regulation in knee OA patients, but not in hip OA patients, compared to control groups[29,30]. Another gene identified to be associated with OA is the *MCF2L* gene, which encodes the guanine nucleotide exchange factor DBS protein[31]. Furthermore, chromosome 7q22 was identified as an OA susceptibility locus. In the European population, the chromosomal region of 7q22 together with the *GDF5* gene reached high significance in a genome-wide analysis[32]. Not only cartilage, but also the surrounding joint

tissues as the synovium and menisci could be affected by catabolic changes[33]. Taking into account the polygenic architecture and multiple variants, the approaches to identify the genetic components of OA require larger meta-analytical efforts[34]. Further interesting aspects are the gender-associated differences in OA. *O'Conner et al.,* found gender specific differences concerning the cartilage thickness (thinner in women), estrogen receptor genes (with higher risk in homozygous individuals) as well as the joint anatomy, all reflecting higher risk of OA development in women[35].

1.2 CARTILAGE

1.2.1 COMPOSITION AND ORGANIZATION

In the human body there exist three different types of cartilage that are differing in their structure and extracellular matrix composition: hyaline, elastic and fibrocartilage. Hyaline cartilage, the most abundant cartilage type, constitutes the transient cartilaginous template of the developing endochondral bones and the permanent articular cartilage (AC), which is covering the surfaces of the articulating bones[36] and therefore is the type of cartilage this study is focusing on. The hyaline cartilage ECM consists a network of collagen fibrils composed of type II, IX and XI collagens, proteoglycans (PGs) carrying glycosaminoglycan (GAG) side chains, hyaluronic acid (HA) and various glycoproteins produced by the highly specialized cells, the chondrocytes[37]. The high negative-charge density of GAGs attracts water and counter-ions into the tissue generating an internal swelling pressure, which enables to withstand compression forces[38]. Due to the high tensile strength of collagen fibrils, cartilage is endowed to resist tensile forces. Compared to other tissues, cartilage is hypocellular, and lacks vessels, lymphatics and nerves. Therefore, nutrients are provided by the synovial fluid *via* diffusion through the matrix[39]. The appearance of chondrocytes in lacunae, also known as chondrons, characterize another important property of cartilage. Here, the chondrocytes are surrounded with different matrix compartments divided into interterritorial, territorial and pericellular sections [40].

Collagens

Collagens are the major component of cartilage accounting for about two-thirds of the dry mass of the AC[41]. The arrangement of collagens into triple helical structures provides a three-dimensional network, which is responsible for its tensile strength as well as its mechanical stability. The predominant collagen in cartilage is collagen type II, a homotrimer of three α1 (II)-chains[42]. Beside collagen type II, AC contains additional collagens such as collagen type I, III, VI, IX, X, XI, XII. and XIV. The typical collagen fibrils are heterotypic containing collagen

II and the quantitatively minor types IX and XI collagens. In degenerative cartilage, the collagen II/IX/X fibrils are degraded by collagenases[43].

Proteoglycan

Proteoglycans consist of a core protein and one or more covalently-linked side chains of glycosaminoglycans (GAGs), such as chondroitin sulfate or keratan sulfate. Aggrecan is the most important and predominant proteoglycan in AC, comprising about 35% of the dry weight. Multiple aggrecan monomers are attached to a hyaluronan polysaccharide chain via link protein, thereby creating a supramolecular structure as represented in Figure 1. The negatively charged GAGs are responsible for the osmotic attraction of water into the ECM, providing the ability to resist compressive loads. The water content in total wet weight is about 80%[44,45]. In addition to aggrecan, other proteoglycans such as versican, with a similar molecular structure to aggrecan, and small leucine-rich proteoglycans (SLRPs), such as decorin and biglycan, are present in lower amount in the AC cartilage, where they fulfill various biological functions, e.g. regulation of collagen fibril diameter and arrangement. In tissue-engineering, heparan sulfate is a highly investigated GAG due to its high affinity for TGF-β1 and -2, two growth factors which play an important role in repair processes, especially in liver tissue[46].

Glycoprotein

Additional non-collagenous molecules in the ECM of AC are the glycoproteins including cartilage oligomeric matrix protein (COMP), matrilins, fibronectin and others. Glycoproteins are proteins post-translationally modified with oligosaccharide side chains (glycans). The main function of glycoproteins is to stabilize the ECM and to support the interaction of chondrocytes with the surrounding matrix[47]. An important glycoprotein of the cartilaginous ECM is fibronectin, consisting of two almost identically monomers linked by disulfide bonds (Figure 1). Although it is a non-cartilage-specific protein, it plays a critical role in cartilage development inducing cell condensation and chondrogenesis. Moreover, cartilage homeostasis is modulated by fibronectin and its upregulation in osteoarthritic joints was observed. Additional glycoproteins found in cartilage are the matrilins. This family have four members (matrilin 1, 2, 3 and 4), whereby matrilin 1 and 3 have been implicated in the fine regulation of collagen fibril growth[48].

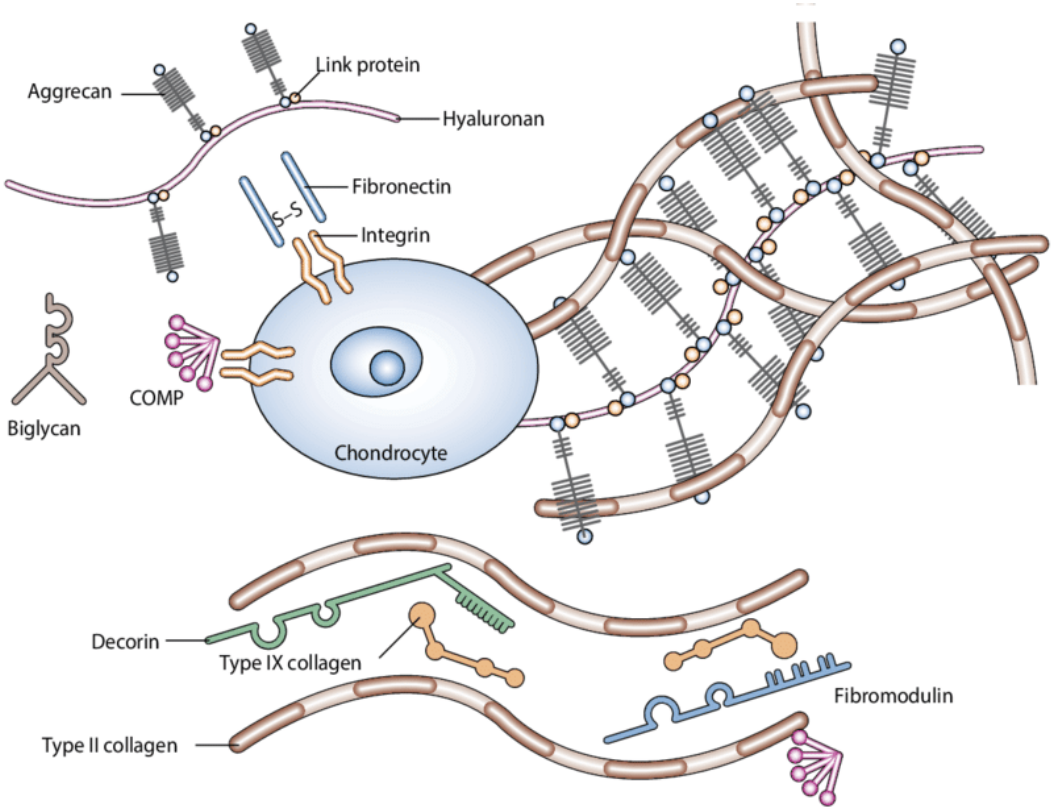

Figure 1: Schematic representation of the extracellular matrix components in articular cartilage. Besides chondrocytes, AC is composed of three main types of proteins: collagens (e.g. collagen type II), proteoglycans (e.g. aggrecan) and glycoproteins including non-collagenous proteins, as COMP, fibronectin, and link protein for example (*Chen et al,* 2006[49])[I].

1.2.2 STRUCTURE OF THE ARTICULAR CARTILAGE

The unique properties of the intact AC together with the synovial fluid are providing joint lubrication for frictionless movement in joints as well as even transmission of loads[50]. Structurally, AC is distributed into four zones based on the differences of ECM composition and cell shape, density and organization as it is represented in Figure 2.

The superficial zone is forming the thinnest layer (10-20% of AC thickness) opposite to the joint cavity. The chondrocytes in this layer are flat and orientated parallel to the surface. Compared to the other zones, the density of collagen is higher while the amount of aggrecan is lower, which causes high resistance towards sheer stress of the articulating bones[51,47]. During OA development the usually parallel oriented fibrils get more disorganized and decrease in number, which is followed by appearance of fibrillations in this zone[52].

[I] Reprinted by permission from Springer Nature, Nature Clinical Practice Rheumatology; „Technology Insight: adult stem cells in cartilage regeneration and tissue engineering “, Chen et al, ©2006

In *the transitional zone* (40-60%) chondrocytes are spherical and fibrils are randomly aligned to the articular surface[51,47]. As, OA progresses, the PG content decreases more significantly in the deeper zones compared to the superficial zone[52].

The radial zone (30%) is the zone with the highest content of PG and has largest collagen fibers. The round and dense chondrocytes represent high synthetic activity. They are vertically oriented as columns towards the surface, likewise as the fibers do[51,47].

The calcified zone is laid up on the subchondral bone. As the name suggests, the ECM is mineralized and contains the hypertrophic chondrocyte marker collagen type X. It is a transitional zone between the soft cartilage and the stiff bone[51,47,53]. The uppermost part of this zone, the so-called tidemark, divides the AC from the calcified layer. During OA, the calcified zone is thickening, which is advancing the tidemark towards the radial zone and therefore contributes to a thinning of AC[54].

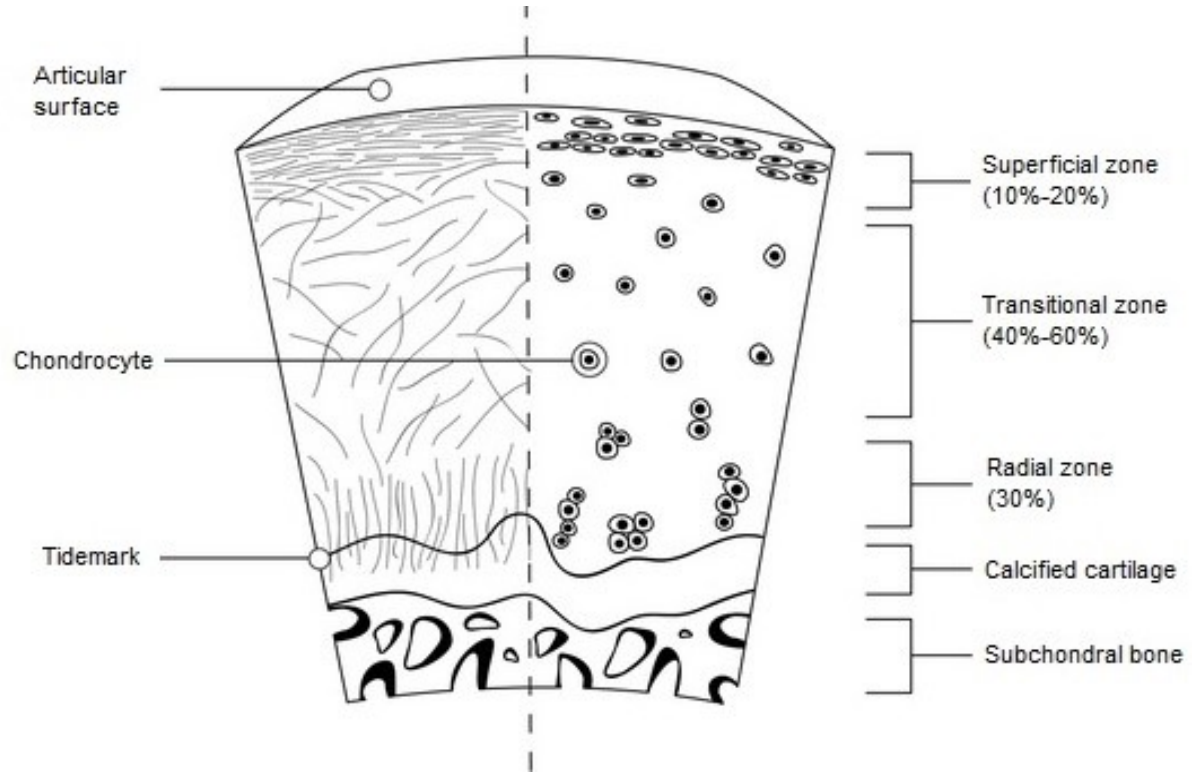

Figure 2: Schematic representation of the structure of articular cartilage. AC is divided into four different functional zones, layered above the subchondral bone. The collagen network is parallel organized with the surface in the superficial, randomly in the transitional zone, and perpendicular in the transitional zone. The border between the radial and calcified zone is marked with the tidemark. The chondrocytes are flat in superficial zone, roundish in the transitional zone and organized into columns in the radial zone (*Ondrésik et al*., 2017[55]).[II]

[II] Reprinted by permission from Springer Nature, Springer Cham; „Knee Articular Cartilage. In: *Studies in Mechanobiology, Tissue Engineering and Biomaterials*. Vol 21“, Ondrésik et al, ©2017

1.2.3 CARTILAGE DEVELOPMENT- ENDOCHONDRAL OSSIFICATION

Endochondral ossification (EO) is the essential process during embryonic development of most bones in vertebrates. It is characterized by sequential morphogenetic steps initiated by condensation and differentiation of skeletogenic mesenchymal stem cells (MSC) into chondrocytes followed by formation of the cartilaginous anlagen in which the chondrocytes proliferate and produce the cartilaginous ECM. Following steps consist of chondrocyte hypertrophy, vascular invasion and replacement of the cartilage by bony skeleton[56]. In long bones, chondrocytes at the metaphysis arrange into the growth plate which is responsible for longitudinal elongation, while at the end of the epiphyses they form the permanent AC covering the articulating surfaces of the bones[57].

Endochondral ossification in the growth plate is an essential morphogenetic mechanism in most of the mammalian bones, except the craniofacial skeleton and part of the clavicle, where intramembranous ossification (IO) occurs. Until the end of puberty, the cartilaginous growth plate in humans is mostly responsible for the linear bone growth, than become silent and it may completely resolve[58]. The individual steps of endochondral ossification are demonstrated in Figure 3. Beginning in the normal growth plate, chondrocytes are well-organized into distinct horizontal zones. The resting zone, or also called reserve zone, contains round, small, stem-cell like chondrocytes that divide rarely and are maintained as replenishment for chondrocytes for the underlying zones[59]. When resting zone chondrocytes enter to the cell cycle, the daughter cells form the proliferative zone, where flat chondrocytes are forming columns in the direction of bone growth. Proliferative chondrocytes arrange into the columns by dividing parallel with the long axis resulting in perpendicularly aligned daughter cells, which rearrange towards the long axis of the column[60]. Later, proliferative zone chondrocytes exit from cell cycle and increase in volume while entering the pre-hypertrophic zone[61,62]. After further enlarging in size, the ECM in the hypertrophic zone is mineralized, the hypertrophic chondrocytes stop expressing collagen type II and begin to express vascular endothelial growth factor (VEGF) to induce blood vessel invasion. In addition, they produce collagen type X, the typical marker for hypertrophic chondrocytes, and MMPs in the terminal layers to degrade the cartilaginous template[61]. Subsequently, chondroclasts and osteoblast precursors are recruited along the invading vessels to degrade the cartilage matrix and build trabecular bone, respectively, at the primary ossification center[63]. At the epiphyseal ends of the bone, a similar scenario occurs, where mesenchymal cells condensate to form the cartilage anlagen. However, at the future joint site cells dedifferentiate and arrange into different layers. Centrally, cell density is decreasing and cells undergo apoptosis to form the future joint cavity by separation. The underlying

interzone contains densely packed, proliferating cells forming the future articular cartilage and other joint tissues. Important is the distinction of articular cartilage and growth plate cartilage as two different origins for chondrocytes[64,65].

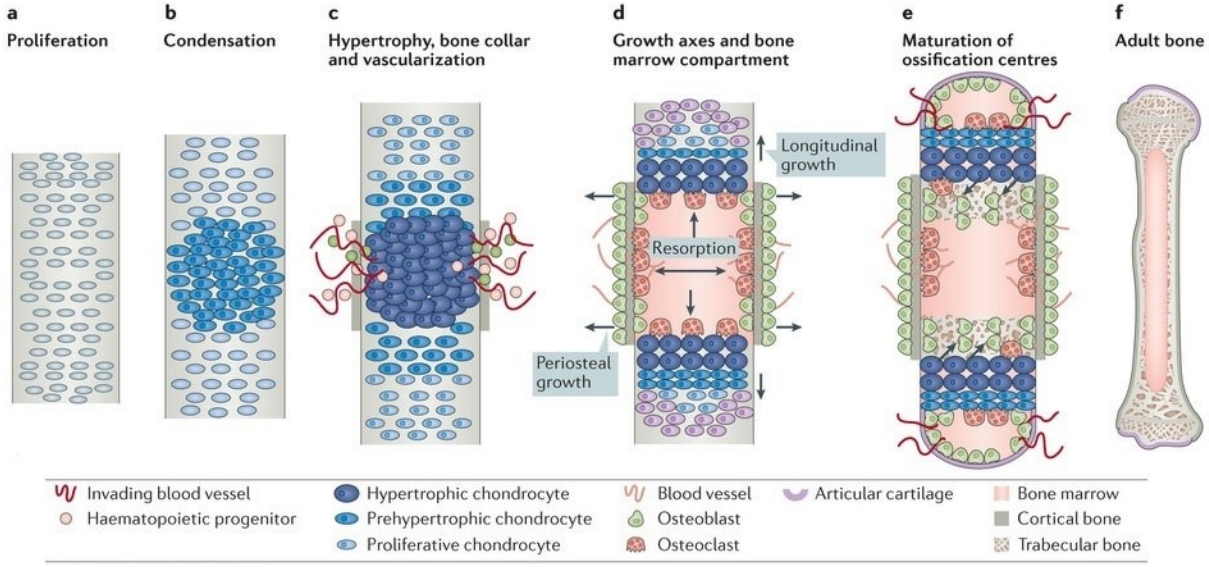

Figure 3: Endochondral ossification. In the first steps of EO, mesenchymal stem cells start to proliferate (a) and condensate (b) before differentiating to chondrocytes to build a cartilaginous template (anlagen). Cells become hypertrophic and vascularization starts (c). The calcified, hypertrophic cartilage is degraded by osteoclasts and replaced by trabecular bone produced by osteoblasts. Parallel with the formation of the bone cavity, the perichondrium around the hypertrophic zone is ossified by IO and become the periosteum forming the cortical bone of the shaft (d). At the center of epiphyses, called secondary ossification center, a similar process removes most of the cartilage, leaving back only the permanent articular cartilage at the ends of the bone. (e). In human, after the end of puberty a remnant of the growth plate remains and the epiphysis and the diaphysis fuse (f) (*Salazar et al*., 2016[66]).[III]

1.2.4 CARTILAGE DEVELOPMENT - TRANSCRIPTIONAL REGULATION

Chondrogenesis describes the process of cartilage development, which is modulated by multiple signaling and transcription factors. One of the most important transcription factors is *SOX-9*. *SOX-9* firstly was described by *Foster et al*. who found mutations in the SRY-box 9 (sex-determining region of y; *SOX-9*) region[68]. This region is a member of the HMG-box (high-mobility group) class DNA-binging protein, which is responsible for several skeletal malformations. For that reason, many researches started to identify the role of *SOX-9* as transcription factor for chondrogenesis[67]. *Foster et al*., for example, could show that heterozygous mutation of *SOX-9* results in campomelic dysplasia, a rare disorder characterized by various skeletal malformations[68]. Analysis of chimeric *SOX-9*$^{-/-}$ mice have demonstrated that

[III] Reprinted by permission from Springer Nature, Nature Reviews Endocrinology; „BMP signalling in skeletal development, disease and repair“, Valerie S. Salazar et al, ©2016

SOX-9 deficient progenitor cells do not differentiate into chondrocytes implicating the pivotal role of this transcription factor in chondrogenesis[69]. Additionally, differentiation of *SOX-9*$^{-/-}$ embryonic stem (ES) cells *in vitro* have failed to produce cartilaginous nodules confirming the essential role of *SOX-9* in cartilage formation[69]. During chondrogenic differentiation, *SOX-9* induces the expression of other *SOX*-family members, *SOX*-5 and *SOX*-6, and cooperates with them in the control of chondrocyte phenotype and the expression of genes encoding for cartilage specific ECM molecules, for example collagen type II and aggrecan, indicating its essential contribution to skeletogenesis[70,71,72]. *SOX-9* is expressed in the early stage of chondrogenesis during the mesenchymal condensation. The lack of *SOX-9* in mouse models results in skeletal defects, for example campomelic dysplasia type I (CMPDI)[73,74]. Despite the important role of *SOX-9* in chondrogenesis, *Liu et al*. reported that *SOX-9* is a non-master pioneer factor, which is not pivotal for activation of marker genes at the onset of chondrogenesis and therefore demands further investigations on transcription activating factors[75]. Maturation of hypertrophic chondrocytes is associated with decrease of *SOX-9* and the upregulation of other transcription factors like runt-related transcription factor 2 (*RUNX-2)*[76]. As aforementioned, cartilaginous remodeling during bone development is regulated by MMPs and collagen type X, which is modulated through Indian hedgehog (Ihh) induced expression of *RUNX-2* in hypertrophic chondrocytes and perichondral osteoprogenitor cells[77,78]. Thus, *RUNX-2* is essentially influencing both maturation of chondrocytes and osteoblast differentiation, and is regarded as a master osteogenic transcription factor[79].

1.2.5 PATHOPHYSIOLOGY OF THE ARTICULAR CARTILAGE DURING OSTEOARTHRITIS

Homeostasis of cartilage is described by a well-organized structure into previously described zones with healthy chondrocytes. Although chondrocytes themselves provide poor self-renewability, they replace ECM in a low-turnover state to maintain an equilibrated environment. This can be negatively influenced by different biomechanical changes due to trauma or congenital, as already mentioned, (secondary OA) or idiopathic (primary OA). As consequence, the production of proteolytic enzymes by activated chondrocytes induces a catabolic metabolism which is schematically represented in Figure 4. The inflammatory response is characterized by elevation of cytokines such as interleukin (IL) 1 and 6, tumor necrosis factor α (TNF-α), c-reactive protein (CRP) and prostaglandin 2 (PGE2). However, cartilage as an avascular and non-innervated tissue is unable to be the source of pain and inflammation. Most likely in early stages of OA these inflammatory factors originate from the surrounding tissues, such as joint capsule, synovia, subchondral bone, muscles or ligaments.

Only a small amount of catabolic proteins expressed from senescent chondrocytes can induce inflammation themselves[1]. Cartilage tissue breakdown is mediated by matrix degrading enzymes such as MMPs (1,3,13) and ADAMTS 4 and 5 (a disintegrin and metalloproteinase with thrombospondin motifs), which are degrading collagen type II and aggrecan, respectively[3]. Therefore, collagen and proteoglycans networks are compromised, introducing a chronic destruction of AC. Loss of fibrillation of proteoglycans due to increased degradation and decreased synthesis, leads to higher water content in cartilage with swelling and over time with loss of viscosity and resiliency[80]. This degeneration process firstly starts in the superficial zone where chondrocyte density diminished due to apoptosis and the remaining chondrocytes become hypertrophic. In addition, superficial fibrillations followed by deep cracks and fissures including also deeper zones, hinder frictionless movements of the joints. Finally, subchondral bone is partly not covered by AC anymore and becomes part of the articulating surface in joints[81].

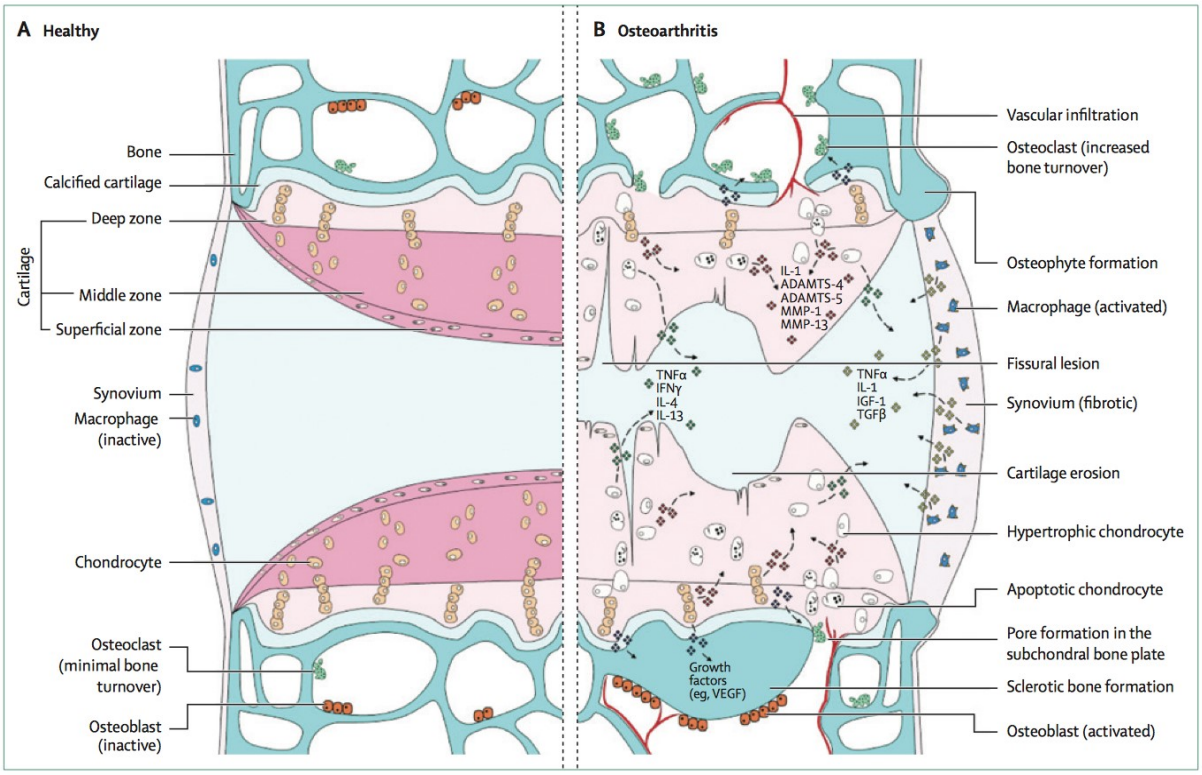

Figure 4: Schematic image of pathophysiology of osteoarthritis. Inflammatory cytokines (TNF-α, IL-1/4, TGF-β, IFN-γ) activate MMPs and ADAMTS, resulting in cartilage erosion with fissural lesions and synovium thickness. Subchondral bone is affected by osteophyte formation, sclerosis and pore formation. Chondrocytes are hypertrophic and apoptotic, osteoclasts are activated (*Glyn-Jones et al.*, 2015[3]).[IV]

[IV] Reprinted by permission from Elsevier, The Lancet; „Osteoarthritis “, S Glyn-Jones,A J R Palmer,R Agricola,A J Price,T L Vincent,H Weinans,A J Carr, ©2015

1.3 CURRENT TREATMENTS

The available treatments for OA focus on pain release and symptomatic therapies to improve quality of life and joint function. The most recommended societies worldwide drawing up guidelines for OA treatments are the Osteoarthritis Research Society International (OARSI), the American College of Rheumatology (ACR) and the American Academy of Orthopedic Surgeons (AAOS). In the German guideline for osteoarthritis of the knee published in 2018, the recommendations of the AAOS and OARSI were considered[12]. In early stages of OA lifestyle changes and conservative treatments are the main strategy. Light to moderate exercises, such as aqua-therapy, are recommended to maintain muscular tone without putting too much pressure on the affected joints. Alternatives such as heat therapy, orthoses or acupuncture are beneficial, but their efficiency is not yet proven[82]. Apart from building up muscles to increase joint stability another desirable effect of physical activity is the weight loss, which in turn reduces overload and as well as inflammation of the joint. Moreover, exercises reduce additional risk factors for OA, for example diabetes and cardiovascular diseases[83]. When non-pharmacological treatments are unsatisfactory, a combination with analgesics like paracetamol, non-steroidal anti-inflammatory drugs (NSAIDs) and later on opioid analgesics, are the most common recommended therapies, because of their double action on pain and inflammation[84]. However, multiple side-effects of these analgesics, particularly NSAID, especially affecting the kidney, the cardiovascular system and the gastro-intestinal-tract, have restricted their application[85].

Additional treatment of OA is the intra-articular (IA) injection of medications, which is providing a more localized and less systemic effect. In these cases, however, attention should be paid to the fact that every articular injection bears the risk of a possible joint infection. The major drugs used for IA treatment are corticosteroids and hyaluronic acid. Corticosteroids suppress inflammation, reduce pain and improve mobility[86]. As a natural glycosaminoglycan, hyaluronic acid is present in normal as well as in osteoarthritic joint fluid. However, the HA content in OA joint is decreased. Its lubricating, shock absorbing and possibly anti-inflammatory properties are accountable for the promising attempts in IA treatments[87,88]. If the prescribed conservative treatments fail, surgical approaches must be considered.

1.3.1 SURGICAL APPROACHES

1.3.1.1 Arthroscopic lavage/debridement

Concerning surgical interventions, the first attempt to be considered is arthroscopic lavage. This method covers the removal of loose damaged tissue, pro-inflammatory cytokines as well as

catabolic proteins from the joint cavity via rinsing with saline solution to improve symptoms and mobility. Arthroscopic debridement is described by shaving cartilaginous or meniscal tears as well as synovectomy or meniscectomy. The outcome of these techniques such as reduced pain, may last for several months, but they do not stimulate cartilage regeneration. In addition, the evidence regarding efficiency is controversially discussed[10,89,90]. An important benefit of arthroscopic inspection of the knee is the diagnostic information provided and the possible combination with further techniques such as microfracture surgery and autologous chondrocyte implantation (ACI).

1.3.1.2 Bone marrow stimulation and osteochondral grafting

Bone marrow stimulation is possible for small cartilage defects not greater than 2 x 2 cm² and in patients without high mobility demands[91]. Different techniques such as microfracturing with an awl or drilling are available to penetrate the subchondral bone and therefore induce new vascularization, offering bone marrow stromal cells as well as growth factors to enter the cartilage defect site and initiate repair processes as demonstrated in Figure 5. Follow-up studies demonstrated that the newly build tissue filling the defect area is fibrocartilage-like, with a lower load capacity compared to native hyaline cartilage. Best outcomes were observed in young patients with smaller defects, because of the higher regenerative potential in younger ages[92]. The technique is approved to be safe, and due to its low costs and simple handling it is recommended as a first-line treatment[93,92].

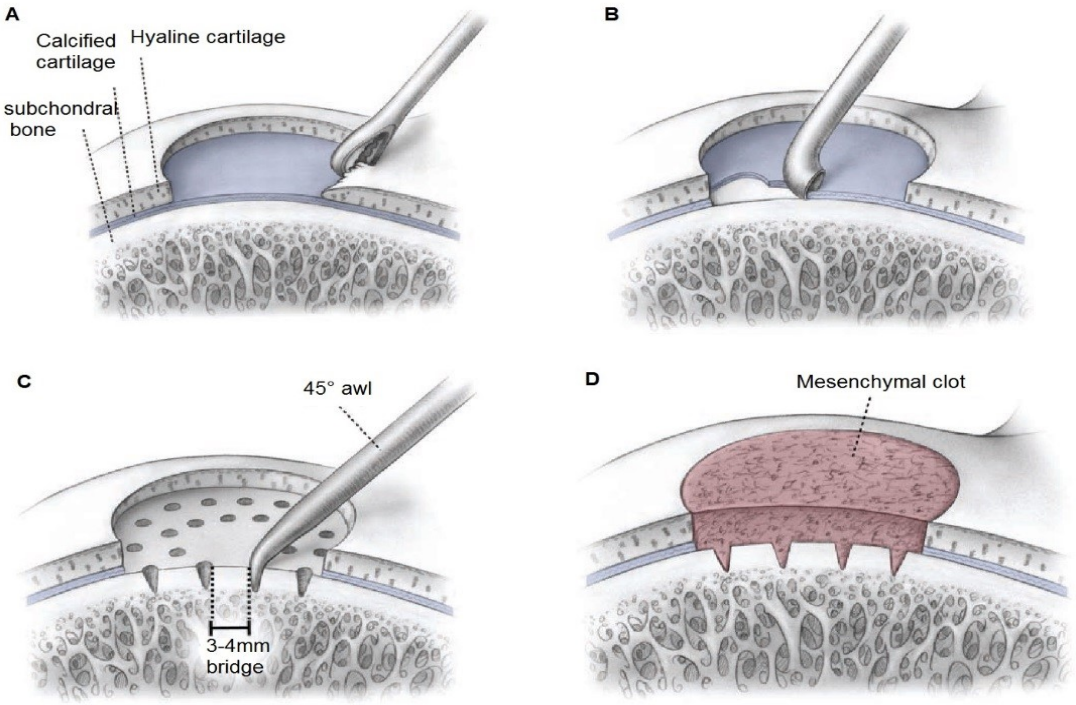

Figure 5: Schematic illustration of the microfracture technique. First, margins of cartilage defects are smoothened (A), followed by removing of calcified cartilage (B). With the help of an awl, subchondral holes are homogenously placed above the cartilage defect (C). A mesenchymal clot is filling the defect (D) (*Mithoefer et al*., 2009[92]).[V]

Osteochondral autologous/allogenic transfer system (OATS) or "mosaicplasty" is an autologous or allogenic transplantation of a cartilage-subchondral bone barrel in defects up to 2 cm². Patients with failed first-line treatments are also candidates for OATS-based therapy. One or more plugs are taken from non-weight bearing areas like the medial or lateral trochlea and are transferred into the chondral defect. The comorbidity of the donor site is a relevant drawback of this technique[94]. As cartilage has difficulties in healing into chondral defects, the bone-to-bone contact has greater and faster healing-in potential. Clinical results are promising and proven to be better than the microfracture technique[95].

1.3.1.3 Autologous chondrocyte implantation (ACI)

Autologous chondrocyte implantation (ACI) is a procedure, which was developed in 1994 by *Brittberg et al*.[96]. The ACI technique requires two operations: In the first arthroscopic surgery healthy cartilage from a low weight-bearing area is dissected to isolate and expand chondrocytes *in vitro*. After three to four weeks the expanded chondrocytes are transferred into

[V] Reprinted by permission from SAGE Publications, American Journal of Sports Medicine; „Clinical efficacy of the microfracture technique for articular cartilage repair in the knee: an evidence-based systematic analysis", Kai Mithoefer, Timothy McAdams, Riley J. Williams, Peter C. Kreuz, et al., ©2009

the smoothened chondral defect and fixed under a periostal flap[97]. In Figure 6 the required steps are demonstrated. Newer generations of the ACI technique take advantage of biomaterial like collagen membranes, fibrins or hyaluronic acids. Chondrocytes are seeded onto these materials, which enables a less traumatic second surgery for reimplantation[98]. The third generation, also known as matrix-associated autologous chondrocyte implantation (MACI), involves three-dimensional scaffolds covered with chondrocytes that are implemented into the defect area[99]. The new-built cartilage is inferior hyaline up to fibrocartilage without the properties of articular cartilage. This is, besides the donor-site morbidity caused by cartilage extraction, one of the disadvantages of ACI[100,94]. In addition, chondrocytes may dedifferentiate during expansion in cell culture, losing their potential to generate cartilage *in vivo*.

To recapitulate, lesions smaller than 2 cm² are supposed to be treated by bone marrow stimulating techniques[101]. If defects are bigger and patients are young and active, ACI should be preferred as it has the best clinical outcome in these defects. Defects involving subchondral bone profit from OATS[102,103]. In advanced stages of osteoarthritic cartilage when degeneration spreads out and defects exceed treatable dimensions for the previous described methods, joint replacement must be considered.

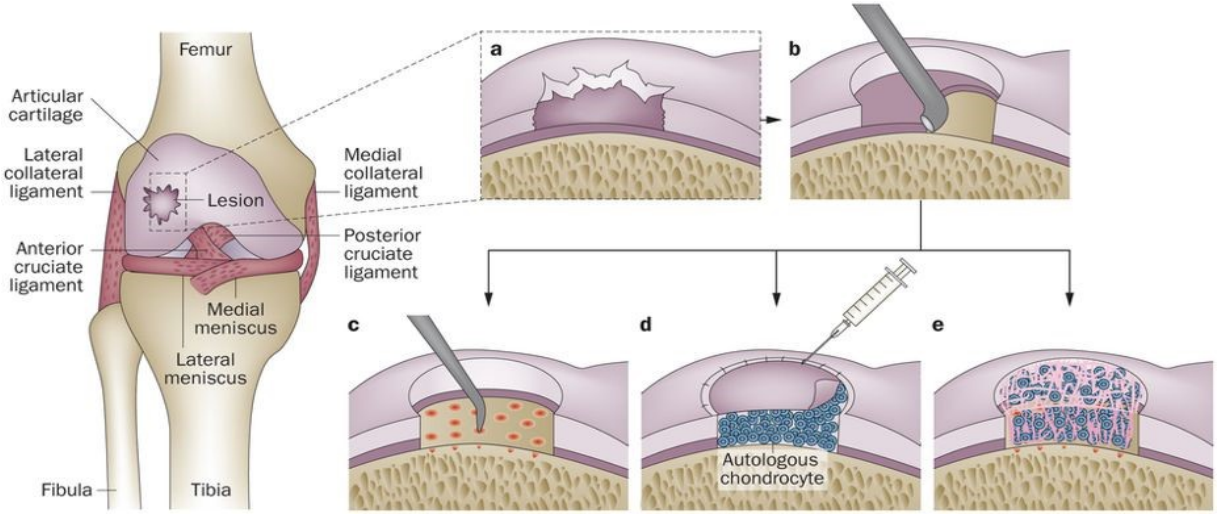

Figure 6: Schematic illustration of tissue engineering techniques for AC. The main weight bearing area of the lateral tibia presents a focal chondral lesion (a). First, margins of cartilage defects are smoothed and calcified cartilage is removed (b). With the help of an awl, microfractures are performed (c). ACI is performed *via* chondrocyte injection below a periostal flap, covering the cartilage defect (d). New tissue engineering attempts to use cell-seeded scaffolds (MACI) that are secured into cartilage defect *via* fibrin glue (d) (*Makris et al*., 2014[104]).[VI]

[VI] Reprinted by permission from Springer Nature, Nature Reviews Rheumatology; „Repair and tissue engineering techniques for articular cartilage“, Eleftherios A. Makris et al, ©2014

1.3.1.4 Joint replacement

The final remaining choice in advanced stages of OA to reduce joint pain and improve movement and life-quality is total joint replacement[105]. There exist different kinds of prothesis to replace either total joint or just parts of it, for example solely the medial condyle in the knee. The outcome of patients with unicompartmental knee arthroplasty (UKA) compared to total knee arthroplasty (TKA) is better regarding mobility and blood loss. In addition, movements in knees with unilateral prothesis are more natural[106]. Metal, polyethylene or ceramic are the most common materials used for these prothesis. Implantations of foreign material are at high risk of infection peri- or postoperative, but another adverse effect is described by periprothetic osteolysis with implant loosening, reducing the life expectancy of joint prothesis to less than 15 years[107]. For this reason, arthroplasty should be only considered in patients older than 60 years to avoid complicated revision surgeries[90].

1.3.1.5 Developing emerging treatments

The novel treatments against OA are predominantly focusing on counteracting the inflammatory component which characterizes OA and are mostly based on blocking antibodies. A major target are TNF-α receptor antagonists such as Adalimumab (Humira; Abbott Laboratories, IL, USA) or Infliximab (Remicade, Böhringer Ingelheim, Deutschland), both monoclonal antibodies (mAB) that are already applied for the treatment of rheumatoid arthritis (RA)[108]. Anyway, in contrast to the successful treatment of RA with Adalimumab, the outcomes for OA are predominantly unconvincing. Yet, new promises are offered by the newly developed monoclonal antibodies against IL-1α and IL-1β[109,110]. Other preclinical studies using mABs against ADAMTS-5 aiming to stop articular surface degradation, have shown beneficial effects such as reduced osteophyte formation and cartilage damage but still present many adverse effects[111]. Also, the expression of VEGF may constitute a possible target in OA treatment. Monoclonal AB against VEGF, such as Bevacizumab, could reduce pain and OA progression in animal models[112]. Another strategy is addressing pain as the main complaint in patients with OA. Tanezumab, a mAB against nerve growth factor (NGF) was found to be efficient in modulating pain, but still no positive effects on disease progression have been reported[113]. Together with the blocking antibody strategies, also the field of novel cell-based therapies using mainly stem progenitor cells or more recently induced pluripotent stem cells (iPSCs) is in continuous development. The properties of adult mesenchymal stem cells and their potential in tissue repair are the pivotal issues of this thesis and therefore will be described in detail in the next chapters.

1.4 HUMAN MESENCHYMAL STEM CELLS

1.4.1 THE POTENTIAL OF MSCS

The drawbacks of the available OA treatments like invasive and multiple surgeries, restricted number of chondrocytes and their unavoidable *in vitro* de-differentiation, push the necessity for alternative strategies focusing on regenerative therapies. In this respect, the use of mesenchymal stem cells (MSCs) represents one of the most promising approaches. MSCs are multipotent cells, meaning they have differentiation potential to cells related to their original germ layer such as chondrocytes, adipocytes, osteocytes, myocytes, fibroblasts and other cells of connective tissue (Figure 7)[114]. They were first described by *Friedenstein et al.* as non-hematopoietic, colony-forming cells with spindle-like shapes[115,116]. MSCs retain commitment to their original lineage when expanded *ex vivo* and exhibit high self-renewal ability. Due to the lack of clear and exclusive identification markers, the International Society for Cell and Gene Therapy (ISCT) introduced three criteria to precise the definition of stem cells and to allow a distinction between the different populations of MSC progenitor cells. These criteria include plastic adherence, *in vitro* differentiation potential towards osteogenic, chondrogenic and adipogenic lineages and finally the expression of the surface protein CD73 as well as the ECM proteins CD90 and CD105 and absence of the hematopoietic antigen CD34 and CD45 as well as markers for B-cells, macrophages and monocytes (for example: CD11b, CD14, CD19 and CD31)[117]. Altogether, MSCs ease of harvest, *in vitro* high-self renewal, multipotency, and additionally, their immunomodulatory, paracrine effects as well as their ability to home to target tissues, provide their clinical relevance in cartilage regeneration and repair. An additional advantage of MSC-based treatment approaches is low immunogenicity, allowing allogenic MSC transplantation, which simplifies their employment and reduces possible side-effects.

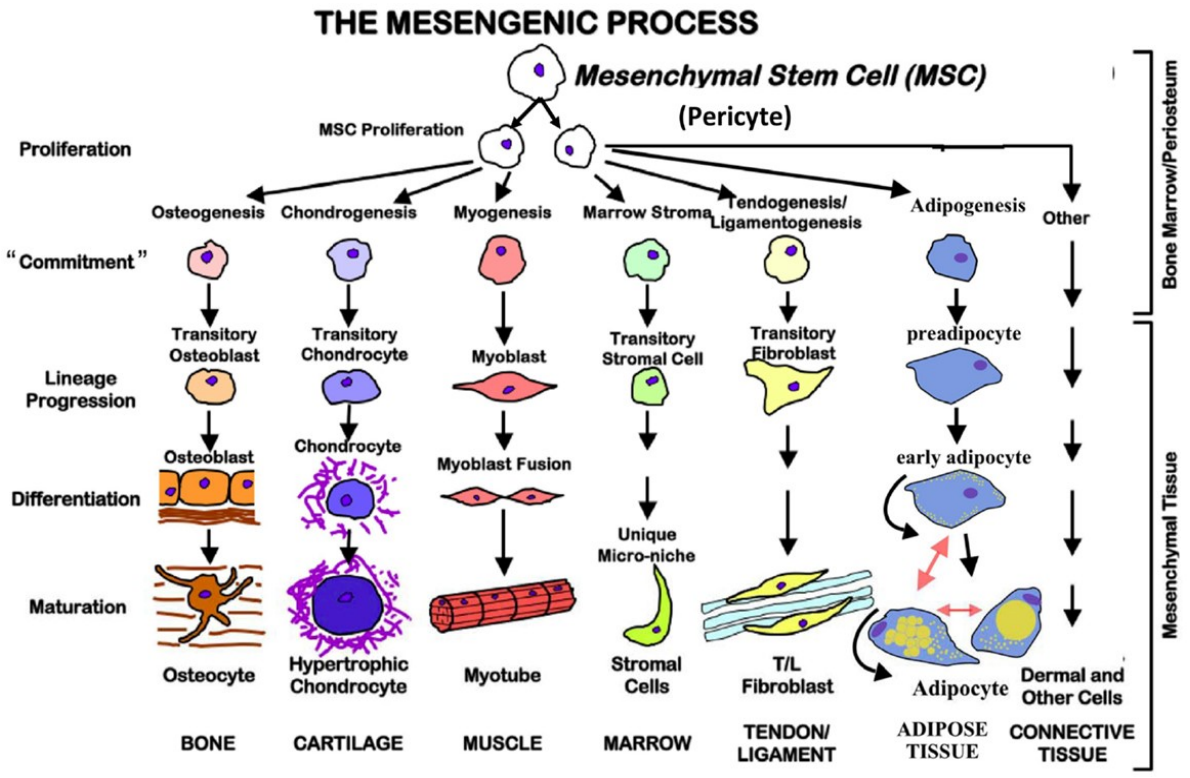

Figure 7: Multilineage differentiation potential of MSCs. Presented are the lineages MSCs are able to differentiate into (*DiMarino, A. M., et al*., 2013[118]). [VII]

1.4.2 ORIGINS OF MSCS

Adult MSCs may be of different origins. They can be isolated from bone marrow where they mainly reside, but also from adipose tissue, skeletal muscle, synovial membrane, periosteum, liver, lung and from peripheral or cord blood. Because of the easy availability, the high chondrogenic potential and the already available comprehensive research, bone-marrow-(BM)-derived and adipose-derived-MSCs (ASCs) are the preferred cell origins for cartilage repair[119]. As BM-MSCs and ASCs are from different origins and display different populations, there exist significant differences regarding their properties as well as donor-dependent characteristics.

Bone-marrow derived MSCs have been the main source to harvest multipotent MSCs. To date, MSCs from bone-marrow have shown the best potential in term of differentiation ability. Nevertheless, when challenged towards chondrogenesis, BM-MSCs tend to form calcified or fibrous tissues. This in concomitance with the comorbidity associated with the isolation procedures and the limited amount of cells present in the tissue have shift the interest of researchers and clinicians towards ASCs[120,121].

[VII] Licensed under CC BY- 3.0; [https://creativecommons.org/licenses/by/3.0/deed.de]: "THE MESENGENIC PROCESS" by DiMarino, A. M., Caplan, A. I. & Bonfield, T. L.

ASCs are much easier to harvest during minimal invasive liposuction or lipoaspirates of subcutaneous tissue from easily accessible parts of the body. The frequency of cells occurring in fat is 300-fold higher compared to bone marrow[122,123]. Their capacity to differentiate into multiple lineages, together with a genetical and morphological long-term stability in culture, highlight ASCs as good alternative to BM-MSCs for clinical applications[124,125].

1.4.3 POTENTIAL MODE OF ACTIONS OF MSCS IN REGENERATIVE MEDICINE

In the past decades it was thought that MSCs could migrate and engraft into the defect area, differentiate into the injured cell lineage and regenerate the damaged tissue[126]. According to this belief, many studies undertook a straight experimental set-up, where MSCs were directly applied to the defect site and afterwards regeneration was analyzed. However, several studies demonstrated that MSCs do not engraft in significant number towards the defect area and for that reason do not explain the reported tissue replacement[127]. These findings initiated a considerable debate about the fate and mechanism of action of MSCs. The novel and nowadays most accepted theory is that MSCs do not actively participate in the regeneration but act in a paracrine manner by releasing chemokines and growth factors which modulate immune response, and enhance cell proliferation, migration and differentiation of native tissue cells. The paracrine activity appears in secretion of bioactive molecules such as VEGF, transforming growth factor beta (TGF-β) and fibroblast growth factors (FGFs), which all support and modulate regenerative processes[128]. Furthermore, MSCs interact with immune cells, where they suppress proliferation and cytokine production of inflammatory T-cells, as well as inhibiting B-cell activity and antibody secretion[129]. First evidences of immunomodulatory actions of MSCs were observed, when MSCs were added to mixed lymphocyte reaction assays (MLR), a mix of mononuclear cells from mismatched peripheral blood. It was observed that T-cell expansion was reduced in presence of MSCs[126,130]. Further, the expression of inflammatory factors (TNF-α, IL-1β, IL-6) by activated macrophages can be reduced in presence of MSCs. A possible explanation for these observations is the expression of TNF-α -stimulated gene protein (TSG)-6 and PGE2. TSG6 is supposed to suppress NF-kB (nuclear factor 'kappa-light-chain-enhancer' of activated B-cells) activity in macrophages and other cells, whereas PGE2 induces the release of IL-10, an anti-inflammatory protein[131,132]. Further studies observed that the secretome of MSCs contains factors, which in part still remain undefined, but support cell survival, stimulate angiogenesis and decrease number of apoptotic cells[133]. In summary, MSCs provide high anti-inflammatory potential and ensure good conditions for tissue repair, although according to current knowledge the majority of the signaling pathways remain unclear.

1.4.4 MSCS DELIVERY OPTIONS

MSCs are considered as a promising therapy for cartilage regeneration due to their direct chondrogenic differentiation ability, secretion of paracrine factors and immunomodulatory effects. However, MSCs are sensible regarding their environment and thus require suitable delivery carriers and methods to avoid apoptosis/necrosis, differentiation into unwanted lineages or de-differentiation of committed cell types[134,135]. Besides static scaffolds, research for OA focuses especially on hydrogels that allow homogenous cell distribution and minimal-invasive intra-articular injection. Hydrogels can be characterized by their synthetic or natural origin and their chemical and physical composition of the protein network. Additionally, a good biocompatibility and low immunogenicity is of outmost importance[136]. Furthermore, the shape adaptability of hydrogels, enables them to be used in different injection devices (e.g., prefilled syringes) and to fill any target space. In this study, a fibrin hydrogel was chosen as cell carrier. Fibrin hydrogel is a degradable, nontoxic biopolymer-based hydrogel consisting of two main components: fibrinopeptides and thrombin. By simulating an important step of blood coagulation cascade, thrombin, a protease mainly isolated from bovine plasma, cleaves fibrinopeptide A and B from fibrinogen and thus fibrin is formed[137]. Fibrin is a clinically approved hydrogel, with proven high biocompatibility[138], low immunogenicity, regulated degradation as well as good properties for cell adherences and migration[138,139]. Fibrin is also remodeled *in vivo* by degradation *via* several proteases such as plasmin. The degradation process can be observed *in vitro* by shrinking of the fibrin hydrogel[140,141]. Variations in the formulation result in different mechanical properties such as alterations in fibrin fiber diameter or pore sizes[142]. For example, to improve stability higher concentrations of thrombin can be used. In this way fibrin gels provide higher resistance to fibrinolysis, while fiber diameters decrease[137].

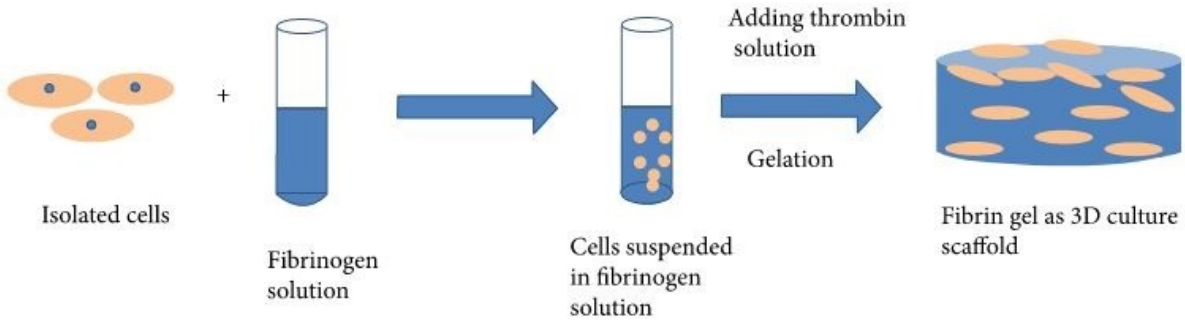

Figure 8: Schematic illustration of fibrin hydrogel as 3D scaffold. Isolated cells are mixed with fibrinogen solution. With addition of thrombin solution, gelation starts and a three-dimensional scaffold is formed (*Li Y. et al,* 2015 [138]).[VIII]

In the cartilage research field, another commonly used scaffold is hyaluronic acid (HA). HA is a naturally occurring component in synovial joint fluid. Hyaluronic acid-based scaffolds are provided as meshes, sponges or more frequently as hydrogels[143]. Due to chemical or physical cross-linking methods, HA hydrogels provide higher resistance against mechanical stress compared to fibrin hydrogels[144]. Furthermore, HA is able to obtain and even promote differentiation capabilities of MSCs towards chondrogenic lineage, which make them attractive especially for cell delivery devices in OA treatment [143]. Nevertheless, due to a short half-life time application of HA is limited, although chemical modifications can prolong this half-life time of HA[145]. Another disadvantage of HA is the non-adhesive surface, which enables MSCs to move, but at the same time make them lose their proliferation capability at higher concentrations[146]. For that reason, HA-based-scaffolds as well as alginate-based scaffolds can be modified by additional arginine-glycine-aspartate (RGD) sequences to improve cellular adhesion. They provide good properties for cell-delivery constructs themselves as well as in mixtures with other substrates such as fibrin or chondroitin sulfate.

Synthetic hydrogels such as polyethylene-glycol (PEG), do have many advantages such as individual tailoring of mesh size, gelation and degradation properties to create an ideal delivery device for cells or drugs. For example, the degradation properties can be adjusted in a way, which allows specific rates for the cell release out of the hydrogel[147]. However, as a synthetic scaffold, PEG hydrogels are confronted with several problems such as limited biocompatibility, immobilization and low viability of cells. Natural hydrogels instead made of ECM components provide a more natural environment for cells[148].

[VIII] Licensed under CC BY- 3.0 [https://creativecommons.org/licenses/by/3.0/]: "Schematic illustration of fabrications of two- and three-dimensional cell culture scaffold" by Li, Y., Meng, H., Liu, Y. & Lee, B. P

Collagen-based scaffolds are another approach for cell delivery. The main components used for these hydrogels are mainly collagen type I , but also collagen type II[149]. For clinical usage it is mainly isolated from animals (for example: rat tendons), as it is a natural and abundant protein in ECM of mammalians. Collagen already provides a natural adherence, which is necessary for cell transplantation. Gelation of collagen is achieved either by increasing temperature or pH, which results in fibrillogenesis[150]. The 3D-environment of collagen hydrogels promotes higher matrix production of chondrocytes compared to control groups as *Rutgers et al*. could show[151]. Further, collagen-based scaffolds can be degraded by collagenases, which retains place for newly build tissue. On the other hand, the good biodegradability provokes limited stiffness for long time-periods as well as low mechanical stability. These properties can be improved chemically or physically, but the methods are limited and influence biodegradation processes. Altogether, collagen is a suitable hydrogel for cell delivery, but it is more useful for cell behavior studies where it is mainly utilized[152].

Alginate is a polysaccharide isolated from brown algae, which is (1,4)-linked to β-d-mannuronic (M) acid and α-l-guluronic (G) acid monomers. The interaction of cations such as calcium, barium or strontium with the G-monomers is responsible for the formation of crosslinking and leads to gelation[153]. With high polymer concentrations, mechanical stability increases and degradation processes are slowed down[154]. To provide a suitable cell delivery environment, alginate hydrogels must be modified to provide cell adhesion, which is not supported by native alginate itself. Therefore, further adhesion molecules such as laminin, fibronectin or collagen are linked to alginate[155]. Proteins containing high concentrations of RGD sequences are used as adhesion ligands as well. Numerous integrin receptors present on cell surfaces are binding to these ligands[156]. The 3D-structure of alginate hydrogels provides MSCs to obtain a rounded morphology, which promotes chondrogenesis[157]. However, native alginate is a non-degradable molecule, which can only be dissolved by release of divalent cross-linking. If alginate previously underwent oxidation, very slowly degradation is possible. However, when degradation appears too slowly it hinders new tissue formation. Further, debates about the biocompatibility of alginate including possible foreign body reactions, evoke doubts about proper usage of alginate as cell delivery device[158].

1.5 INTEGRINS

Integrins are transmembrane proteins which connect the cytoskeleton of a cell to the ECM. Acting as chemo- and mechano-transducers, they are responsible for the activation of several

outside-in and inside-out signaling pathways, involved in cell proliferation, migration, shape and orientation as well as survival and differentiation[159].

1.5.1 STRUCTURE OF INTEGRINS

Integrins are heterodimeric transmembrane receptors composed by an α and a β glycoprotein subunit that are non-covalently associated and have a large extracellular domain, whereas the intracellular or cytoplasmatic domain is short[160]. The human diversity of integrin subunits consists of 8 β and 18 α subunits that can form together 24 different heterodimeric integrin receptors. Integrins can be further divided into subgroups according to their ligand specificity such as collagen, laminin, RGD and leucocyte-specific receptors (Figure 9).

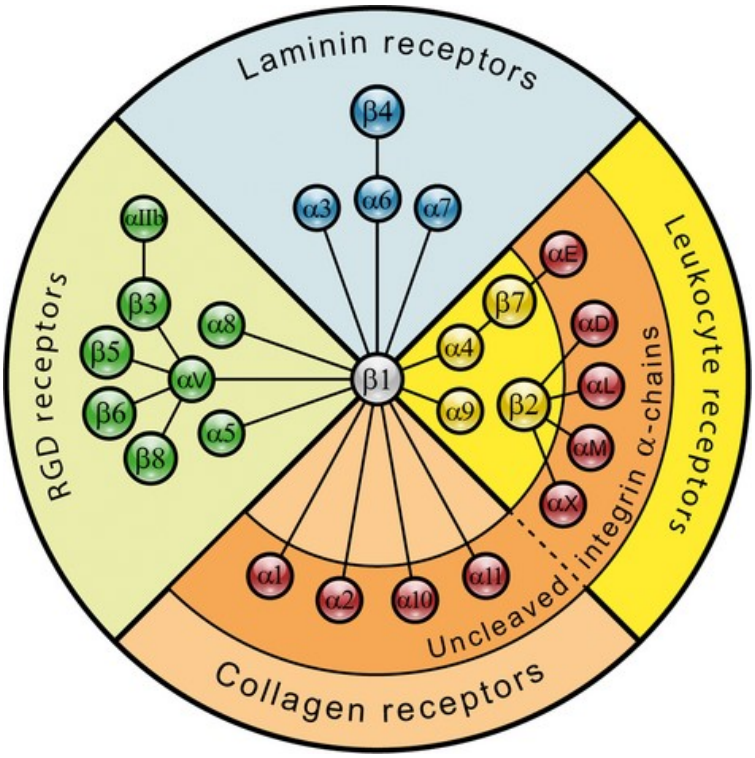

Figure 9: The integrin family in vertebrates. According to the binding specificity, integrins can be classified into four groups: collagen receptors, RGD receptors, laminin receptors and leukocyte receptors (*Barczyk et al*., 2000[161]).[IX]

To be functional, activation of integrins is required, which is initiated by inside-out-signaling leading to conformational changes. For most integrins the cytoplasmatic β tail gets activated by phosphorylation *via* talin or kindlin, leading to separation of the α and β parts and further to integrin activation. In addition, the extracellular tail of the integrin pass through a conformational change, which increases the affinity to its ligands[162,163]. The signal transduction

[IX] Reprinted by permission from John Wiley and Sons, Peridontology 2000; „Role of integrins in the periodontal ligament: organizers and facilitators“, Donald Gullberg, Anne Isine Bolstad, Malgorzata Barczyk, © 2013

from extracellular ligands into the cell is so called outside-in signaling. The binding of an extracellular ligand results in several conformational changes such as separation of the transmembrane domain, which induces interactions with intracellular enzymes transferring the molecular information from the outside to the inside[162].

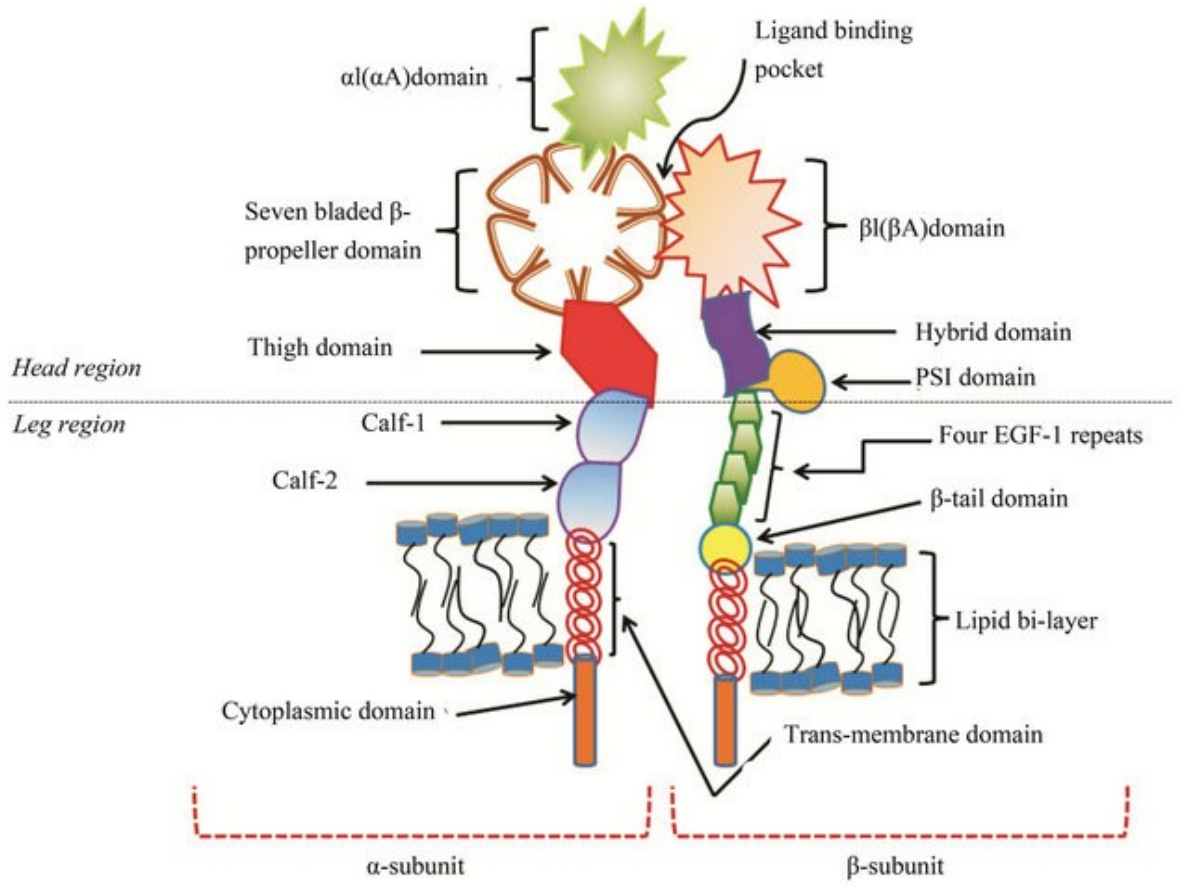

Figure 10: Schematic illustration of integrin structure. Integrins are heterodimers consisting of an α- and a β-subunit. The extracellular head-region of the α-subunit contains the αI(αA)-domain, seven-bladed β-propeller domain for calcium binding and the αI domain with a binding-site for metal ions. The thigh domain connects the calf-1 and calf-2 domain as parts of the leg region. β-subunit similarly consists of a βI(βA)-domain, which provides a ligand pocket together with the β-propeller domain of the α-subunit. The leg region is formed by four EGF-1 repeats that are connected to the PSI (plexin-semaphorin-integrin) and hybrid domain of the head region (*Goswami, S, 2013* [164]).[X]

The group of collagen-binding integrins consists of the subunits α1, α2, α10 and α11, all coupling with the β1-subunit [165]. Integrin α1β1 was described to be expressed in trophoblasts after implantation, indicating a pivotal role during embryogenesis[166]. However, mice deficient in integrin α1, could develop normally and are fertile[167]. Together with integrin α2β1 it is involved in the FAK (focal adhesion kinase) and p38 MAPK (mitogen-activated protein kinase)

[X] Licensed under [https://creativecommons.org/licenses/by/4.0/] "Representation of prototype αI-domain containing integrin heterodimer": by Goswami, S.

pathway for the induction of MMP-13, which is activated for example during ostelysis[168]. Moreover, both collagen receptors are involved in chondrogenic differentiation of MSCs, as a strong activation of these receptors was observed by *Goessler et al*[169].

Integrin α11β1 is a commonly investigated collagen receptor, which was first described in fetal muscles by *Gullberg et al.*[170]. Nowadays, it is found in fibroblasts, bones and muscles. Loss of integrin α11β1 results in disorganized periodontal ligaments and dwarfism, indicating its pivotal role in fibroblasts for cell migration and collagen organization[171]. Moreover, *Popov et al*. found out that silencing of α2 and α11, two collagen type I receptors, leads to increased apoptosis, reduced cell adhesion and motility of MSCs as well as challenging bone development in mutant mice[215].

The subunit integrin α10 was first described by *Camper et al*. as a collagen type II binding integrin expressed by chondrocytes[172]. It is expressed in growth plate and AC and therefore playing an important role in chondrogenesis as *Bengtsson et al*. already described in 2005, and eventually in AC homeostasis. In their study, mice lacking integrin α10 displayed mild chondrodysplasia with changes in cartilage structure and defects of chondrocyte shape, revealing the importance of integrins for cell-matrix interactions during endochondral ossification[173]. Furthermore, *Varas et al.* could show that integrin α10 is expressed in bone marrow MSCs and its expression is upregulated during chondrogenesis, suggesting integrin α10 as a potential biomarker for chondrogenic potential of MSCs[174]. Recently, it was found that equine MSCs selected for high integrin α10 expression have the potential to hinder the onset of OA in an equine impact model[175]. This first preclinical trial demonstrated the safety and efficacy of intra-articular injection of allogenic integrin α10-selected adipose derived MSCs in a large animal. To date, no integrin α10 mutation has been identified in humans. However, in 2013 an autosomal recessive chondrodysplasia caused by a nonsense mutation in *ITGA10*, affecting the Norwegian Elkhound and Karelian Bear Dog breeds was reported[176]. Integrin α10 protein loss leads to disproportionate dwarfism, with anatomical features resembling the human spondylo-methaphyseal dysplasia. This canine phenotype further supports the important role of integrin α10 in cartilage and bone formation. More recently, integrin α10 was also found to be expressed in human glioblastomas, and glioblastoma cells selected for high integrin α10 expression show increased proliferation and sphere formation[177]. Moreover, function-blocking antibodies against integrin α10, significantly suppressed tumor growth[178], spotlighting integrin α10 for its potential as a therapeutic target in treating glioblastomas.

1.5.2 MODELS OF INDUCED OSTEOARTHRITIS

Osteoarthritis is mainly a degenerative disease, which is why it is appearing mostly in elderly people. In order to mimic the natural etiology of OA, spontaneous OA models that are very close to the primary OA in humans, appear most suitable. However, a long period of time is needed for developing OA, which goes along with higher maintaining costs. Also, larger numbers of animals are required to conduct the study, while higher variations of outcome are to be expected. In summary, all these disadvantages, make the spontaneous OA-models to some extent unattractive[179,180]. Another possibility is to induce OA. Often performed are the so-called injection models using mono-iodoacetate, collagenases, papain, carrageenan or others[181]. These models are primarily used for studying pain related effects of OA caused by inflammation, toxicity or cartilage damage[182,183]. The appearance of high numbers of dead chondrocytes and accelerated cartilage destruction are not comparable to the pathomechanism responsible for OA development in human. For these reasons, injection methods provide restricted validity for researches on the pathomechanism of human OA[180]. On the other hand, the surgically induced OA-models mimic predominantly post-traumatic development of OA in humans. Partial/total meniscectomy, destabilizations of the medial meniscus (DMM), resection of the anterior cruciate ligaments and osteotomy are besides numerous other methods commonly used models to induce OA, all with the goal to destabilize the knee[184,185]. The knee is the most frequently joint investigated. All surgical models offer high reproducibility. In particular, the DMM-model, causes mild-instability with slower progression of OA which is mimicking in a more resembling way human OA[186,187]. The applicability of the DMM model to mice also offers the possibility to implement knock out animals to study the precise role of a protein of interest during OA. For these reasons, the DMM model is currently the most commonly used surgical method to induce OA in mice and also the method of choice for this study.

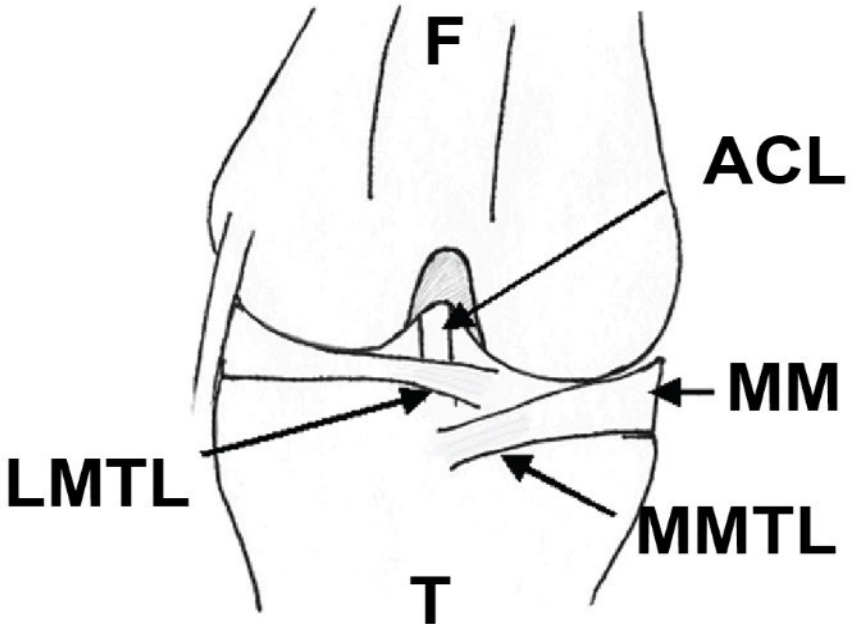

Figure 11: DMM-Model: right knee of a mouse, frontal view. The destabilization of the medial meniscus is achieved by cutting the MMTL. F= Femur, T= Tibia, MM= medial meniscus, MMTL= medial meniscotibial ligament, LMTL= lateral meniscotibial ligament, ACL= anterior cruciate ligament (*Glasson et al*., 2007[188]).[XI]

1.5.3 OA ANIMAL MODELS

Osteoarthritis can be observed in different types of animals. Large animals such as sheep, goats or horses provide anatomic similarities to the human joint components especially regarding cartilage thickness. Therefore, they are crucial to obtain more clinically relevant data prior to therapeutic interventions[185]. On the other hand, small animals, like rodents for examples have been mainly used as models for osteoarthritis, because of inexpensive and standardized housing. Regarding the joint size and cartilage thickness, rats provide thicker AC compared to mice as *Gregory et al.* could show in their study[189]. However, cartilage loading in rats is different to humans and therefore rat models are not always comparable to humans[190]. In rabbit, the destabilization of the medial meniscus, leads to a successful induction of OA[191]. However, *Pederson et al*. introduced the fact that structural differences with higher density of chondrocytes as well as notably thinner cartilage are observed comparing human and rabbit AC as well as *Glasson et al*. did in mice AC[192,193]. Due to the considerable experience gained in our laboratory, modest costs and extensive knowledge in literature regarding mouse models, the mouse was the preferred animal for the present work.

[XI] Reprinted by permission from Elsevier, Osteoarthritis and Cartilage; „The surgical destabilization of the medial meniscus (DMM) model of osteoarthritis in the 129/SvEv mouse“, S.S. Glasson,T.J. Blanchet,E.A. Morris, © 2007

1.6 AIMS OF THE THESIS

As there is currently no disease-modifying osteoarthritis drug or treatment that can halt the progression of the disease or regenerate damaged joint cartilage, adult mesenchymal stem cell (MSC)-based therapies represent promising, minimally invasive treatment options for alleviating osteoarthritis and repairing cartilage lesions. In vitro differentiation of MSCs into different lineages can be modulated by a variety of factors including growth factors, cell-matrix interactions and mechanical stimulation. Recently, a subpopulation of monolayer-expanded bone marrow-derived MSCs expressing α10 integrin was identified with high chondrogenic potential in pellet culture, suggesting that α10β1 may be a unique biomarker for quality assurance of MSCs used for cartilage repair. The main objective of this thesis is to determine the therapeutic effect of human BM-MSCs sorted for α10β1 integrin (hereafter referred to as $\alpha10^{high}$ MSCs) expression in a post-traumatic osteoarthritis (PT-OA) in vivo mouse model. Specifically, the following objectives have been identified:

- To demonstrate the improved chondrogenic potential of platelet lysate-treated, α10β1 integrin-sorted human MSCs ($\alpha10^{high}$ MSC) in pellet culture.
- To identify a suitable hydrogel carrier for in vivo delivery of MSCs.
- To compare the effect of transplanted human $\alpha10^{high}$ MSCs and unsorted human MSCs on the progression of OA in the destabilization of the medial meniscus (DMM) PT-OA mouse model.
- To identify the transplanted human MSCs in the joint eight weeks after surgery.

2 MATERIAL AND METHODS

2.1 *IN VITRO* ANALYSIS

2.1.1 PRIMARY CELLS

The primary cells used for this study were human mesenchymal stem cells (MSCs) isolated from bone marrow (BM). The cells were isolated, characterized and kindly provided by Xintela AB (Lund, Sweden; CEO: Evy Lundgren-Åkerlund). Human BM-MSCs were firstly characterized by presence of the typical mesenchymal stem cell surface markers: CD105, CD73, CD90 and the absence of the hematopoietic markers: CD14, CD34, CD45[117] by flow cytometry (BD AccuriTM C6, BD Bioscience, USA). Cells were cultured in DMEM/Ham's F12 1:1 medium (Dulbecco's Modified Eagle Medium; Gibco™ Thermo Fischer Scientific, USA) supplemented with 5% platelet lysate (Stemulate®; Cook general biotechnology, USA) and 1% penicillin/streptomycin (Gibco™ Thermo Fischer Scientific, USA). After expansion, a portion of cells were stained using a proprietary monoclonal integrin α10 antibody (Xintela AB) and live cells were subjected to fluorescence-activated cell sorting by FACSAria (BD Bioscience, USA) in order to select a subpopulation with elevated integrin α10 expression, namely $\alpha10^{high}$ MSCs. Discrimination of live/dead cells was assessed by 7-AAD staining (BioLegend). Sorted cells were washed in culture medium and re-seeded for recovery and expansion for one more passage before being aliquoted and frozen. In parallel, a portion of non-sorted cells, namely unsorted MSCs, to be used as control, were expanded. Cells at passage three (unsorted MSCs) and passage four ($\alpha10^{high}$ MSCs), were shipped overnight in dry ice to the Laboratory of ExperiMed (Hospital for General, Trauma and Reconstructive Surgery – Ludwig-Maximilians-University, Munich) and stored in liquid nitrogen until used in the various *in vitro* and *in vivo* experiments. Cells were thawed, seeded and cultured to be used for studies of the chondrogenic, adipogenic and osteogenic differentiation potentials at passage four and five, respectively.

2.1.2 CULTURE CONDITIONS

2.1.2.1 Cell culture conditions

For general expansion and subsequent experiments, cells were handled under sterile conditions in a primary cell culture laminar flow hood (Heraeus Instruments, Germany). The basic culture medium contained DMEM/Ham's F12 1:1 medium (Dulbecco's Modified Eagle Medium/ Nutrient Mixture F-12 Ham; Merck, Germany) supplemented with 5% platelet lysate (Stemulate®; Cook general biotechnology, USA) and 1% penicillin/streptomycin (Life

Technology, USA). Cells were grown in monolayers in a hypoxic (4% O_2) humidified incubator (MCO-5M, Sanyo, Germany) under constant conditions at 37 °C and 5% CO_2. Media was changed every 3-4 days and cell confluency never exceeded 80-90%.

2.1.2.2 Passaging and counting of cells

MSCs grown in monolayer were detached from the plastic using Accutase™ (Thermo Fischer Scientific, USA). Accutase™ is a gentle, less toxic cell-detachment solution with proteolytic and collagenolytic enzyme activity. In brief, cells were covered with Accutase™ for less than 5 min at 37 °C and 5% CO_2 until cells detached. To neutralize Accutase™ the double amount of fresh culture media was added. For counting, 10 µl of re-suspended cells was injected into Neubauer chamber (Brand, Germany). To determine the total number of cells per milliliter, cells were counted in all four quadrants (A, B, C and D) divided by 4 and multiplied by 10^4: cells/ml = [(A+B+C+D)/4] x 10^4.

For re-plating, a defined number of cells was centrifuged at 300 g for 5 min (Universal 16 R centrifuge, Hettich Zentrifugen, Germany) and re-suspended in fresh culture media and poured into suitable flasks.

2.1.2.3 Cryopreservation and thawing of cells

For cryopreservation a pre-cooled freezing media containing 70% of culture media, 20% FBS (Sigma Aldrich, Germany) and 10% dimethyl sulfoxide (DMSO, Merck, Germany), was used. Cell aliquots in cryovials (Thermo Fischer Scientific, USA) were firstly placed at -80 °C in freezing containers with isopropanol and subsequently stored in liquid nitrogen.

For thawing, cryovials were briefly placed in a water bath at 37 °C until suspension melted and immediately mixed with 5 volumes of fresh culture media and afterwards centrifuged for 5 min at 300 g (Universal 16 R centrifuge, Hettich Zentrifugen, Germany). Aspiration of supernatant was followed by resuspending cells with fresh and pre-warmed culture media. For culturing, cells were transferred in T-175 or T-225 cell culture flasks (Thermo Fischer Scientific, USA) and after 24 hours culture media was changed in order to remove non-attached cells.

2.1.2.4 Cell culture dishes

Dishes and flasks used in this study for *in vitro* cell culture were T-75, T-175, T-125 cell culture flasks, 6-well and 96-well-plates and 3,5 cm culture petri dishes, all purchased from Thermo Fischer Scientific (USA), Greiner bio-one, (Germany), Sarstedt AG & Co. (Germany) and Corning Inc. (USA).

2.1.3 TRILINEAGE DIFFERENTIATIONS

2.1.3.1 Osteogenic differentiation

For osteogenic differentiation MSCs were plated into 6-well-plates and expanded to 70-80% confluency. DMEM-high glucose media (Thermo Fischer Scientific, USA) supplemented with 10% FBS, 10 mM ß-Glycerolphosphat, 50 µM L-ascorbic-acid 2-phosphate, 100 nM dexamethasone (all Sigma-Aldrich, Germany) and 1% penicillin/streptomycin (Merck, Germany) was used to induce differentiation. Control groups received basic culture media. Media was changed twice per week. After 21 days osteogenic differentiation was ended and matrix mineralization was detected *via* Alizarin Red staining. In brief, cells were washed with PBS (phosphate-buffered saline) and fixed with 4% Paraformaldehyde/PBS solution (PFA; Merck, Germany) for 15 min at room temperature (RT). Fixative was washed with distilled water (dH_2O) and cells plus eventual deposited matrix were stained with 40 mM Alizarin Red Stain solution (Osteogenesis Assay Kit, Millipore, USA) for 20 min at RT. In order to remove unbound staining, dishes were washed with dH_2O three times. Pictures were taken (10x magnification) on AxioVert 40CFL microscope with AxioCam 105 color camera (Zeiss, Germany). To quantify osteogenic differentiation, the Osteogenesis Assay Kit (Millipore, USA) was used. Alizarin-stained plates were incubated with 10% acetic acid (Sigma-Aldrich, USA) for 30 min at RT, scraped from bottom, transferred into tubes (Eppendorf, Germany) and heated at 85 °C for 10 min (Thermomixer comfort, Eppendorf Germany). After centrifugation for 15 min at 14000 g (Centrifuge 5415 D, Eppendorf, Germany), pH of supernatant was neutralized with 10% ammonium hydroxide (Sigma Aldrich, USA). To measure the optical density at 405 nm a Multiskan FC microtiter-plate reader (Thermo Fischer Scientific, USA) was used. Finally, to calculate the absolute Alizarin Red content, all sample values were compared to a standard curve of serial Alizarin Red solutions.

2.1.3.2 Adipogenic differentiation

For adipogenic differentiation cells were plated into 6-well plates. When cell density reached approximately 90-100% confluence, DMEM-high glucose media (Thermo Fischer Scientific, USA) supplemented with 10% FBS, 1 µM dexamethasone, 0,1 mg/ml insulin, 0,2 mM indomethacin, 1 mM 3-isobutyl-1-methylxanthine and (all Sigma-Aldrich, USA) 1% penicillin/streptomycin (Merck, Germany) was added to induce differentiation for five days. For the following two days, cells were maintained in a DMEM-high glucose conservation media composed of 10% FBS, 0,1 mg/ml Insulin and 1% penicillin/streptomycin. Induction and conservation media were consecutively changed for three weeks. Controls were kept in basic

culture media. To quantify adipogenic differentiation lipid vacuole formation was visualized by Bodipy-staining. After 21 days, cells were washed with PBS, fixed for 25 min at RT with 4% PFA (Merck, Germany) and then incubated with Bodipy staining (1:2500, diluted in dH_2O Thermo Fischer Scientific, USA) for 15 min. After washing unbound solution, pictures were taken with AxioObserver Z1 using AxioCam MRm color camera (Zeiss, Germany) (10x magnification). Lipid vacuoles were analyzed and quantified with ImageJ (https://imagej.nih.gov/ij/; USA) and Microsoft Office Excel (Microsoft, USA). A threshold for dark background was adjusted to detect the bright-green colored areas representing lipid vacuoles.

2.1.3.3 Chondrogenic differentiation

Chondrogenesis was induced using pellet culture. The chondrogenic basic medium consisted of DMEM High Glucose (Thermo Fischer Scientific, USA), dexamethasone (10 µM), L-ascorbic-acid 2 Phosphate (0,195 mM), sodium pyruvate (1 mM), 1% ITS+3 (insulin, transferrin and selenite) (all Sigma-Aldrich, USA) and penicillin/streptomycin (100 IU/ml, Merck, Germany). Aliquots of 2 x 10^5 cells were transferred in 96 V-bottom non-treated polypropylene plates (Corning Inc., USA) in respective medium. Negative controls obtained chondrogenic basic media, the correspondent differentiation media was supplemented with TGF-ß1 (20 ng/ml) and BMP-2 (100 ng/ml) (both R&D Systems, USA). The whole plate was centrifuged at 300 g for 5 min (CT 4 22 Centrifuge, Thermo Fischer Scientific, USA) to induce pellet formation. Pellets were cultured in a humidified hypoxic incubator (2% O_2, 5% CO_2; MCO-5M, Sanyo, Japan) at 37 °C for 28 days. Media changes were performed three times a week. After 28 days, pellets were washed once with PBS (Merck, Germany), then fixed with 4% paraformaldehyde for two hours at RT. Next, pellets were rinsed 3x5 min with PBS and incubated in 30% sucrose (Merck, Germany) for 3 hours at RT. Next, pellets were placed in disposable cassettes and enclosed in cryomedia (Tissue-Tek O.C.T compound, Sakura, USA). Gradual sample freezing was achieved by placing the cassettes on a copper plate placed on dry ice. Samples were stored, wrapped in parafilm (Thermo Fischer Scientific, USA), at -20 °C until use. The cryotome Microm HM500O (Thermo Fisher Scientific, USA) was used for cutting cryosections of 7 µm thickness. Slices were collected onto SuperFrost Plus glass slides (Thermo Fischer Scientific, USA) and stored at -20 °C.

2.1.3.4 Safranin-O-staining on pellets

Proteoglycans are together with collagen type II the major components of the ECM in cartilage. Safranin-O is a basic stain, which binds with strong affinity to the acidic proteoglycans. The

content of proteoglycans is proportional to the intensity of the staining. Pellet sections were rehydrated twice with PBS and then incubated with 0.1% Safranin-O- staining solution (Sigma Aldrich, USA) for 5 min. To dispose redundant staining solution, slides were turned on Watman-paper (Roth, Germany). Finally, slides were mounted with Roti-Histokitt® (Roth, Germany). Pictures (5x magnification) were taken with AxioVert 40 CFL using AxioCam 105 color camera (Zeiss, Germany).

2.1.3.5 Immunohistochemistry

Immunolocalization of aggrecan and collagen type II as chondrogenic markers was performed as follow. Slides were let stand 30 min at RT, rehydrated and then endogenous peroxidase were quenched for 20 min in 30% H_2O_2 in absolute methanol. Afterwards sections were washed in PBS and then incubated with 0.2% hyaluronidase in PBS (pH=5; Sigma-Aldrich, USA) for 30 min at 37 °C. For aggrecan staining, specimens were blocked in 1% BSA/PBS (bovine serum albumin; pH=7,4; Roth, Germany) for one hour at RT, followed by incubation with the polyclonal primary antibody (AB1031, Chemicon/Milipore, USA) diluted 1:200 in the blocking solution at 4 °C overnight. For collagen type II staining, sections were blocked in 25% M.O.M.™ Mouse IgG Blocking Reagent (Vector Laboratories, USA) in PBS for one hour and afterwards incubated for 5 min in 12.5% M.O.M.™ Diluent in PBS. The mouse monoclonal primary antibody for collagen type II (II- II6B3-s, DSHB, USA) was diluted 1:10 in protein concentrate, applied on sections and incubated at 4 °C overnight.

Next day, sections were washed in PBS and for the aggrecan-staining, the biotinylated goat anti-rabbit antibody of the Vectastain® Rabbit ABC Kit (Vector Laboratories, USA) was diluted in blocking solution and incubated for one hour. The biotinylated anti-mouse antibody for collagen type II staining was diluted in PBS and incubated for 10 min. Detection of the secondary antibody was achieved with the Avidin-Biotin Complex (ABC) reagent Kit, prepared 30 min before application and applied for 30 min. DAB Staining was prepared by diluting 0,027g DAB (3,3'-Diaminobenzidine; Sigma-Aldrich, USA) in dH_2O and TRIS-HCl (Tris(hydroxymethyl)aminomethane hydrochloride; pH=7,6; Sigma-Aldrich, USA) and adding just before use a solution of 20% H_2O_2 (Roth, Germany). DAB reaction lasted 7 min in dark and was stopped with dH_2O. Nucleic counterstaining was performed with Mayer's Hämalaun (Roth, Germany) and thereafter rinsed in tap water. Finally, sections were dehydrated in 90%, 100%, EtOH, 2x Xylol (3 min each) and mounted with Roti-Histokit® (Roth, Germany). For negative controls, primary antibody incubation was skipped. Pictures (10x) were taken Axioobserver Z1 using AxioCam MRm colour camera (Zeiss, Germany).

2.1.4 MESSENGER RNA ANALYSIS

2.1.4.1 Total RNA Isolation

From cells

For the analysis of RNA expression of differentiation markers during adipogenic and osteogenic differentiation the RNeasy® Mini KIT (Qiagen, Netherlands) was used. RNA was isolated by washing the cells with PBS, adding RLT-Buffer mixed with 1% ß-Mercaptoethanol (Merck, Germany) to lyse cells. Cells were detached using a cell scraper (Sarstedt, Germany). RNA was transferred into QIAshred Spin Columns and centrifuged for 2 min at 10000 rpm to homogenize the lysate (Biofuge pico, Heraeus, Germany). To purify the isolated RNA, 70% ethanol in 1:1 ratio was added to the lysate and afterwards transferred into RNeasy® Mini spin column and centrifuged for 15 sec at 10000 rpm. RW1-Buffer was added to column and again centrifuged for 15 sec/10000 rpm. On-column DNase digestion was performed with 10 µl DNAse (Qiagen, Netherlands) solved in 70 µl RDD-Buffer for 15 min. Another washing with RW1-Buffer and subsequent centrifugation followed. Next RPE-Buffer was added and centrifuged for 2 min/10000 rpm. This step was repeated once and the columns were transferred in new collection tubes to be dried by a further centrifugation for 1 min/10000 rpm. To elute total RNA, RNase free water was added to columns and centrifuged. Finally, to evaluate concentration and purity of the RNA, measurements with a spectrophotometer (NanoDrop, Thermo Fischer Scientific, USA) at A_{260} and A_{280} were performed.

From pellets

To isolate RNA from pellets of chondrogenic differentiation, pellets were washed with PBS and put in QIAzol Lysis Reagent (Qiagen, Netherlands) and stored at -80 °C. In order to disaggregate the ECM-rich pellet structure, samples passed through three freezing and thawing cycles. Pellets were homogenized in ceramic bead tubes (Qiagen, Netherlands) with a homogenisator (Precellys 24, Bertin Technologies SAS, France) using maximum speed for 30 sec. Protein/RNA separation was performed by adding chloroform (Merck, Germany), then tubes were inverted and then centrifuged at 12000 g for 15 min at 4 °C. The upper aqueous layer was harvested and supplied with 70% EtOH in a 1:1 ratio. Samples were then transferred in a RNeasy® Mini spin column and the protocol was followed as described above.

2.1.4.2 cDNA-synthesis

CDNA was synthesized by the Transcriptor First Strand cDNA Synthesis Kit (Roche, Switzerland) according to the manufactures protocol. RNA samples corresponding to 1 µg were

filled up to 11 µl with H_2O, afterwards 2 µl hexamer-random primers (50 ng/µl) were added and samples were incubated for 10 min at 65 °C. Each sample was enriched with a mixture containing a PCR-Buffer, deoxynucleotides (10 mM), 40 U RNase Inhibitor and 15 U of reverse-transcriptase. The prepared mixtures were incubated in a thermocycler (PEQLAB Biotechnologie GmbH, Germany) for 1 hour at 50 °C following the cDNA synthesis program (Table 1).

RNA denaturation mixture		
RNA	1 µg	65 °C for 5’
DEPC-treated H_2O	to 11 µl	
Random hexamer primers	2 µl	

cDNA synthesis mix	
5x-Buffer	4 µl
RNAse inhibitor	0,5 µl
Desoxynucleotide	2 µl
Reverse Transciptase	0,5 µl

Synthesis	
RNA denaturation mix + cDNA synthesis mix	25 °C for 10’ 50 °C for 60’ 85 °C for 5’ 4 °C *forever*

Table 1: Reaction mixes and program for cDNA synthesis

2.1.4.3 Light cycler (LC)-PCR

Quantitative Reverse Transcriptase-PCR (qRT-PCR) was performed using the Taq Man Probes for integrin α10 (*ITGA10*) and α11 (*ITGA11*), collagen type II (*COL2A1*), *PPAR-γ, RUNX-2* and hypoxanthine-guanine phosphoribosyl-transferase (*HPRT)* (all from Integrated DNA Technologies, Inc, USA). cDNA samples, dH_2O, Prime Time Gene Expression Master Mix were pipetted in triplicates in a 96-well plate (Table 2). To collect samples on the bottom of each well a short centrifugation (30 sec) was performed. PCR reaction was carried out in a LightCycler® 96 instrument provided with LightCycler® 96 software (Roche, Germany). The relative gene expression was normalized in relation to the housekeeping gene *HPRT* by the comparative ΔΔCt (crossing point) method. The n-fold change of gene expression levels relative to *HPRT* was performed by comparative $2^{-\Delta\Delta Ct}$ method. Minimum of two independent repetitions were performed.

Taq Man Probes Reaction Recipe	
Prime Time Gene Expression Master Mix	10 µl
cDNA (diluted 1:5 in dH_2O)	5 µl
Primer Mix	1 µl
dH_2O	0,5 µl

Table 2: Taq Man probes LightCycler® reaction setup

Oligonucleotides used for LightCycler®PCR	
HPRT	*P:5'-/56-FAM/CTTGCTGGT/ZEN/GAAAAGGACCTCTCGAA/3IABkFQ/-3'* *f:5'AACAAAGTCTGGCCTGTATCC-3'* *r:5'CCCCAAAATGGTTAAGGTTGC-3'*
Integrin α10	*P:5'-/56-FAM/CATTGTGAA/ZEN/CCAGCCTCAGCAGC/3IABkFQ/-3'* *f:5'TGTCACAGACTTGAACTTGGC-3'* *r:5'CGATGTCAGGTGGTAAGGTG-3'*
Integrin α11	*P:5'-/56-FAM/TGCCCCACA/ZEN/GAGGAATCACAGC/3IABkFQ/-3'* *f:5'CAGGTTGCAGATGATGGAGAC-3'* *r:5'ACAGCACAGAGTACAGGAGTA-3'*
PPAR-γ	*P:5'-/56-FAM/TGCCCCACA/ZEN/GAGGAATCACAGC/3IABkFQ/-3'* *f:5'CAGGTTGCAGATGATGGAGAC-3'* *r:5'ACAGCACAGAGTACAGGAGTA-3'*
RUNX-2	*P:5'/56-FAM/TTAACTGAGA/ZEN/GAGGAAGGCCAGAGGC/3IABkFQ/-3'* *f:5'AGGGATGAAATGCTTGGGAA-3'* *r:5'GATGATGACACTGCCACCTC-3'*

Table 3: Probes and primer pairs used for LightCycler® PCR with Taq Man Probes. P= Probe, f= forward, r= reverse.

2.1.5 PRELIMINARY TESTING OF CELL BEHAVIOUR IN FIBRIN SEALANT

In vitro cell survival in fibrin sealants

To determine survival rate of cells in fibrin hydrogels, live/dead assay was performed. Therefore, cells were double-stained with fluorescein-diacetate (FDA) and propidium iodide (PI), (both from Sigma-Aldrich, USA). FDA is esterized in the cytoplasm of live cells and fluorescent green, whereas PI intercalates in the DNA of dead cells and appears red. The FDA stock solution was prepared by dissolving 10 mg of FDA in 2 ml pure acetone. The working solution, consisted of a 1:500 dilution in PBS of the stock solution (Merck, Germany). For the FDA/PI solution, a 1:1 ratio of FDA stock solution together with the purchased PI solution (1mg/ml in water) was mixed. Cell staining was performed by adding 500 µl of FDA/PI solution

to 1 ml of cell suspension in well culture dishes for 2 min followed by washing with PBS. Live/dead analysis was performed subsequently by fluorescence microscopy with microscope AxioObserver Z1 mounted with Axiocam MRm (5x, Zeiss, Germany). Assay was performed every second day for one week.

Remodeling of fibrin hydrogels

Fibrin gels are well established and widely used bioadhesives in surgeries. They trigger minimal inflammation, are non-toxic and provide excellent biocompatibility. Three different commercially available products were tested, which differ in their formulation: Artiss® and Tisseel® from Baxter (USA) and Beriplast P® from CSL Behring (USA).

	Artiss®	Tisseel®	Beriplast P®
Fibrinogen	67-106 mg/ml	90 mg/ml	67-106 mg/ml
Thrombin (human)	2,5-6,5 units/ml	500 IU	400-625 units/ml

Table 4: Fibrinogen and thrombin formulation of Artiss®, Tisseel® and Beriplast P®.

The different sealants were tested and compared regarding cell survival, chondrogenic differentiation and remodeling. The company's recommendation for the thrombin: fibrinogen ratio was 1:1. For the *in vitro* remodeling of fibrin sealants 25 µl of fibrinogen were dropped into a 96 well (non-culture treated, Corning Inc, USA). Following, another 25 µl of thrombin containing 500.000 human $\alpha10^{high}$ MSCs were added to the fibrinogen. Hydrogels were incubated at 37 °C for five min and subsequently transferred with the aid of a spoon into 24 well dishes, which were coated with agarose (Biozym, Germany) to avoid cell attachment to the plastic dish. Medium was changed every second day. Remodeling was observed every second day for one week with stereoscope (Stemi 2000 CS, Zeiss, Germany).

2.2 *IN VIVO* ANALYSIS

2.2.1.1 Housing and breeding

For the *in vivo* experiments twelve weeks old female C57BL/6j mice of the (Charles River, Germany) were used. Animals were kept at the central animal facility of the LMU downtown hospital under the FELASA-guideline. The trial was approved by the government of Upper Bavaria (animal application: 55.2-1-54-2532-150-13). Animals were kept in individually ventilated cages (IVC Sealsafe, Tecniplast, USA) under SPF l conditions. The autoclavable cages contained HEPA-filters for air supply and were of a size of 365x207x140 mm (LxWxH). A maximum of five animals were put together in one cage. Every twelve hours light was switched on/off to simulate a day/night cycle. Temperature was set at 20-22 °C and humidity

at 45-55%. Each cage is equipped with a small house rendering as shelter as well as material for bedding, gnawing and nesting, which was changed once in a week. Water and food were at free disposal. After shipment, two weeks of acclimatization to accustom to the new environment was 'observed'.

2.2.1.2 Experimental setup

Animals (n=41) were randomly distributed into the following groups described in Table 5. Each animal was operated on its right knee. The sham group obtained a small incision of the skin without opening the knee capsule and was used as control group. After eight weeks of observation, mice were sacrificed by cervical dislocation.

Group	Treatment	Animals + Reserve
A	Artiss® + Integrin $\alpha10^{high}$ MSC	11+1
B	Artiss® + unsorted MSC	11+1
C	Artiss® without cells (empty)	11+1
D	Sham	5
Total number of animals		**41 (38+ 3 Reserve)**

Table 5: Experimental groups

2.2.1.3 *In vivo* osteoarthritis induction

To induce OA in mice knee joints the well-known destabilization of the medial meniscus (DMM)- model described by *Glasson et al* was performed[188]. In this procedure the medial meniscus (MM) is destabilized by dissection of the medial meniscotibial ligament (MMTL). This ligament connects the meniscus and the medial joint surface of the tibia. By dissection of the MMTL the medial meniscus is no more anchored and moves further lateral. The medial meniscus usually provides a larger region to transfer loads from femur to tibia. Further, the softening effect of the menisci disappears, which results in a shifted biomechanical axis. Especially the posterior femur as well as central parts of the tibia are affected. The consequent joint instability, set the stage for the development of human-like posttraumatic OA.

2.2.1.4 Operation protocol

Pre-operative protocol

Preoperative, mice were weighted and their state of health was evaluated. Next, animals were narcotized *via* intraperitoneal application of a mixture of Fentanyl (0,05 mg/kg KG, Fentanyl-Janssen, Janssen-Cilag, Germany), Midazolam (5 mg/kg KG, Dormicum, ratiopharm) and

Medetomidin (0,5 mg/kg KG, Antisedan, Orion, Finland). Following the right leg of the animals was shaved and disinfected with Cutasept F (Paul Hartmann AG, Germany). For the whole time of operation mice were laying on a heating plate at 37 °C to keep animal body temperature constant. To avoid eyes desiccation, Bepanthen® balm (Bayer Vital, Germany) was applied. As prophylaxis, clindamycin antibiotic (45 mg/KG, Clindaseptim® Vetiquol, Austria) was given before the right leg was covered with sterile sheets.

Destabilization of the medial meniscus

A second disinfection of the operation area was performed before the incision of the skin medial to the ligamentum patellae. The knee capsule was opened with a microsurgical scissor (Mikro-Iris, Aesculap, Germany). Adrenalin (1:1000; InfectoPharm, Germany) was applied in-situ if needed, to reduce bleeding and enable clear sight of the joint. The fat tissue located on top of the medial meniscus was carefully dissected with the help of a fine tweezer (Aesculap, Germany) without affecting the meniscus. The patella was dislocated laterally for a clear sight of the operation area. After displaying and identifying the intercondylar region and the medial meniscotibial ligament (MMTL), this was cut through with a micro scalpel, leading to the aimed destabilization of the medial meniscus. Subsequently, and depending on the different groups, the intra-articular injection took place. Therefore, fibrinogen and thrombin were mixed in a 1:1 ratio and injected with a 1-2 µl pipette. Group A-C received 3µl of fibrin glue (Artiss®, USA) into the right knee. In group A and B, the thrombin component was previously supplemented with 50000 cells of $\alpha 10^{high}$ MSCs and unsorted MSCs, respectively. To close the knee capsule, a continuous and absorbable suture (7-0, Vicryl, Ethicon, Germany) was used. The patella was relocated and followed by the skin suture, which was performed with individual sutures (5-0, Prolene, Ethicon, Germany).

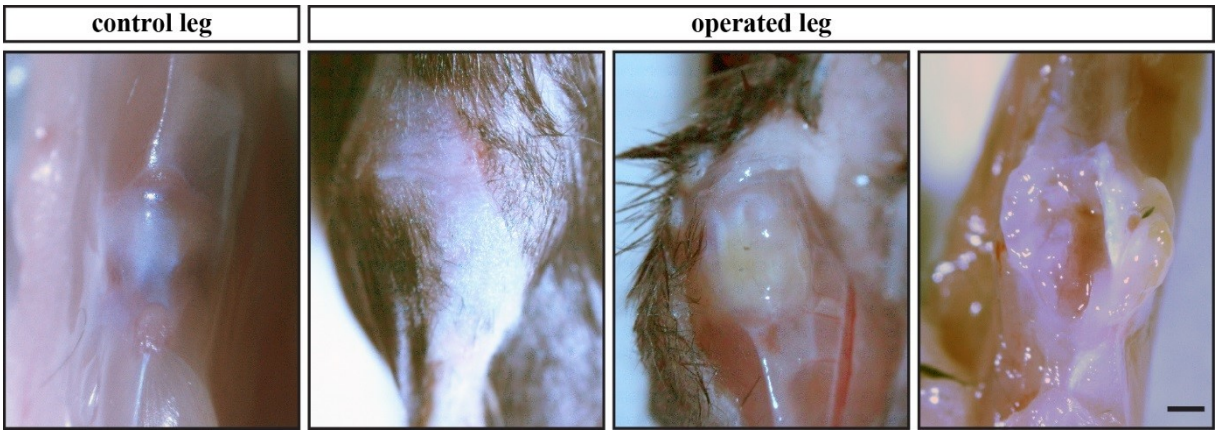

Figure 12: Controls of operated right knees. Success of operation was examined one-week post-operation. Wound healed with no superficial or profound infections. Scale bar: 1 mm.

Because of the expected post-operative pain, Buprenophin (0,1 mg/kg KG, Buprenophin animal, Bayer Vital, Germany) was applied intraperitoneally. To neutralize narcosis, 0,2 ml salin solution mixed with Naloxon (1,2 mg/kg KG, Narcanti®, Bristol-Meyer, Germany), Flumazenil (0,5 mg/kg KG, Anexate®, Roche, Germany) and Atipamezol (2,5 mg/kg KG, Antisedan®, Zoetis, USA) was injected intraperitoneal. Afterwards animals were transferred in a cage warmed *via* infrared light and observed until awakening and then transferred in the IR cages.

Post-operative follow-up

Animals were checked daily for changes in movement or behavior. Analgesia was performed until the third postoperative day with intraperitoneal injections of Buprenophin (0,1 mg/kg KG, Buprenophin animal, Bayer Vital, Germany). A score-sheet was filled daily for the first three days and then every third day (see 7.5 Appendix – Scoring sheet).

Animal sacrifice

Eight weeks postoperative, animals were sacrificed *via* cervical dislocation. Previously, blood serum was harvested.

2.2.1.5 Testing short-term faith of cells *in vivo*

In order to test cell survival embedded in fibrin gel *in vivo*, a pre-operative test with two mice was performed. For this purpose, before application, cells were labeled with CFDA-SE (carboxyfluorescein diacetate-succinimidyl ester) (Sigma Aldrich), a dye, which is esterized by live cells generating green fluorescence. Briefly, cells were incubated with 15 µM CFDA-SE for 15 min at RT, and afterwards embedded in the fibrin gel as previously described. Post operation, inspection of live cells after one day and one week was performed. A control leg, which received no cell application, was used as negative control. Fluorescence pictures were taken with Axio Observer Z1 mounted with Axiocam MRm, Zeiss, Germany.

2.2.1.6 Histology

Fixation and decalcification

Knee joints of euthanized mice were deskinned, dissected and briefly rinsed in PBS. Samples were fixed overnight at 4 °C in pre-cooled 4% paraformaldehyde (PFA, Merck, Germany) or Saint Marie (SM, 95% EtOH, 1% acetic acid, 4% H_2O) fixative solutions under constant shaking. Next day, PFA samples were washed in PBS (3x15min), whereas SM-fixed samples underwent a descending ethanol row to rehydrate: for each step 2 hours at 4 °C in 90%, 80%

and 70% ethanol/dH_2O and afterwards overnight in 50% ethanol/PBS at 4 °C. Finally, SM-fixed samples were washed with PBS 3x15 min.

To smoothen bones, samples were incubated for approximately four weeks in decalcification solution composed of 10% EDTA/PBS (Roth, Germany) pH of 8,0. Solution was renewed two times per week.

Paraffin embedding

Decalcified samples were washed in PBS 3x15 min and afterwards passed through an ascending row of ethanol (50%, 70%, 80%, 90%, 2x100%), 2x Xylol and 2x paraffin (Roth, Germany), each step lasting 2 hours. To embed samples in fresh paraffin the next day, the embedding station HistoCore, Arcadia C (Leica, Germany) was used.

Sectioning

For sectioning a microtome Hyrax M55 (Zeiss, Germany) was used. Sagittal slices of 6 µm were cut and collected on SuperFrost Plus™ glass slides (Thermo Fischer Scientific, USA). Before storing at room temperature, slides were incubated at 37 °C overnight.

2.2.1.7 Safranin-O/Fast-green staining

Safranin-O/Fast-green staining was performed to analyze Proteoglycan loss in cartilage. After deparaffinization samples were rehydrated through a stepwise row of 2x Xylol, 2x100%, 90%, 80%, 70%, 50% EtOH and dH_2O, each step lasting 4 min to rehydrate samples. A 0,5% Mayer's Haemalaun staining solution (Roth, Germany) was used for 2 min and followed by washing with tap water at least three times. After dipping in 1% acetic alcohol (Merck, Germany), slides were incubated in a 0,02% Fast-green solution (Sigma-Aldrich, USA) for 1 min. Next, slides were immersed in 1% acetic acid for 30 sec and then a 1% Safranin-O solution (Sigma-Aldrich, USA) was applied for 30 min. For dehydration slides passed through 4x 95% ethanol, followed by 2x 100% ethanol and 2x Xylol, each step for 3 min. Finally, slides were mounted with Roti® Histokitt (Roth, Germany).

2.2.1.8 Toluidine-blue staining

As an acidophilic staining, Toluidine-blue stains negatively charged molecules such as extracellular proteoglycans, which afterwards display metachromatic and purple color. Therefore, it allows an evaluation of proteoglycans loss in the AC of the osteoarthritic knee joints. For Toluidine-blue staining slides were deparaffinized and dehydrated as described above in Safranin-O/Fast-green staining. Next, a 0,1% Toluidine-blue solution (Sigma-Aldrich,

USA) was applied for 7,5 min. To dispose redundant staining solution, slides were turned on Whatman-paper (Roth, Germany). Next 2% potassium ferrocyanide $K_4[Fe(CN)_6]$ (Sigma-Aldrich, USA) as counter-staining was used to incubate slides for 3 min and afterwards slides were cleaned with Whatman-paper. Lastly, slides were mounted with Roti® Histokitt (Roth, Germany).

2.2.1.9 Immunohistochemistry on knee sections

Immunohistochemistry was performed for aggrecan and collagen type II. The protocol was followed as described in 2.1.3.5.

2.2.1.10 Pathological scoring of articular cartilage

For the evaluation of joint pathology, cartilage degradation and proteoglycan loss were considered. Pictures of toluidine blue and Safranin-O/Fast-green sagittal sections were serially stained and blindly scored from three independent observers. A modified scoring system according to *Little et al.* was used to score structural damages as described in Table 6[194]. Cartilage surface of tibia and femur were separately surveyed and a cumulative score of tibia and femur was calculated. In this way, score values for structural damage can be between 0 and 14. For proteoglycan loss, a modified scoring system from *Nicolae et al.* based on toluidine blue staining was implemented as described in Table 6[48].

Structural damage *(according to Little et al.*[194]*)*	
0	normal cartilage
1	roughened surface, small fibrillations
2	fibrillation to superficial layer / loss of superficial lamina
3	horizontal cracks/clefts to calcified cartilage
4	mild loss of non-calcified (n.c.) cartilage (<10% surface area)
5	moderate loss of n.c. cartilage (10% - 50% surface area)
6	mild loss of n.c. cartilage (>50% surface area)
7	erosion of cartilage to subchondral bone
Proteoglycan loss based on Toluidine Blue staining *(according to Nicolae et al.*[48]*)*	
0	normal staining
1	reduced staining
2	focal patchy loss of staining
3	no staining

Table 6: Histopathological scoring system for structural damage and proteoglycan loss.

2.2.2 DETECTION OF GRAFTED CELLS ON KNEE SECTIONS

2.2.2.1 DNA extraction

To extract DNA from paraffin-embedded tissue sections the TaKaRa DexpatTM Easy Kit (TAKARA BIO INC., Japan) was used. The kit enables the isolation of PCR-ready genomic DNA (gDNA) from mammalian formalin-fixed/paraffin-embedded tissues. Briefly, the pre-heated (100 °C, 1 min, Thermomixer comfort, Eppendorf, Germany) TaKaRa Dexpat^{TM} Easy solution was pipetted directly on tissue section and then scraped away with a scalpel (Carbon steel safety scalpel #15, B. Braun, Germany). All the solution/tissue mix was pipetted and transferred into microtubes and incubated at 100 °C for 10 min, while tubes were gently inverted three times. To divide the paraffin layer from DNA, tubes were centrifuged (13000 rpm, 10 min, 4 °C, Centrifuge 5415 D, Eppendorf, Germany) and cooled down on ice afterwards. The aqueous layer, in between the paraffin and the gel-like layer containing the gDNA and was collected with a pipette and stored at 4 °C until used.

2.2.2.2 DNA purification by ethanol precipitation

The gDNA was purified by ethanol precipitation as described in the manufacture's manual of TaKaRa Dexpat^{TM} Easy Kit. Genomic DNA was mixed in a 1/10 volume ratio with 3M sodium acetate (Sigma-Aldrich, USA). Further 2,5-fold of volume of ethanol was added. Solution was mixed by inversion and then rest at -20 °C for 60 min. Next, samples were centrifuged (12000 g; 15 min; 4 °C) and supernatant removed. Another centrifugation (12000 g; 15 min; 4 °C) was performed after adding 70% EtOH. After supernatant was discarded and samples air-dried, gDNA was solved in TE buffer (Qiagen, Netherlands). The collected DNA was stored at 4 °C until used.

2.2.3 PCR ON GENOMIC DNA

The semi quantitative RT-PCR was performed for the housekeeping gene *glycerolaldehyde-3-phosphate dehydrogenase* (GAPDH) as input control and for the human *Charcot-Marie-tooth-Disease gene* (*hCMT1A*), as human-only expressed gene[195]. Therefore, a master mix containing PCR buffer, H_2O, 0.2 mM dNTPs, 1.5 mM $MgCl_2$, 0.25 pmol gene-specific primers and 1 U Taq DNA polymerase (Roche, Switzerland) and the extracted DNA was transferred in PEQSTAR 2X (PEQLAB Biotechnologie GmbH, Germany).

PCR reaction mix		PCR program
10 x buffer with $MgCl_2$	2 µl	95 °C for 10´
dNTPs	0,4 µl	
Primer forward	0,1 µl	95 °C for 30´´ *Annealing T°C for* 30´´ 72 °C for 1´ — *X cycles*
Primer reverse	0,1 µl	
Taq polymerase	0,25 µl	
H_2O	16,15 µl	72 °C for 10´
Extracted DNA	1,0 µl	4 °C *forever*

Table 7: PCR reaction mix and program. For each gene, annealing temperature and cycle number are different (see Table 8).

The amplified PCR products were pipetted on 2% agarose gels (Biozym, Germany) to be visualized afterwards by ethidium bromide (Merck, Germany) staining. PCR product size was referred to a 100bp molecular weight standard (New England Biolabs, USA). The gel imaging system (Vilber Lourmat, Germany) was used to take pictures of PCR product bands.

Target gene	Primer	Annealing temp.	Cycle nr.	Product size	Reference
Housekeeping gene					
GAPDH	*F 5'-caactacatggtttacatgttc-3'* *R5'-gccagtggactccacgac-3'*	50 °C	30	181 bp	(*Böcker et al.*)[196]
Human genes					
hCMT1A	*F 5'-gaaattcatttaaaagcattttaac-3'* *R 5'gctaatagtcatgtttaaaatcatttt-3'*	51,5 °C	41	345 bp	(*Cheng et al.*)[195]
SRY	*F 5'agtttcgcattctgggattctct-3'* *R 5'gcgacccatgaacgcatt-3'*	60 °C	25	100 bp	(*Cheng et al.*)[195]

Table 8: Nucleotide sequences and related information of the PCR primers

2.2.4 ENZYME-LINKED IMMUNOSORBENT ASSAY (ELISA)

During the development of OA proteolytic enzymes such as MMPs or ADAMTS degrade the cartilage tissue generating neo-epitopes of ECM molecules. The c-telopeptides of collagen type II (CTX-II) is the most characterized degradation epitope originating during the course of OA. To quantify the amount of CTX-II in mice serum, the CTX-II ELISA-Kit from MyBioSource,

(#MBS706197, Canada) was utilized. A microplate is pre-coated with antibody specific against CTX-II. The bond antibodies bind any CTX-II that is present in the added samples. When the biotin-conjugated detection AB is pipetted in wells, it binds to CTX-II as well. Finally, avidin conjugated horseradish peroxidase (HRP) is added and together with the substrate solution catalyze a color reaction. The amount of CTX-II present in the sample is proportional to the developing color. After stopping color reaction, intensity is measured. According to manufacturer's manual samples and standards were assayed in duplicates. As recommended, samples were diluted with sample diluent of the prescribed Kit in a ratio of 1:100. First, 100 µl of diluted samples and standards were pipetted into provided wells, whereas negative controls were loaded with 100 µl of PBS. Next, samples were covered and placed in an incubator (Memmert, Germany) for 2 hours at 37 °C. Afterwards, the remaining liquid was removed without washing and 100 µl of biotin-antibody was added to each well. The microplate was covered and samples were incubated for 1 hour at 37 °C. Next, samples were washed three times with the provided washing buffer to remove all liquid. HRP-avidin complex was added to each well and incubated for 1 hours at 37 °C. As described above, washing was repeated for five times and TMB substrate was added for 30 min in the dark. After the reaction was stopped with stop solution, the optical density was measured with the Multiskan FC microtiter-plate reader (Thermo Fischer Scientific, USA) at 450 nm. Concentrations were calculated against a standard curve built with known concentrations of CTX-II given in the kit.

2.2.5 COMPUTER PROGRAMS

To evaluate quantitative data and create graphs, Microsoft Office Excel 2016 (Microsoft, USA) and GraphPad Prism 8 software (GraphPad Software, USA) were used. Photomicrographs were processed with AxioVision LE software (Carl Zeiss, Germany) and adapted in figures with Adobe Photoshop CS6 and Illustrator CS6 (Adobe System, USA). With ImageJ 1.52g (https://imagej.nih.gov/ij/, USA) morphometric analyses were handled. Reference management was performed with Mendeley 1.19.2 (Mendeley Ltd, USA).

2.2.5.1 STATISTICS

Statistical significance was tested by using the unpaired Student's t-test and the *p*-value of 0.05 was defined to be statistically significant. Quantitative data was presented with GraphPad Prism 8 software (GraphPad Software, USA). Three to two independent experiments in triplicates were performed. Mean values and standard deviations are shown.

3 RESULTS

3.1 *IN VITRO* ANALYSIS

3.1.1 MORPHOLOGICAL CHARACTERIZATION OF CULTURED MSCS

The morphology of human BM-MSCs in monolayer culture was observed by phase-contrast microscopy. Integrin α10^{high} MSCs (passage four) and unsorted MSCs (passage three) showed the typical spindle-like shapes and no obvious differences in shape or size were observed between them (Figure 13).

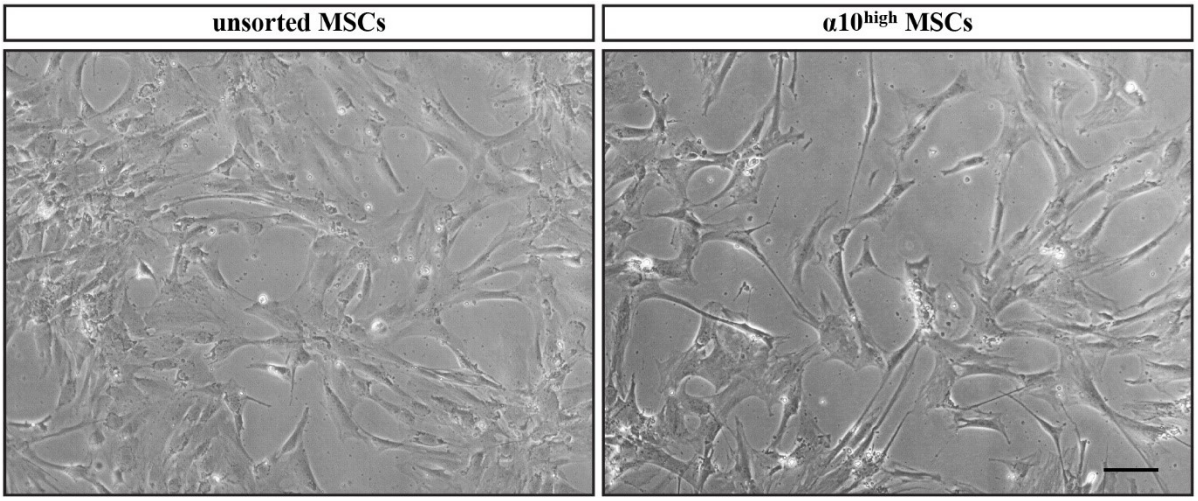

Figure 13: Phase-contrast microscopy of monolayer cells cultivated on plastic dish. Cells showed typical fibroblastic morphology without differences between the two groups. Scale bar 100 µm.

3.1.2 TRILINEAGE DIFFERENTIATION OF MSCS

To assess the multipotency of the α10 selected MSCs, a trilineage differentiation towards the osteogenic, adipogenic and chondrogenic lineages was performed.

3.1.2.1 Osteogenic differentiation

Cells were stimulated for 21 days and analyzed for mineral deposition with Alizarin Red (AR) staining (Figure 14-A). In stimulated groups, mineral deposits in the ECM were detected indicating a successful osteogenic induction, whereas in control groups no spontaneous mineral deposition was found (Figure 14-B). The quantitative analysis of the mineral deposition did not revealed differences between the unsorted and α10^{high} MSCs group. Despite these results, mRNA analysis of the cultured cells at the end of the differentiation period revealed an approximately 3-fold higher expression of the osteogenic transcription factor *RUNX-2* in the unsorted group compared to α10^{high} MSCs group (Figure 14-C).

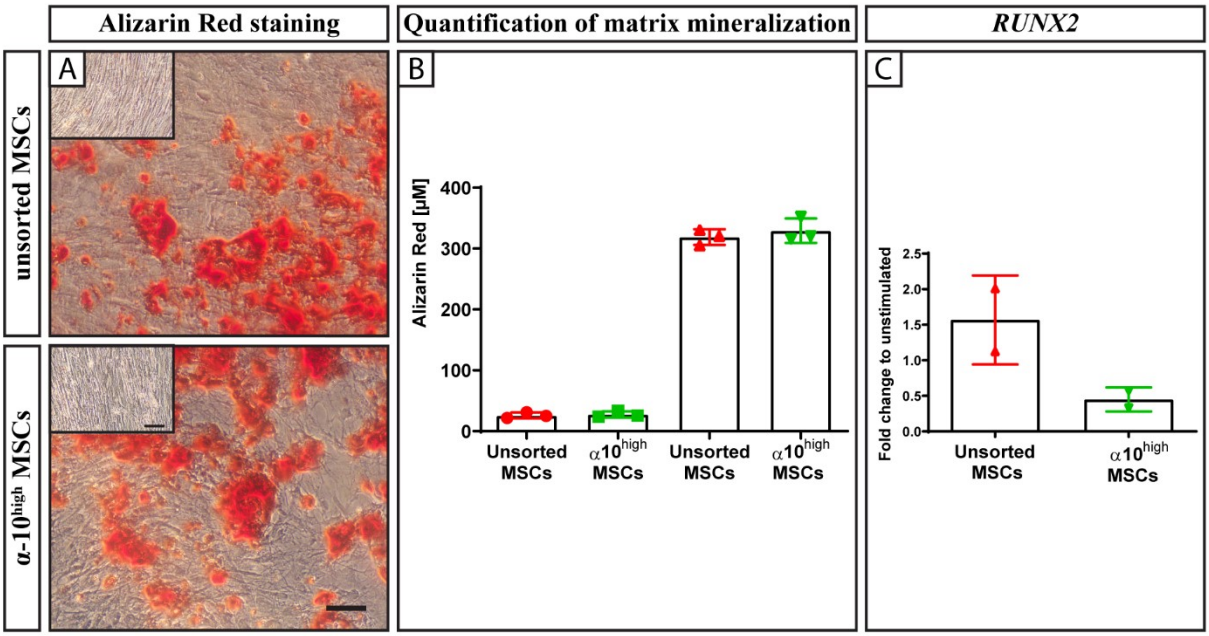

Figure 14: Mineral deposition and quantification by Alizarin Red staining and *RUNX-2* mRNA expression of α10^{high} and unsorted MSCs after 21 days of osteogenic differentiation. (A) Representative AR staining indicating mineral deposition in red. Control wells grown with normal growth medium (small boxes) do not display AR staining. (B) Quantification of Alizarin Red concentration from one representative experiment. Media with standard deviation of the three replicates are shown. (C) *RUNX-2* mRNA expression analysis. Fold changes to the non-stimulated groups were calculated relative to the expression of the house keeping gene *HPRT*. A representative result from two independent experiments is shown. Scale bar 100 µm.

3.1.2.2 Adipogenic differentiation

To demonstrate the potential for adipogenic differentiation of α10^{high} and unselected MSCs, the lipid vacuole formation in response to adipogenic stimulation was analyzed. Lipid vacuoles were seen in the stimulated groups, but not in negative controls, indicating the success of adipogenic stimulation (Figure 15). When comparing the area covered by lipid vacuoles, no difference between the two cell groups could be seen. However, at day 21, the mRNA expression level of the adipogenic transcription factor *PPAR-γ* (*PPARG*), relative to the non-stimulated groups, was slightly higher (1-fold) in the unsorted MSCs compared to the α10^{high} group.

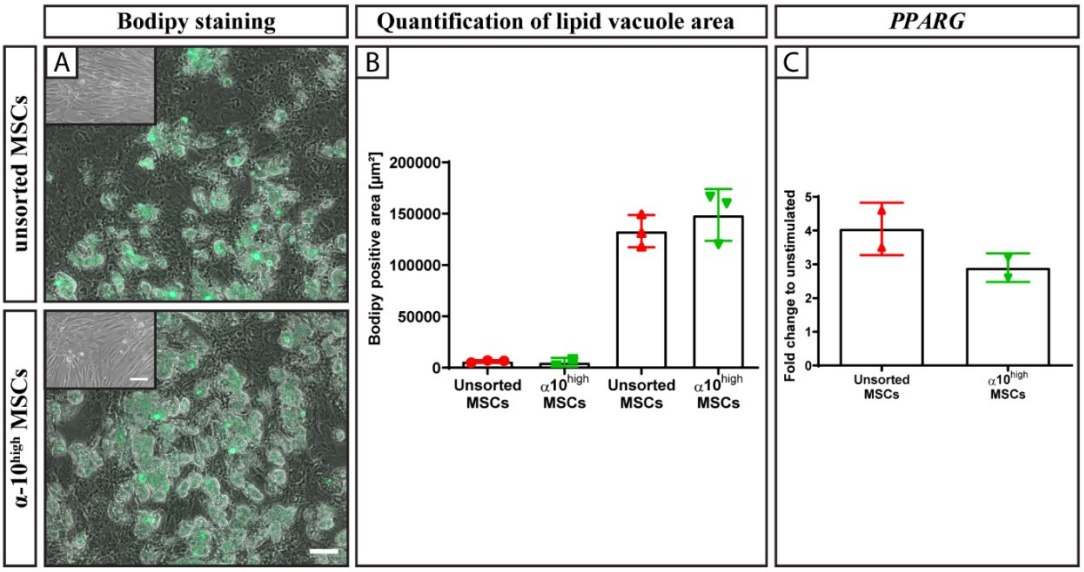

Figure 15: Bodipy staining of lipid vacuoles, quantification of differentiation and *PPAR-γ (PPARG)* expression analysis of α10^{high} and unsorted MSCs after 21 days of adipogenic differentiation. (A) Bodipy (light green) stained lipid vacuoles were detected in stimulated MSCs but not in unstimulated controls (small boxes). (B) Quantitative analysis of the area (µm²) covered by lipid vacuoles. (C) *PPARG* mRNA expression analysis by qRT-PCR. Shown is one representative out of two independent experiments with mean and standard deviation of three replicates. Scale bar 100 µm.

3.1.2.3 Chondrogenic differentiation of MSCs

Of particular importance for this study was to confirm that the elevated expression of integrin α10 in MSCs leads to higher chondrogenic potential. MSCs were chondrogenic differentiated in 3-dimensional pellets for 28 days. Quantification of the pellet size, which reflects the deposition of extracellular matrix, revealed no significant differences between sorted and unsorted MSCs (Figure 16).

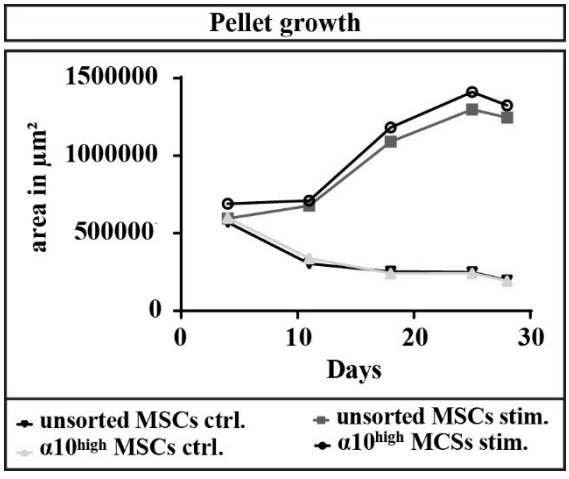

Figure 16: Analysis of pellet size during chondrogenic differentiation. Average pellet area (µm²) of each group was measured weekly. A representative result out of two independent experiments is shown.

Deposition of PGs, reflecting the synthesis of a typical chondrogenic matrix, was assessed by Safranin-O staining on pellet sections. As shown in Figure 17, the homogenous and intense staining observed in the α10^{high} MSCs pellet was not reproducible in its unsorted pellet counterpart. Importantly, α10^{high} pellets exhibited stronger and more even Safranin-O staining than the unsorted pellets (Figure 17).

Furthermore, an immunolocalization of aggrecan and collagen type II, the two major structural components of mature cartilage tissue was performed. As expected, aggrecan staining followed the Safranin O pattern. The chondrogenic marker collagen type II also showed a more uniform and strong staining in the α10^{high} MSCs compared to the pale and peripheral restricted staining in the unsorted group. Furthermore, a weak signal of the hypertrophic marker collagen type X in the pellets of the unsorted group was observed, whereas no positive staining was detected in the α10^{high} cells pellets, indicating that these pellets did not undergo hypertrophic differentiation.

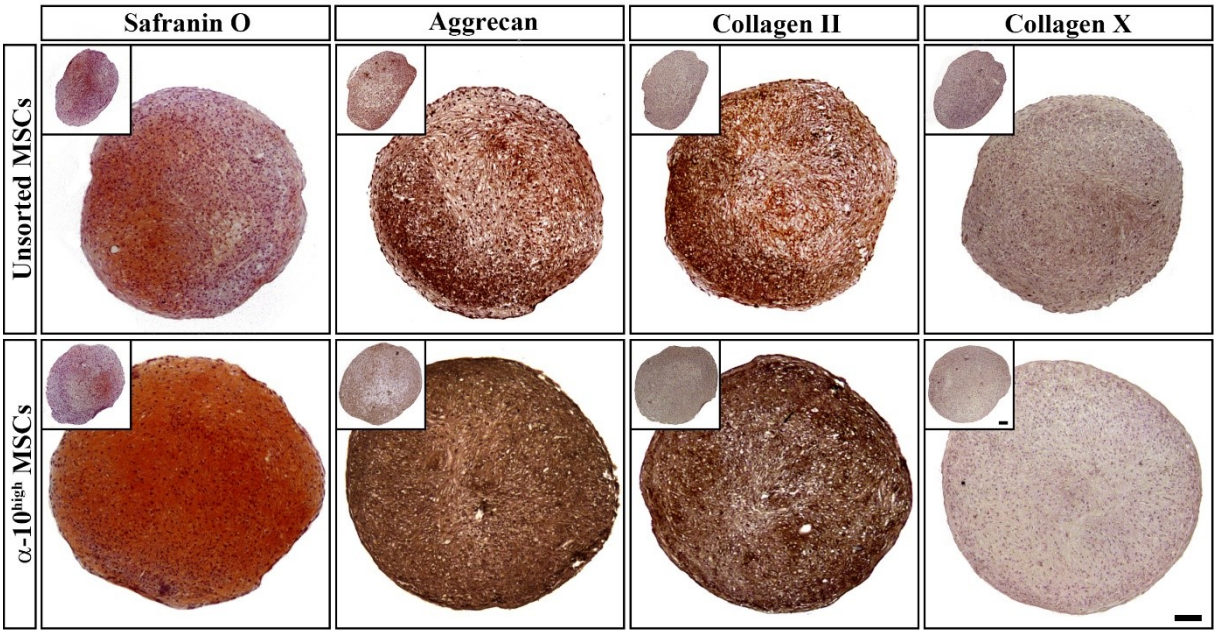

Figure 17: Histological and immunohistochemical analysis of chondrogenic differentiation pellets after 28 days of stimulation. Representative micrographs illustrate 7 µm pellet sections of α10^{high} MSCs compared to unsorted MSCs stained for Safranin-O, aggrecan, collagen type II and collagen type X. Box inserts, show same staining's for the correspondent non-stimulated pellets. Scale bars: 100µm.

The histological and immunohistochemical findings were further supported by the expression levels of integrin α10 and α11 mRNAs. Analysis *via* quantitative PCR of the transcripts at day 28 revealed high expression of the chondrocyte-related integrin α10 and low expression of the fibroblastic-related integrin α11, in the pellets formed by the α10^{high} MSCs. The unsorted

counterpart showed the opposite expression tendency, revealing their unmatured chondrogenic phenotype.

Altogether, these results indicate the higher chondrogenic potential of the integrin α10 expressing MSCs.

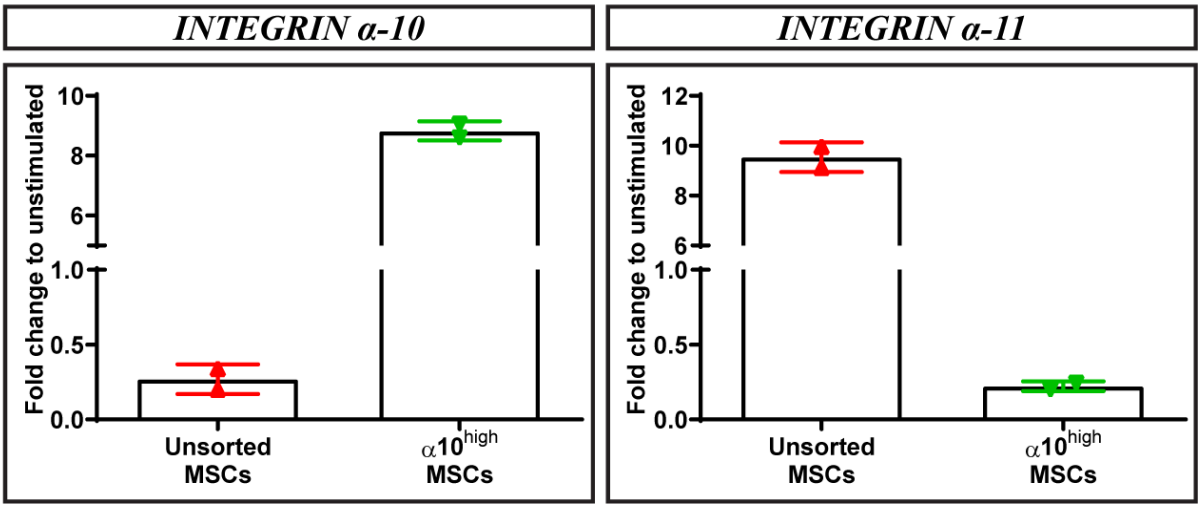

Figure 18: Expression levels of integrin α10 and α11 mRNAs in chondrogenic pellets of α10^{high} and unsorted MSCs compared to non-stimulated MSCs. The α10^{high} group displayed a high expression level of integrin α10 together with a downregulation of integrin α11. Shown is one representative out of two independent experiments.

3.2 *IN VIVO* ANALYSIS

3.2.1 PRE-OPERATIVE TESTING

3.2.1.1 Remodeling of fibrin hydrogels

In this study, a clinically approved bi-component fibrin hydrogel was used as a vehicle for the delivery of MSCs into the knee cavity of mice. Three different formulations from two manufacturers were tested, namely: Artiss® and Tisseel® from Baxter and Beriplast P® from CSL Behring. The ease of handling, cell survival, remodeling as well as chondrogenic differentiation in hydrogel were investigated.

The three tested hydrogels have different formulations but work according to the same principle: soluble fibrinogen is converted into polymerized fibrin by the addition of thrombin. Tisseel® and Beriplast P®, two fast gelling hydrogels, were difficult to handle. Polymerization started immediately when the fibrin and thrombin solutions came into contact, which posed a challenge to homogenous cells distribution. In contrast, the Artiss® hydrogel is a slow-gelling hydrogel in which resuspension could be accurately performed due to a slow and gradual polymerization.

Next, hydrogel remodeling was examined by visualizing the shape and volume shrinking after eight days incubation with human BM-MSCs. Artiss® showed a faster remodeling rate than Tisseel® and Beriplast P® hydrogels (Figure 19 and quantification in Figure 20).

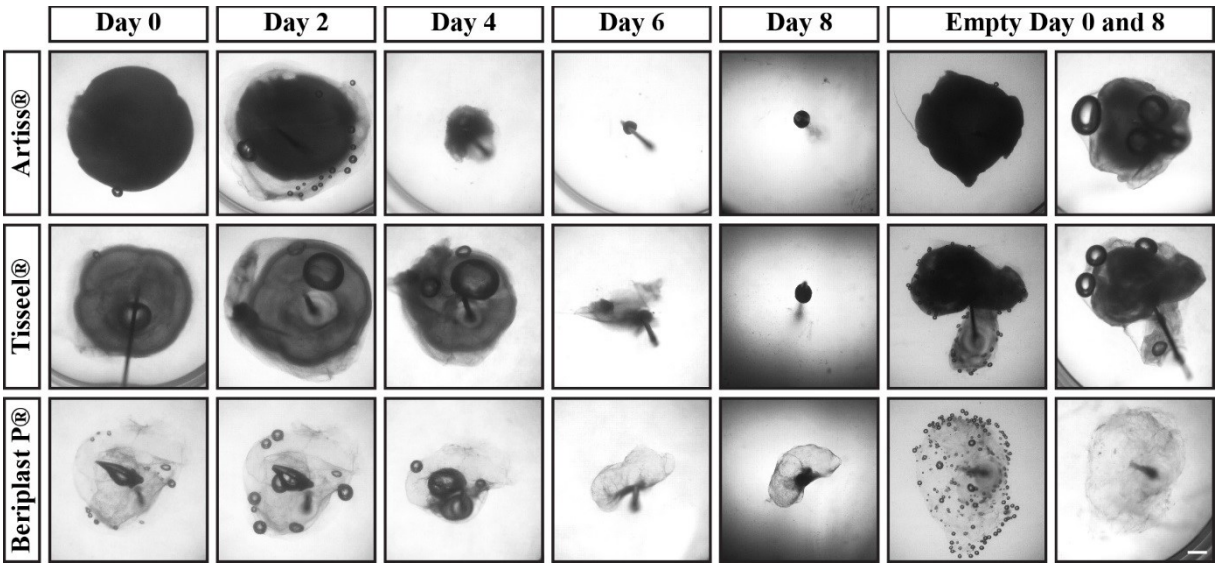

Figure 19: Remodeling capacity of the three tested fibrin hydrogels over one week. The gross appearance of the three hydrogels demonstrated shrinkage in volume and area. Empty hydrogels (without cells) served as negative controls. Scale bar 1mm.

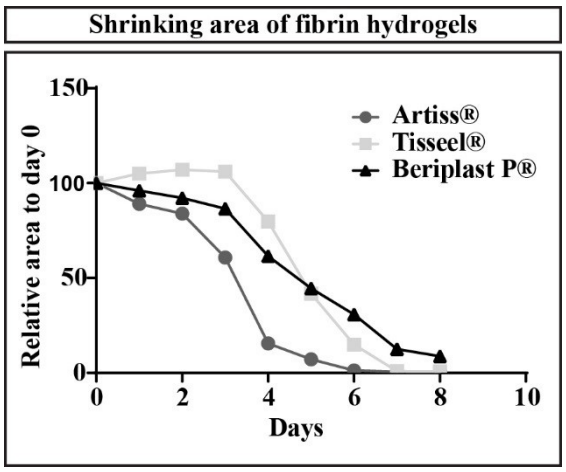

Figure 20: Shrinking area during remodeling of fibrin hydrogels over eight days. Shown is the percentage of loss area from day 0 to day 8.

3.2.1.2 *In vitro* cell survival in fibrin hydrogels

Cell survival in the three different fibrin hydrogels was analyzed with the aid of a live/dead assay for one week (Figure 21). Dead cells stained with propidium iodide (PI) can be seen as red stained areas, whereas alive cells stained with fluoroacetate (FDA) appear in green color. From day one to day five, the area of cells stained with red, in example dead cells, increased,

but there was no remarkable difference between the three groups. On day eight, more dead cells can be observed in the Tisseel® hydrogel compared to Artiss® and Beriplast P®.

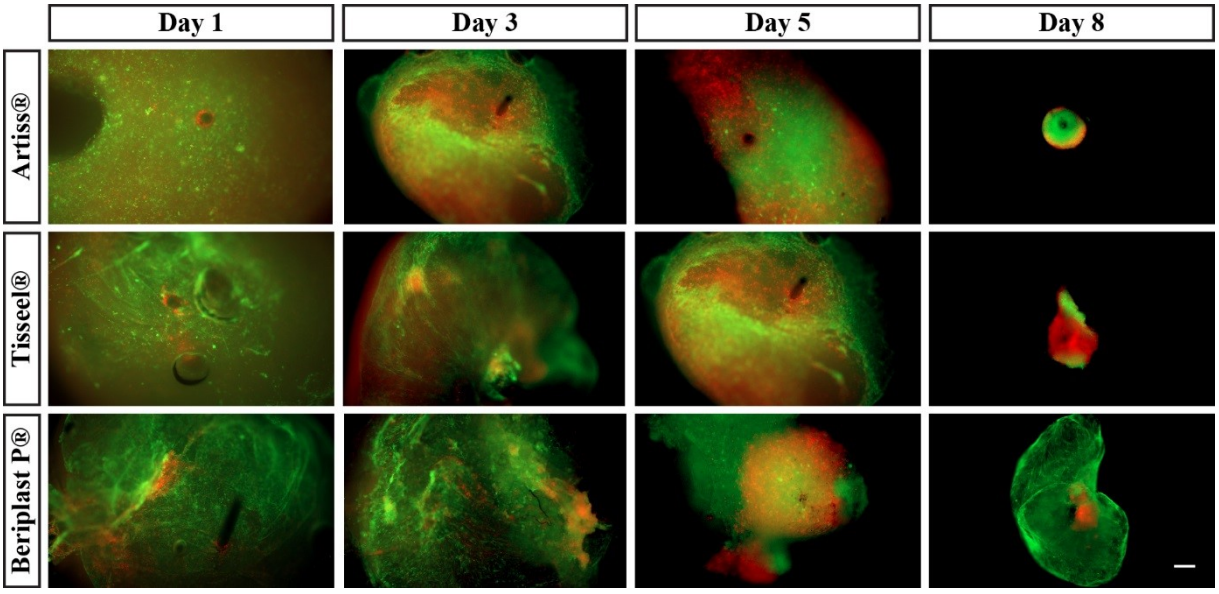

Figure 21: Live/Dead assay of human BM-MSCs in fibrin sealants. In all three fibrin sealants, no obvious difference of alive (green) and dead (red) cells were detected. Scale bar 200µm.

3.2.2 OPERATION AND POST-OPERATIVE FOLLOW-UP

For the *in vivo* study, destabilization of the medial meniscus (DMM) model was applied to induce osteoarthritis in 39 *C57bl6/j* mice. No infections or animal death were observed post operatively. The animals recovered well from operation and were unrestricted in their mobility. On the day of dissection, the legs of mice were inspected macroscopically and showed well-healed scars in all groups. After skin removal, almost no differences were observed between the operated and non-operated knees, reflecting the good performance of the surgical procedure (Figure 22).

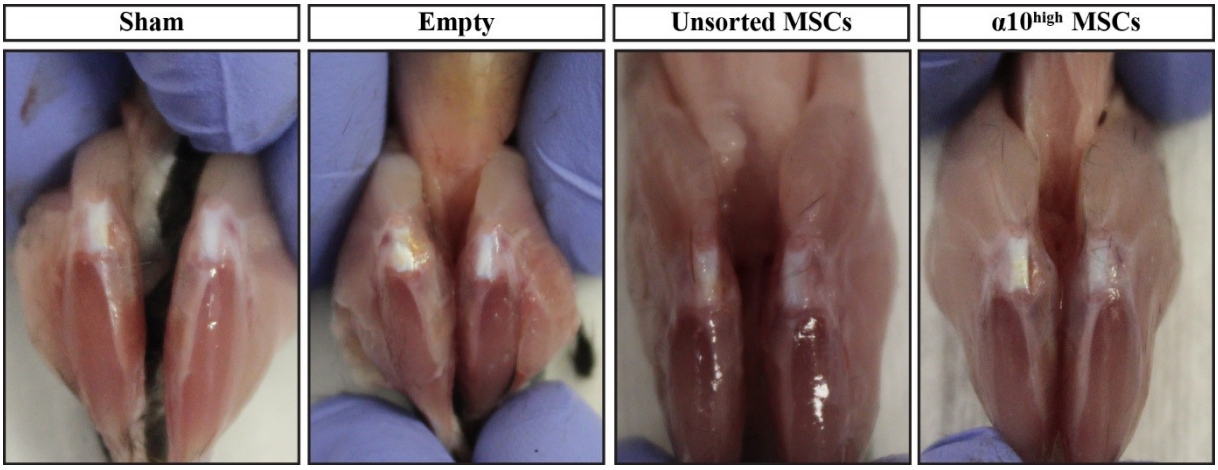

Figure 22: Gross appearance of the legs of mice on the day of dissection. Representative examples of the four groups. The operated right knee showed good wound healing and almost no differences in the joint capsule appearance compared to the non-operated left knee.

3.2.3 DETECTION OF GRAFTED CELLS IN THE DISSECTED KNEES

In vivo survival analyses of MSCs in Artiss® hydrogel were performed one day and one week post operation. For the detection of grafted cells, MSCs were fluorescently labeled with CFDA-SE. On the first post-operative day, the knee capsule of one mouse was opened to detect grafted cells. CFDA-SE staining showed that the injected cells were retained inside the knee capsule and were resistant to the mechanical stress induced by the needle injection (Figure 23). One week after surgery, cells were still detectable but in a lower number compared to day one post-operation. However, it remains to be clarified whether cells migrate out of the knee capsule or simply die. Due to the cell application technique, a small number of cells were detected at the top of the closed capsule. In the non-operated legs, transplanted cells were not detected.

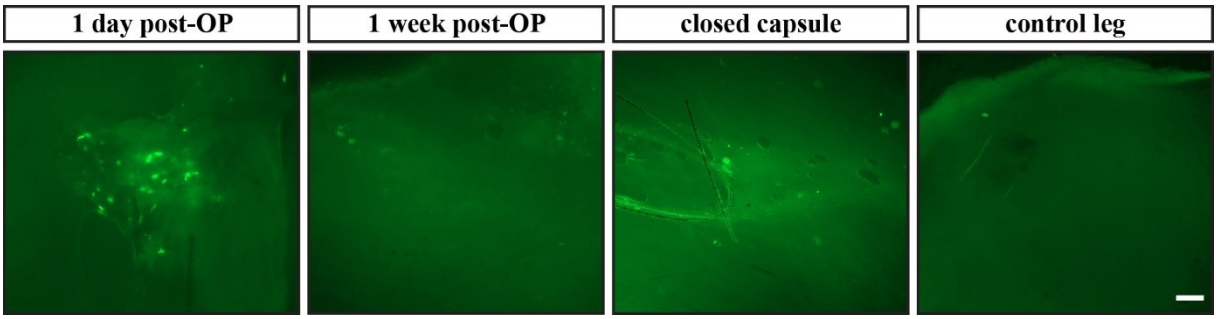

Figure 23: Detection of transplanted cells with Artiss® hydrogel in the mouse knee with CFDA-SE staining one day and one-week post operation. The labelled cells are visible in bright green color at both time-points in the operated, closed capsule, but not in the control.

3.2.4 HISTOPATHOLOGICAL ANALYSIS

3.2.4.1 Structural damage

In order to evaluate the extent of cartilage degeneration upon destabilization of the medial meniscus, a modified scoring system from *Little et al.* was implemented[194]. The cumulative maximal score for tibial and femoral articular cartilage is shown in the graph in Figure 25. Safranin-O (Figure 24) and Toluidine-Blue (Figure 26) staining were performed to detect cartilage damage and proteoglycan loss.

Eight weeks after surgery, Safranin-O staining revealed structural damages of the cartilage in all operated groups (Figure 24 and Figure 25). The empty group with solely hydrogel carrier showed an intermediate erosion score with a value of 6,55 ± 1,51. Mice which received unsorted MSCs exhibited the highest erosion score (7 ± 2,1). However, the mean value of this group was similar and non-significantly different from the empty group. On the other hand, the $\alpha 10^{high}$ MSCs had the best outcome in term of preventing erosion upon DMM with mean erosion score of 4,66 ± 2,0, reaching statistical significance *versus* the empty (**p*=0,0380) and unsorted (**p*=0,0211) groups (Figure 25). In all operated groups, the femoral condyles revealed higher scores (average around four) than the tibiae which averaged around three (not shown). General signs of ectopic calcification were detected in small extent among all groups. As expected, sham group did not show any detectable structural change in either the AC or the subchondral bone.

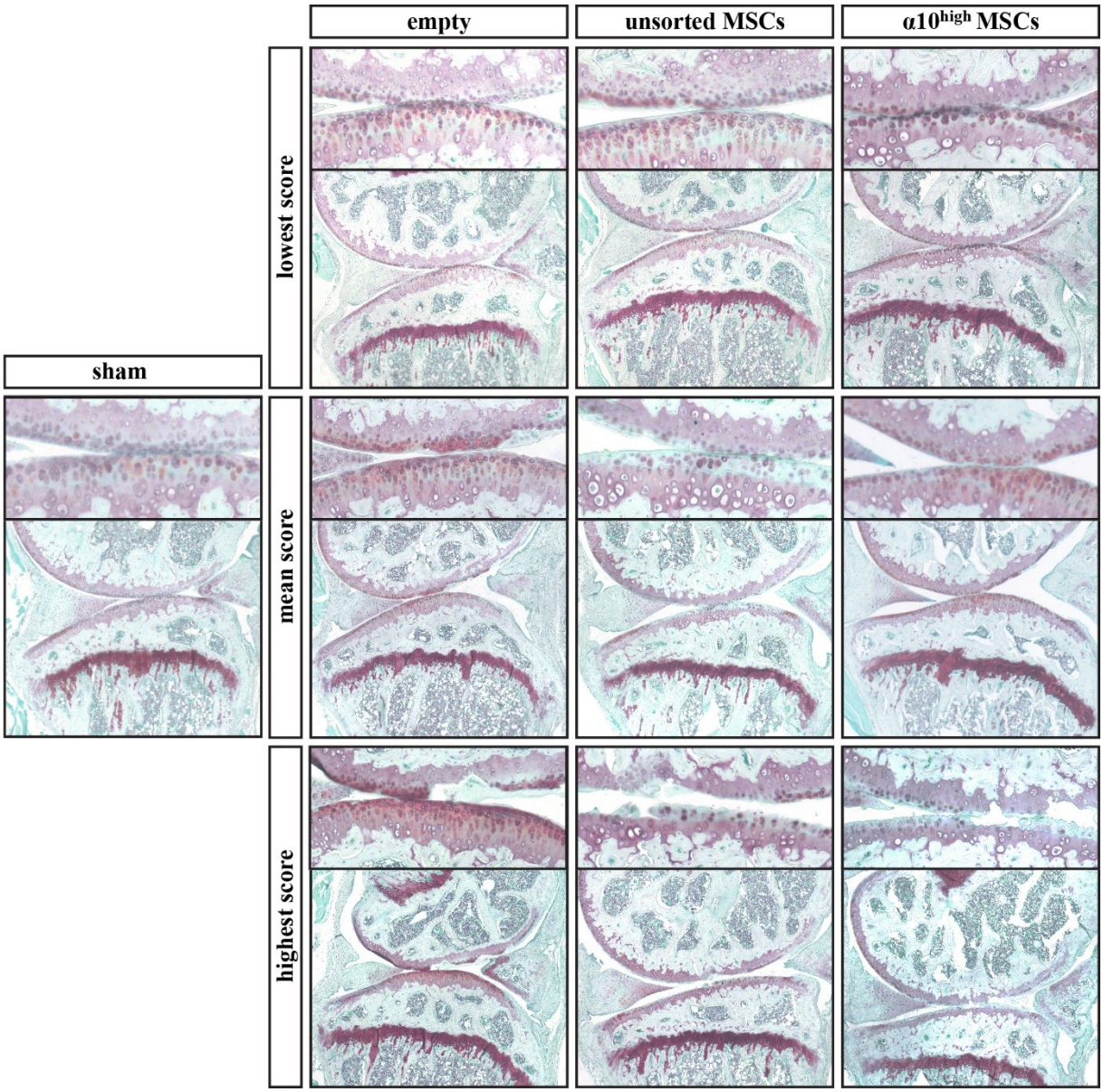

Figure 24: Histological analysis of cartilage damage. Safranin-O/Fast-Green staining of the femoral condyle and tibial plateau was performed on 7 µm sections of the mice knees dissected eight weeks after operation. Representative micrographs of each group as example of the highest, mean and lowest scores are shown.

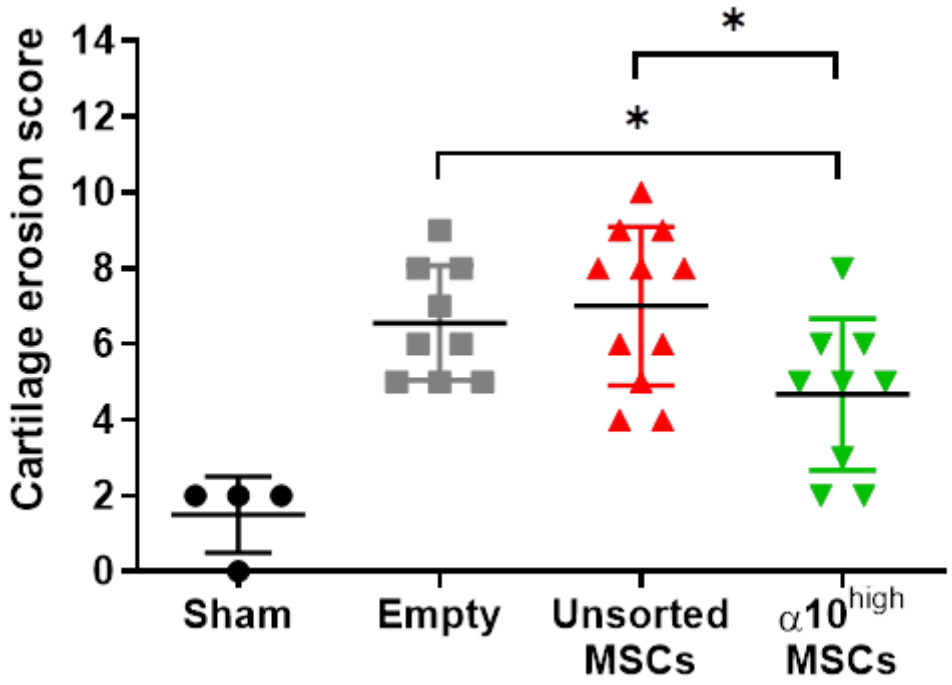

Figure 25: Scoring for structural damage of the AC. A modified scoring system with cumulative scores for the AC of femoral condyle and tibial plateau was implemented to analyze cartilage erosion eight weeks after operation[194]. The mean and standard deviation are shown. Statistical analysis with parametric unpaired *t*-test revealed significant differences between the $\alpha10^{high}$ MSCs group *vs* the empty (**p*=0,0380) and *vs* unsorted (**p*=0,0211).

3.2.4.2 Proteoglycan loss

General histological examination with Toluidine Blue staining did not reveal any massive loss or significant differences in the proteoglycan content of the AC among the groups (Figure 27). With a mean value of 1,17 ± 0,41, the empty group revealed the highest scores compared to the unsorted (0,71 ± 0,75) and $\alpha10^{high}$ (1 ± 0,58) groups. Of notice, the unsorted MSCs group have the most animal with score 0. However, no significant difference was observed in between any of the experimental groups. Similar to the cartilage degeneration, PG loss affected more the femur condyles than the tibial plateaus.

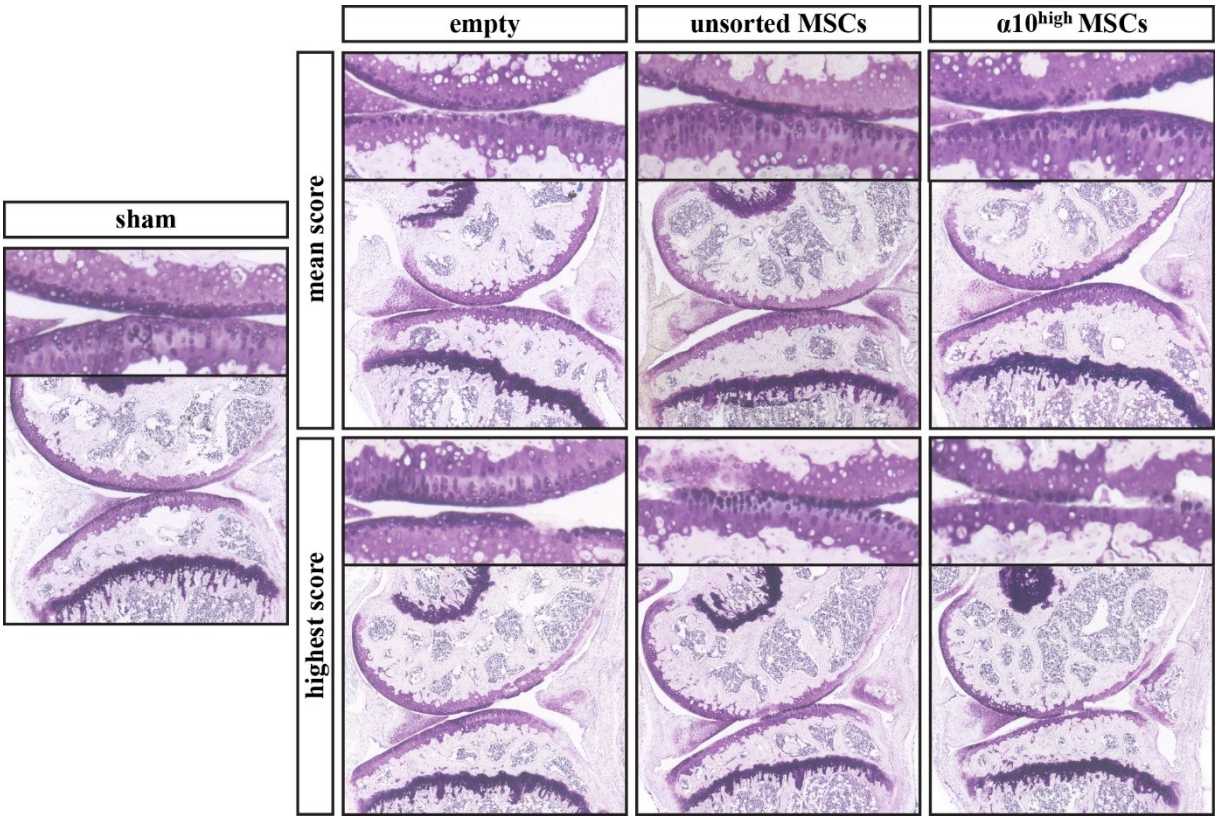

Figure 26: Histological analysis of proteoglycan loss. Representative micrographs of mean and highest score examples from the knees of mice stained with Toluidine Blue eight weeks after surgery.

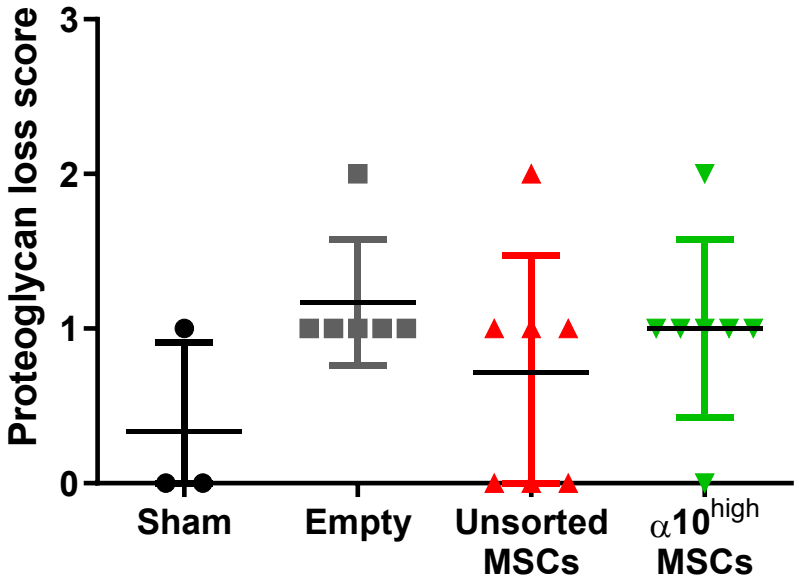

Figure 27: Quantification of the proteoglycan loss. A modified scoring system was utilized to analyze the proteoglycan loss eight weeks after operation[194]. Mean and standard deviation are shown.

3.2.4.3 Aggrecan expression

Immunohistochemical analysis for aggrecan expression was performed to qualitatively monitor expression changes of the main proteoglycan in AC (Figure 28). Here, similar to the evaluation of PG loss no tremendous differences in aggrecan deposition in between the operated groups were detectable. Chondrocytes appear regularly arranged in the three typical articular cartilage zone (superficial, middle and deep). The sham group, displayed the strongest aggrecan staining. Samples with higher scores for proteoglycan loss also showed reduced aggrecan staining. Qualitatively, the $\alpha10^{high}$ MSCs group showed the least aggrecan loss compared to the other operated groups.

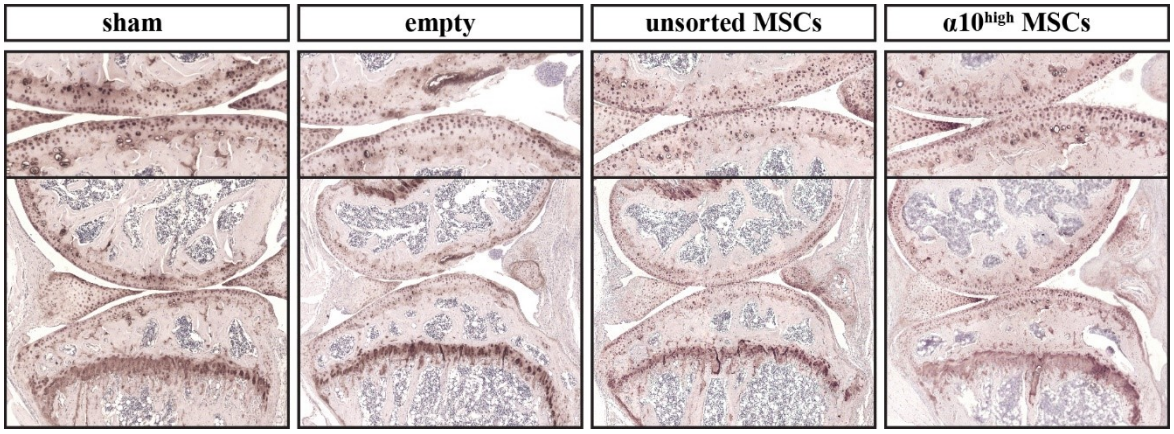

Figure 28: Immunohistochemical analysis of aggrecan expression. Representative micrographs of aggrecan immunostaining on mouse knee joints, eight weeks post operation.

3.2.4.4 Collagen type II expression

Immunohistochemical analysis for collagen type II was performed to analyze possible differences in the expression and distribution of the main structural component of cartilage tissue (Figure 29). The qualitative examination of immunostaining revealed a slight decrease of collagen type II in the empty group, suggesting that the addition of cells, either unsorted or $\alpha10^{high}$ cells, might help to preserve the collagenous network of articular cartilage in the post traumatic OA model. In addition, $\alpha10^{high}$ and unsorted groups showed more intense staining in the deep zone compared to the other zones, suggesting that eight weeks after trauma, the deep zone of AC is less affected than the superficial layer, and that overall, the addition of MSCs hindered the loss of collagen type II at least in the deeper areas of the AC.

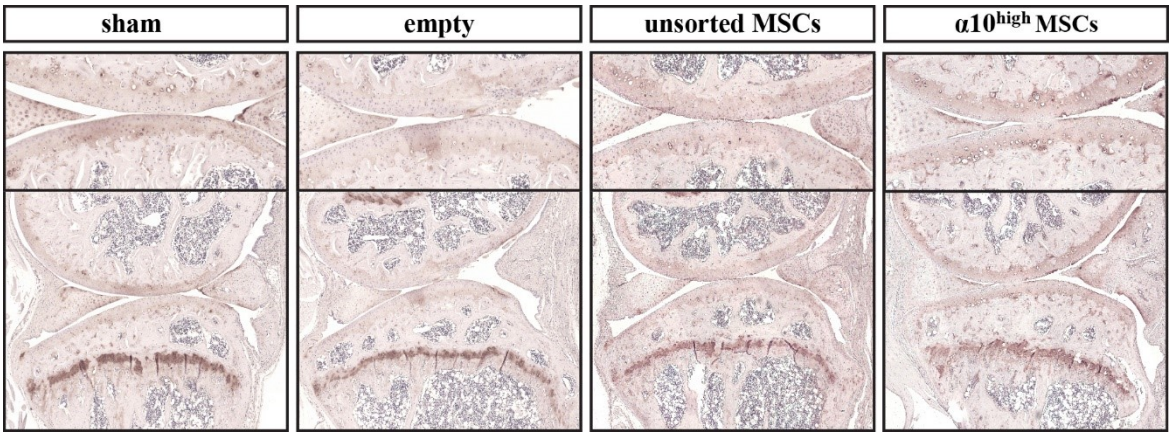

Figure 29: Immunohistochemical analysis of collagen type II expression. Representative photomicrographs of collagen type II immunostaining in knees at eight weeks postoperatively.

3.2.4.5 Detection of collagen type II degradation in blood serum

Before sacrificing the animals, serum samples were collected and tested for CTX-II, a neo-epitope of collagen type II cleavage that is released in the blood stream and indirectly reflects collagen type II degradation. A clear tendency of reduced CTX-II levels was observed in the $\alpha10^{high}$ MSCs group compared to all others (Figure 30). A significant difference was recorded between the unsorted and $\alpha10^{high}$ MSCs.

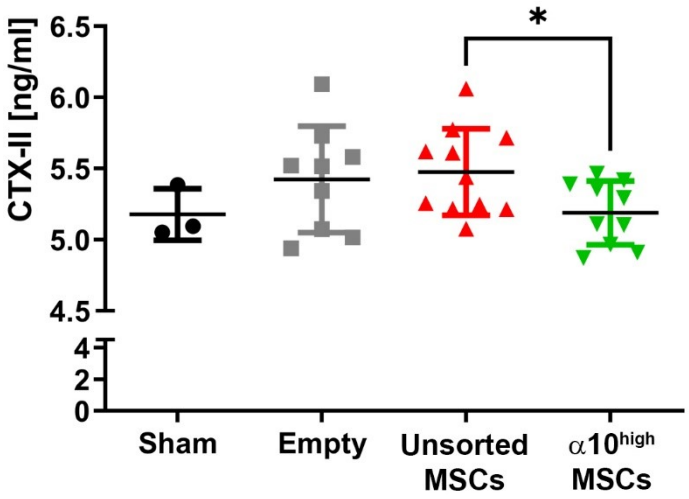

Figure 30: CTX-II serum levels eight weeks post operation. Scatter plot of serum CTX-II values, indicates reduced levels of collagen type II degradation neo-epitope in the $\alpha10^{high}$ MSCs group. Mean and standard deviation are shown. Statistical significance calculated by parametric unpaired t-test where *p=0,0282.

3.2.4.6 Detection of injected cells

Primer set pre-testing

In order to identify grafted human cells in the operated knees eight weeks after injection, the analysis of genes that are expressed exclusively in male or only in human was performed. To this aim, two genes have been tested, namely the *sex determining region of Y* gene *(SRY)* and the *Charcot Marie tooth disease* gene *(CMT1A*).

In the first experiment, two samples with 100 ng/µl DNA of human muscle cells (male) and mouse myoblast cells (female) were tested for *CMT1A* and *SRY* gene detection. As expected, no gene was detectable in female mouse cells (labeled as M in Figure 31), whereas clear signals were observed in human male gDNA samples (labeled as H in Figure 31) for both sets of genes. To test the detection sensibility/threshold of the two genes, a mixtures of human and mouse DNA in ratios of 0.0005% and 0.0001% with a total gDNA concentration of 50 ng/µl (labeled as A and B in Figure 31, respectively) was prepared. As shown in Figure 31, the detection potential of *CMT1A* was more powerful compared to *SRY*, as it was able to detect human gDNA in the lower ratio mixture. These results were crucial in deciding whether to use *CMT1A* primers for the detection of human cells in mouse tissue in the subsequent experiments.

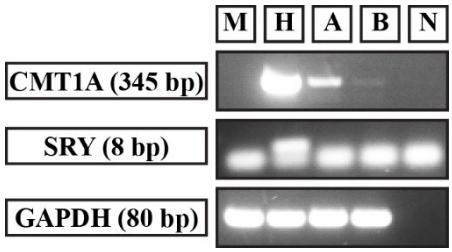

Figure 31: PCR analysis of human *CMT1A* and *SRY* genes in human, mouse and mixed genomic DNA samples. M = mouse DNA (50ng/µl); H = human DNA (50ng/µl); A: 0.0005% human/mouse DNA; B: 0.0001% human/mouse DNA; N = negative control. Signals for *CMT1A* at 345 bp reveal the presence of human DNA at all tested ratios, whereas *SRY* signal was detected only in the pure human male cells gDNA sample.

Detection of injected human MSCs in the mouse joint cavity

To verify that the injected human cells are still present in the joint cavity of the mice eight weeks after surgery, genomic DNA (gDNA) was extracted and purified from the knee region of paraffin-embedded slices. A ratio of 0.0005% human/mouse cells served as positive control in concentrations of 200 ng/µl (Figure 32, A) and 25ng/µl (Figure 32, B) for PCR of the *CMT1A* gene.

Only the mixed control sample A gave the expected 354 bp signal after the PCR amplification (Figure 32). Neither the knee samples nor the human/mouse control with the concentration of 25ng/µl gDNA demonstrated *CMT1A* expression. Murine *GAPDH* analysis served as input control, and its positive signal for all tested samples prove the successful DNA extraction from the mouse tissue sections. These results indicate that the injected MSCs either died or left from the joint cavity or their presence was too low to be detected by such a technique.

Figure 32: Representative PCR analysis for *CMT1A* gene expression of human MSCs in mouse knee tissues eight weeks post operation. Positive control (A) = 0.0005% human/mouse cells, 200ng/µl. (B) = 0.0005% human/mouse cells, 25ng/µl. No positive signal for CMT1A expression was seen in the operated groups (Empty, Unsorted MSCs or $\alpha 10^{high}$ MSCs). *GAPDH* expression served as input control.

4 DISCUSSION

Articular cartilage is the highly specialized tissue of diarthrodial joints, which enables frictionless movement and the ability to withstand compressive and tensile forces. Due to its hypocellular and avascular nature, the AC has limited capacity for self-regeneration. Damage of the AC, whether due to degenerative processes or traumatic injuries, leads to loss of function and progressive degradation of cartilage. To date, there is no disease modifying treatment available to heal or successfully halt the progression of cartilage conditions, like OA. Current treatments are mainly restricted to reduce symptoms, in particular pain relief, by the application of NSAIDs or intra-articular injection of corticosteroids or hyaluronic acid[197]. Surgical approaches such as autologous chondrocytes implantation or transplantation of osteochondral plugs are invasive techniques, which only provide limited success. In later stages, when joint morphology is irremediably altered and pain management is insufficient, joint replacement becomes necessary but is confronted with different conditions and scenarios that hamper successful operation[198]. The need for alternative and satisfying regenerative treatments for early and late stages of OA is enormous. In this regard, a new hope for disease modifying treatments is represented by MSCs. In comparison to chondrocyte-based strategies, MSCs offer new possibilities due to their high renewable capacities as well as their ability to differentiate into multiple lineages. Furthermore, the ease of harvest and the efficient *in vivo* expansion provides advantages of MSCs over the use of chondrocytes. Many *in vivo* trials demonstrate the positive effects of MSCs during tissue repair processes. However, to date, the mechanisms by which MSCs influence tissue regeneration remain unclear. One possible mechanism of action is described by their paracrine activity, which has been shown to reduce inflammation by improving the native environment required for tissue regeneration. Taking in account the multipotency of MSCs, another possible mechanism of action is the targeting of MSCs to the damaged tissue, with the subsequent differentiation and direct regeneration of the defect. Therefore, studies that aim to increase the potential of differentiation capacities to one or more lineages are of particular interest in regenerative medicine. Importantly for cartilage repair, *Varas et al*. demonstrated that MSCs expressing high levels of integrin α10, a collagen type II receptor abundantly found in cartilage, exhibit greater chondrogenic differentiation potential[174].

The aim of the present study was to investigate the potential of MSCs expressing integrin α10 in the protection against post-traumatic osteoarthritis. The experimental set-up included the following milestones:

- Ensuring the multilineage differentiation potential of MSCs sorted for integrin α10

- Selecting a suitable cell carrier for the *in vivo* injection of the cells, which could support remodeling, cell survival and chondrogenic differentiation.
- Investigating the effect of $\alpha10^{high}$ MSCs in the murine post-traumatic DMM model.

In this study it was found that $\alpha10^{high}$ MSCs retain the typical multipotency of MSCs with a higher potential towards the chondrogenic lineage. The clinically approved fibrin hydrogel was implemented as cell carrier, which can support *in vitro* remodeling and cell survival. Of outmost importance, the $\alpha10^{high}$ MSCs exert positive effects in reducing cartilage degradation when injected into the PT-OA murine model. A detailed discussion of these findings contrasted with the literature is presented in the following sections.

4.1 *IN VITRO* ANALYSIS

The human bone marrow-derived MSCs used in this study were harvested, characterized and kindly provided by Xintela AB (Sweden). Cells were grown under the exposure of platelet lysate (PL), which is known to promote expansion and differentiation potential of MSCs and, most importantly for this study, to positively modulates integrin α10 expression levels. *Chevallier et al*., observed spontaneous expression of osteoblastic genes during cultivation of MSCs in the presence of PL instead of FBS[199]. Similar results were also found by *Hildner et al.*, where ASCs cultured in PL-enriched chondrogenic differentiation medium showed higher chondrogenic potential than fetal calf serum-enriched ASCs[200]. Additional advantages of PL over FBS include elimination of the transmission risk of animal-derived pathogens, high reproducibility due to the elimination of lot-to-lot variations typical of FBS and more ethical research.

Varas et al. observed a higher chondrogenic potential when MSCs were cultured with FGF2. They showed upregulation of integrin α10, concomitant with an improvement in chondrogenic potential. In conclusion, integrin α10 was proposed as possible chondrogenic differentiation marker for MSCs[174]. Further studies have demonstrated a similar upregulation of integrin α10 in MSCs expanded with PL. However, when regarding future applications in humans, FGF-2 treatment has an important side-effect. *Bocelli-Tyndall et al*. observed the expression of HLA-DR in MSCs treated with FGF-2. The expression of HLA-DR on MSCs may increase apoptosis and provoke immunological response when non-autologous cells are applied in humans[201]. According to *Bernardo et al*., HLA-DR expression in MSCs treated with PL was not observed[202]. In addition, PL can be produced from the patient itself, which avoids immunological reactions and is therefore more attractive for future human applications. All the above-mentioned reasons lead to the decision to choose PL for the present study.

After sorting for integrin α10 expression, cell behavior such as proliferation rate and shape in culture did not change. However, in many cases, the commitment of a multipotent cell type towards a particular mesenchymal lineage hinders their potential to differentiate towards other lineages. *Alberton et al.* have shown that overexpression of the tendon master regulator *Scleraxis* (*Scx*) shifts the phenotype of primitive MSC towards a tenogenic progenitor. Moreover, differentiation towards osteogenic or chondrogenic lineage was hindered in human MSCs transfected with *Scx*.[203]. *RUNX-2* is a transcription factor, which regulates osteogenic differentiation at different time-points. This requires binding to OSE2 (osteoblast-specific-element 2), the promoter region responsible for osteogenesis. In early-stages, *RUNX-2* positively influences osteogenesis in an inducing way, whereas it is an inhibitory regulator in later stages[204]. *Lin et al*. observed that *RUNX-2* silenced in rat osteoblasts *via* lentivirus vectors expressing small interfering RNS (siRNA) suppresses *in vitro* differentiation and matrix mineralization[205]. The essential role of *RUNX-2* in osteogenesis is further demonstrated by the results of *Zhang et al.* In their study, *RUNX-2* overexpression *via* recombinant adenovirus-transduction into ASCs resulted in increased matrix mineralization *in vivo* and *in vitro* as well as in inhibition of adipogenesis [206]. Similar results are obtained regarding the adipogenic differentiation potential. *PPAR-γ* (peroxisome proliferator-activated receptor gamma) is a member of the nuclear hormone receptor subfamily involved in lipid metabolism. It represents an early and independent transcription factor for critical genes, which is activated by several ligands including fatty acids, which triggers adipogenic differentiation[207,208]. Together with the 9-cis retinoic acid receptor (RXR), *PPAR-γ* binds to a peroxisome proliferator response element (PPRE) to activate adipogenic genes such as the phosphoenolpyruvate carboxykinase (PEPCK) and adipocyte lipid binding protein (aP2)[209]. *Wang et al*. found that silencing *PPAR-γ* via siRNA transfection in chicken preadipocytes results in a lower differentiation potential of these cells[210]. Moreover, *Lee et al.* have shown that silencing of *PPAR-γ* following osteogenic induction not only inhibits adipogenesis, but even promotes osteogenesis by inducing critical genes for osteogenesis like *RUNX-2*, *BMP2*, *ALP* (alkaline phosphatase) and *OC* (osteocalcin)[211]. Regarding chondrogenic differentiation, *SOX-9* is an essential transcription factor required for chondrogenesis, and its overexpression leads to enhanced chondrogenesis of murine MSCs. *Sitcheran et al.,* showed a suppressed chondrogenesis due to NF-κB-induced destabilization of *SOX-9* mRNA[212]. *Xing et al.* found a similar involvement of the NF-κB signaling in adipogenesis, where NF-κB-dependent suppression of *PPAR-γ* occurs[213]. These findings are of great interest considering that inflammation is playing an important role in the development of OA.

In the present study, matrix mineralization of unsorted and α10^{high} MSCs upon osteogenic induction was visualized and quantified with Alizarin Red staining. The results indicated successful osteogenic differentiation of stimulated MSCs and quantification of Alizarin Red staining did not revealed differences in mineralization potential between the two groups. However, a higher expression of *RUNX-2* was observed in the unsorted group. In view of the previous described literature, the upregulation of *RUNX-2* would suggest a higher osteogenic potential for unsorted MSCs. Similar results were observed for the adipogenic differentiation potential. Unsorted and α10^{high} MSCs showed similar lipid vacuoles production upon adipogenic stimulation, although unsorted MSCs exhibited higher expression of the adipogenic transcription factor *PPAR-γ.* Chondrogenesis was analyzed after 28 days of stimulation in pellet culture. Pellets were assessed with Safranin-O staining, immunohistochemistry against the chondrogenic markers aggrecan and collagen type II, mRNA expression analysis for integrin α10 and α11, and pellet growth measurement. While only slight differences in pellet growth were observed, staining with Safranin-O and for aggrecan and collagen type II clearly demonstrated the higher chondrogenic potential for α10^{high} MSCs in comparison to the unsorted group. The results of mRNA expression were consistent with the findings of *Varas et al*., demonstrating upregulated *ITGA10* and downregulated *ITGA11* expression in α10^{high} MSCs compared to the unsorted MSCs during chondrogenesis[174]. These results, support the original findings presented by *Gouttenoire et al*. and *Varas et al.*, indicating integrin α11 as marker for primitive MSCs, and integrin α10 as marker for MSCs committed to the chondrogenic lineage[214,174]. These results are interesting when compared with the findings of *Popov et al*., who described an upregulation of integrin α11 in MSCs during osteogenesis[215].

In summary, MSCs selected for high expression of integrin α10 exhibit typical spindle-like cell shapes when cultured in monolayers and display successful differentiations towards mesenchymal lineages especially towards chondrocytes. In conclusion, the cell sorting does not influence typical characteristics of stem cells. When compared to the existing literature, these results are in agreement with those found by *Varas et al*. and *Uvebrant et al*[174,216], and support the hypothesis that integrin α10 serves as a biomarker for a subpopulation of MSCs with high differentiation potential for cartilage repair.

4.2 *IN VIVO* ANALYSIS

In vivo cell-therapy studies play a fundamental role in testing the safety, behavior and effects of the designated cells in the intended target environment. The following discussion of the *in*

vivo analysis will consider the studies performed to select the appropriate cell carrier, the use of $\alpha10^{high}$ MSCs in the PT-OA murine model and its analysis.

4.2.1 FIBRIN HYDROGEL AS CELL-CARRIER

Providing an adequate environment for cell delivery is of outmost importance for the successful outcome of an *in vivo* trial. In this work, cell delivery was ensured by fibrin hydrogel. In preliminary testing, a slow-gelling fibrin gel (Artiss®, Baxter, USA) was preferred because the properties of this hydrogel enabled homogenous cell distribution, good remodeling, good cell survival and chondrogenic differentiation of MSCs. Fibrin hydrogel has been reported to support differentiation, cell adhesion and distribution with reduced adverse effects[217,218]. *Christman et al*. transplanted myoblasts into infarcted myocardium using fibrin hydrogel and observed improved cell survival of transplanted cells. Here, the beneficial effect of fibrin on cells can be attributed to its structure, which served as a temporary matrix/scaffold where cells can bind to RGD sequences and enable new ECM synthesis[219]. *Dragoo et al*., placed ASCs with the aid of a fibrin glue scaffold into a full-thickness cartilage animal-model. Their results for cartilage regeneration were promising, showing a smooth articulating surface after repair[220]. *Chang et al*. tested fibrin as a cell delivery construct with autologous chondrocytes in rabbits and showed neocartilage formation eight weeks after injection[221]. These results indicate fibrin gel as a useful cell carrier. Furthermore, the latter group found that the number of chondrocytes is not critical for cartilage formation when fibrin is used. More important is the high thrombin concentration, which positively correlates to the number of cross-links required for a suitable cell environment. The low concentration of thrombin and therefore a lower number of cross-linking results in an unstable matrix, which hinders proper matrix production of chondrocytes. Moreover, increasing concentrations of chondrocytes do not result in successful matrix production, either[221]. Another interesting issue is the correct ratio of thrombin and fibrin. *Catelas et al*. have tested different ratios of fibrin and thrombin and the behavior of the encapsulated MSCs *in vitro*[222]. In-line with other studies, fibrin and not thrombin plays the more important role for cell behavior, whereas thrombin is more important for a solid matrix formation, as mentioned above. In fibrin sealants with lower concentrations of fibrin, MSCs are elongate and proliferate easily, whereas higher concentrations of fibrin results in greater osteogenic differentiation potential. However, the appropriate fibrin/thrombin ratio depends on the respective experiment and needs to be optimized for each purpose[222,223]. In the study of *Guo et al.*, injection of 5 million/ml BM-MSCs in hydrogel with a 1:1 ratio of fibrin and thrombin into rat myocardium achieved better results than injection of MSCs alone, in terms of cell survival and differentiation, suggesting a beneficial and protective effect of fibrin itself on

cells[224]. To note, the number of BM-MSCs used in the present study is 10-times lower compared to the study of *Guo et al*[224]. Moreover, these experiments were performed in the knee joint of mice which provides only limited space for the injection of cells. The available knowledge for an appropriate number of cells and a suitable ratio of thrombin and fibrin for AC repair is limited and further investigations are needed. However, the fibrin/thrombin ratio and the number of cells chosen for the present study resulted in high cell survival *in vitro*. An additional important aspect to keep in mind is the biodegradability of fibrin gel as a main factor for mechanical instability. If degradation occurs too rapidly with early loss of the scaffold, adherence of cells and cell integration into the hydrogel can be reduced leading to apoptosis. Matrix production and cell division need to occur at the same or higher rate as hydrogel degradation to support cell organization and survival[225]. *In vitro* studies combining fibrin/hyaluronic acid hydrogels show improved mechanical properties of the construct itself regarding compressive modulus, while remaining biodegradable. Thus, they are promising for improvements of hydrogel-based cell delivery methods[135]. In this study, the commercially available and fully approved Artiss® was chosen to take a step towards possible pre-clinical study in larger animals and/or humans.

4.2.2 ANIMAL MODEL

In this study, twelve weeks old female mice of the C57BL/6j strain underwent surgery on the right knee and were analyzed eight weeks post-operatively. When comparing the mouse joint to human joint, one obvious anatomical difference is the size. The smaller joint affects differences not only in the biomechanical loading but also in AC structure. According to *Glasson et al.,* articular cartilage of mice is 50 times thinner and the relative amount of calcified cartilage is higher compared to humans[193]. However, due to the ease of handling small animals together with the commonly and wide-spread use of mice, this animal model simplifies comparisons between different studies. In addition, the mouse model enables further studies for a better understanding of the genetic and molecular pathomechanism of OA due to the use of the genetically modified mice and the fact that the entire mouse genome has been sequenced[189]. An important factor to consider is the prevalence of OA in male mice compared to female. *Van Osch et al*. found more severe spontaneous and collagenase-induced OA in male mice, whereas *Ma et al.* observed the same in surgical induced OA models[226,227]. The explanation lies in different hormonal activity and expression. While ovarian hormones are suggested to protect from OA, male hormones such as testosterone are reported to exacerbate OA in male mice. In this pilot study, female mice producing moderate OA were selected. Testing the therapeutic effect of cells in a milder OA model is more akin to a potential human clinical trial where intra-articular injection of cells would be used to treat early OA patients.

Destabilization of the medial meniscus (DMM) model was used to induce post-traumatic osteoarthritis (PT-OA) in mice. The study of *Glasson et al*. was the first to described the DMM model in 2007 and therefore served as main reference in this study[188]. Compared to other surgical induced OA models, the DMM model allows for a slow onset of disease, good reproducibility and high similarity to human OA[228]. For a good comparison, it is important to choose the correct control group. According to *Teeple et al.,* the contralateral leg is not an ideal control because unloading of the operated leg may lead to inflammation in the contralateral knee[180]. Therefore, in this study, an un-operated group, the so-called sham group, which received only a small skin incision, served as control group. The mice used were twelve weeks old, which is according to *Poole et al*. above the recommended minimum age of ten weeks[229]. Moreover, in twelve weeks old-mice DMM reproducibility was higher compared to four-month old mice as reported by *Huang et al.*[230]. Eight weeks after surgery was chosen as the timepoint for knee dissection and histological analysis as OA severity increasing from week four to week eight post-operatively[188]. In all groups, a mild to moderate OA was observed with major effect on the medial parts of the femur and tibia using this DMM model. Interestingly, the femur displayed higher scores of cartilage damage and erosion compared to the tibial counterpart, which is inconsistent with observations from other studies where the tibia is the more involved joint part[186]. The high reproducibility and successful induction of OA is the reason why this method has now become established as the surgical PT-OA model in our laboratory.

4.2.3 EFFECT OF α10 ^{high} MSCS ON PT-OA

The ultimate proof of the effect of the α10^{high} MSCs on PT-OA is their use in an *in vivo* model. The α10^{high} group displayed the best outcome in term of erosion score after eight weeks post operation and cell injection. Injecting α10^{high} MSCs-encapsulated fibrin gel into the joint cavity after the operation significantly reduced cartilage structural damages eight weeks after surgery compared to the unsorted MSCs/fibrin and empty fibrin hydrogel groups. On the other hand, the separate scoring for proteoglycan loss on Toluidine Blue stained sections showed similar results for all operated groups. Furthermore, immunohistochemistry did not indicate difference in the deposition of aggrecan among the groups indicating that proteoglycan metabolism was apparently not affected by the MSC/fibrin gel treatment. In general, cartilage damage upon DMM was not so strong in either group, including the ‘empty’ one. This might be due to the fact that the fibrin sealant, which is also present in the empty group, might have cushioning properties against joint loading, as has been described for several other viscosupplements[231]. In this regard, the lack of a control DMM group without fibrin sealant is a limitation of this study, but since the aim of the experiments was to investigate the regenerative potential of α10^{high}

MSCs compared to unsorted one, the observations still validate the capacity of α10^{high} MSC subpopulation to reduce OA progression.

The regenerative therapeutic potential of stem cells, due to their high proliferative, differentiating and immunomodulatory properties, may be of great interest for therapies for OA[232]. Interestingly, *Schelbergen et al.* found that cartilage destruction was not positively affected by injection of adipose-derived MSCs at day seven or 14 post-DMM[233]. In contrast, a positive effect was found when ASCs were injected in a collagenase-induced model of OA, which is characterized by marked synovitis compared to the DMM model. The authors suggested that eventually the healing capacity of ASCs could be related to counteracting synovial inflammation[233]. Similar immunomodulatory effects of injected adipose derived MSCs using collagenase-induced OA model were reported by *Ter Huurne et al.* and *Maumus et al*. [234,235]. For example, *Ter Huurne et al*. observed reduced synovial thickening and inflammation already with a single injection of ASCs in early stages of OA. This study suggests that the time point of cell injection has a major importance as the anti-inflammatory effect is highest during the acute inflammatory phase, which is normally at the beginning of the disease progression. At later time points, the injection of ASCs in this model was less effective[234]. *Maumus et al.* demonstrated the feasibility of a xenogeneic model using equine ASCs (eASCs) and evaluated the immunosuppressive effect of IFN-γ (Interferon gamma)-primed eASCs. The improved anti-inflammatory and therapeutic efficiency, as well as reduced synovitis *in vivo* compared to non-primed cells, highlight the immunomodulatory potential of MSCs[235]. Another approach showing the immunomodulating effects of MSCs on OA was shown *by Khatab et al*. In their study, human bone marrow MSCs were stimulated with IFN-γ and TNF-α. The secretome released by these cells was injected into a collagenase-induced mice model and compared it to injection of MSCs[236]. The positive effects on pain and structural damages revealed that MSCs-secretome can be as effective as MSCs injection[236], further suggesting that MSCs might act in a paracrine manner in the target tissue. Therefore, it is a legitimate theory that MSCs anti-inflammatory properties are required in early stages of OA, while their homing and chondrogenic potential is more desirable in advanced stages of OA with significant structural erosion.

The ELISA assay for CTX-II showed slightly, but significantly reduced levels of collagen degradation product in the serum of the DMM operated group which received α10^{high} MSCs compared to the other groups. CTX-II, the C-telopeptide of collagen type II, is a frequently analyzed serum or urine biomarker for indirect diagnosis of cartilage destruction[237]. *Ishikawa et al*. have demonstrated a positive correlation between human OA grades and urinary CTX-II

levels[237]. *Duclos et al.* suggested CTX-II levels in rabbit serum as possible predictive biomarker for OA[238]. Consistent with the low grades of degradation seen in histopathological analysis, we did not expect high values or tremendous differences of CTX-II between the groups. It is important to keep in mind, especially for further studies, that degradation of collagen type II might start at different phases of the disease therefore more time points for CTX-II measurements should be implemented in follow-up studies.

4.2.4 FATE OF INJECTED MSCS

Survival assay of cells embedded in fibrin gel *in vivo* was performed with CFDA-SE and visualized with a fluorescence microscopy on day one and day seven postoperatively. At both time points, fluorescently-labelled MSCs were detectable, but in much lower amount after one week than after one day of surgery. Thus, these results confirm the successful MSC transplantation and cell survival in fibrin hydrogel *in vivo* in the first week. As the CFDA-SE staining is a short-/mid-term cell-labelling with rapid loss of signal, the detection of injected MSCs was performed *via* RT-PCR for the human *Charcot-Marie-Tooth-disease* gene (*CMT1A*) from DNA isolated from knee tissue sections at eight weeks post DMM[239]. At this late time point, it was not possible to detect *CMT1A* in any of the groups. This finding might suggest that either cells did not adhere and survived in the joint tissue for eight weeks, or that the number of cells that eventually integrated in the joint tissue were under the threshold sensitivity of the detection method used. Interestingly, *Cheng et al*. tested the sensitivity for *SRY* and *CMT1A*, as in this study, but revealed higher sensitivity for *SRY*-gene with 0.03% human DNA[195], in contrast to higher sensitivity of *CMT1A* as described in the current work. *Kehoe et al*. were able to detect CM-Dil-labelled MSCs after intra-articular (IA) injection in mice for at least 28 days, where cells were primarily distributed along the synovia. Additional experiments to investigate possible migration and off-target homing of MSCs failed to detect cells in other organs four weeks after IA injection[240]. Furthermore, *Schelbergen et al.* could not to detect murine ASCs five days post IA injection in mice[233]. *Mak et al.* transfected MSCs with GFP-lentivirus and detected them *via* fluorescence microcopy at two and four weeks after IA injection in mice. Interestingly, the number of cells detected between the two time points was shown to decrease in the MRL strain and to increase in the C57Bl6 mouse strain[241]. The authors argued that in the MRL strain, MSCs could be already primed for immediate regenerative effects early in the post injury period and may subsequently migrate or differentiate, which would reduce the positive staining for MSCs. The same method was used by *Ter Huurne et al*. In this study, MSCs could be detected near to the synovium 24 hours after IA-injection, but detection was not possible five days post injection[234].

The diverse results for cell detection described in the above studies rather indicate that cells injected *in vivo* do not provide a clear statement about either migration or attachment of MSCs in the joint. Moreover, if cells were detectable, the chosen time-points were earlier compared to the eight weeks selected in this study. Regarding the results, eight weeks may be too late for a successful detection of the injected MSCs. Therefore, earlier time-points should be preferred. Another important point influencing successful cell detection is the different methods used for this purpose. In most of the studies, cells were labelled prior to IA injection, which simplified detection and provided higher sensitivity. In this work, cell labelling was performed only in the short-term (one and seven days) as an internal control for the successful cell delivery. Cell labelling before injection is a possible improvement that should be considered in future experiments, although long-term labelling still faces several problems.

4.2.5 MSCS MODE OF ACTIONS

The mechanism of action of MSCs on AC regeneration remains to be elucidated. Due to their homing and differentiation potential, one hypothesis is that MSCs migrate towards damaged cartilage and regenerate the damaged tissue through differentiation into chondrocytes as *Andersen et al* could demonstrate with human adipose derived MSCs sorted for integrin α10 were injected into the joint cavity of rabbit knees. Further, homing of cells to the cartilage defect side as well as the presence of cartilage specific molecules such as collagen type II and aggrecan was observed at least for ten days after injection. Altogether, their results indicate that MSCs sorted for high expression of integrin α10 are able to home to cartilage defects *in vivo* and differentiate towards chondrocytes-like cells [239]. Nonetheless, the emerging and most acclaimed theory of the recent years is that MSCs act in a paracrine manner, releasing beneficial cytokines and growths factors which support the immuno-modulation of the joint environment and help resident cells to respond to injury. It is not possible to rule out one mechanism of action or another, as these are highly depended on the experimental design. *Ter Huurne et al.* were able to show that a single injection of MSCs in a collagenase-induced OA model in mice reduced the extent of synovitis as measured by synovial thickness scoring. Additional positive effect on cartilage destruction, in terms of reduced macrophage activity, was also observed[234]. Similar findings were reported by the group of *Schelbergen et al.* who could show the beneficial effect of ASCs injected in the murine DMM model[233]. It is important to note that the DMM-model has smaller inflammatory component compared to the collagenase-induced OA-model. In a similar collagenase-induced-mouse-model for OA, naïve or IFN-γ-primed equine MSCs were injected and both groups displayed chondroprotective and immunomodulatory effects on AC, with the primed cells showing higher efficiency[235]. *Mak et al.* generated focal cartilage defects

in mouse and found that injected MSCs were able to form proteoglycan-rich ECM close to the defect[241]. In an antigen-induced rheumatoid arthritis (RA) model, performed by *Kehoe et al*., reduced PG-loss was observed, which was consistent with lower grades of cartilage destruction and reduced inflammation in groups treated with murine MSCs[240]. However, RA is a different and mainly inflammatory disease, and therefore the chondroprotective and immunomodulatory effects of MSCs observed in this study are difficult to compare with OA. In summary, all these studies reveal positive effects of MSCs in animal models of cartilage conditions, although the mechanism of action remain unclear.

4.2.6 CONCLUSION AND OUTLOOK

In the present work, it is shown that a MSCs subpopulation selected for the expression of the collagen binding integrin α10 (α10^{high} MSCs) *in vitro* retains multilineage differentiation potential, with a clear commitment towards the chondrogenic lineage, as indicated by their improved chondrogenic potential. As a proof of principle, α10^{high} MSCs were challenged *in vivo* using the surgery-induced DMM OA model, and showed a modest but significant role of α10^{high} MSCs in protecting against PT-OA. These results highlight the promising potential of stem-cell based therapies for the treatment of OA and demonstrate the efficacy of the fibrin hydrogel-based method for MSC delivery into the joint.

The mechanism of action of α10^{high} MSCs and their fate after intraarticular injection remains to be clarified. This study demonstrates a superior chondrogenic differentiation potential of α10^{high} MSCs *in vitro*, but in the specific *in vivo* experimental set-up and PCR detection method, it was not possible to detect implanted cells eight weeks post operation. *Wike et al*. performed a study in which MSCs were injected into 15 mm cartilage lesions via autogenous fibrin vehicle and results were analyzed arthroscopically after 30 days and histologically after eight months. They could find improved cartilage regeneration with fibrous tissue, but no significant long-term effect was observed[242]. A suiting experiment is the drilling model, where MSCs are transferred into a focal cartilaginous defect. Compared to the DMM-model, cartilage damage present from the beginning and do not have to develop first.

To improve the experimental setup for future studies, multiple cell injections could provide long-term maintenance of MSCs in the joint. As no MSCs were detected in the joint after eight weeks in the present study, it is plausible to speculate that the cells start to exert their positive effect within a few days of injection. *Schelbergen et al.* couldn't detect ASCs five days after injection[233]. Cell-labelling prior to injection, would provide a better monitoring of MSC. The most preferable option would be a 3-dimensional, real-time visualization of cells to obtain

information on their fate, survival, migration and differentiation. In this way, effective cell delivery and engraftment could prove the success of stem cell-based therapy. The labelling of cells for long-term observation is still facing several problems, such as stability of the selected marker, sustained expression of reporter genes for bioluminescence imaging, or the influence of differentiation capacity or phenotypes of MSCs eventually caused by MRI detectable particles, just to name a few examples[243].

Identifying the mechanism by $\alpha10^{high}$ MSCs exert a beneficial effect against the development of severe PT-OA remains of outmost importance. Detailed analysis of their transcriptome and proteome, as well as characterization of the cargo of their released extracellular vesicles (exosome and microvesicles) will certainly shed new insights into their mechanism of action.

5 REFERENCES

1. Mora JC, Przkora R, Cruz-Almeida Y. Knee osteoarthritis: Pathophysiology and current treatment modalities. J Pain Res. 2018 Oct 5;11:2189-2196. doi:10.2147/JPR.S154002

2. Bannuru RR, Schmid CH, Kent DM, Vaysbrot EE, Wong JB, McAlindon TE. Comparative effectiveness of pharmacologic interventions for knee osteoarthritis: A systematic review and network meta-analysis. Ann Intern Med. 2015 Jan 6;162(1):46-54. doi:10.7326/M14-1231

3. Glyn-Jones S, Palmer AJ, Agricola R, Price AJ, Vincent TL, Weinans H, Carr AJ. Osteoarthritis. In: The Lancet. 2015 Jul 25;386(9991):376-87. doi:10.1016/S0140-6736(14)60802-3

4. Leardini G, Salaffi F, Caporali R, Canesi B, Rovati L, Montanelli R. Italian Group for Study of the Costs of Arthritis. Direct and indirect costs of osteoarthritis of the knee. Clin Exp Rheumatol. 2004 Nov-Dec;22(6):699-706

5. Salmon JH, Rat AC, Sellam J, Michel M, Eschard JP, Guillemin F, Jolly D, Fautrel B. Economic impact of lower-limb osteoarthritis worldwide: a systematic review of cost-of-illness studies. Osteoarthritis Cartilage. 2016 Sep;24(9):1500-8. doi:10.1016/j.joca.2016.03.012

6. Fuchs J, Rabenberg M, Scheidt-Nave C. Prävalenz ausgewählter muskuloskelettaler Erkrankungen: Ergebnisse der Studie zur Gesundheit Erwachsener in Deutschland (DEGS1). Bundesgesundheitsblatt Gesundheitsforschung Gesundheitsschutz. 2013 May;56(5-6):678-686.German. doi:10.1007/s00103-013-1687-4

7. Altman R, Asch E, Bloch D, Bole G, Borenstein D, Brandt K, Christy W, Cooke TD, Greenwald R, Hochberg M, et al. Development of criteria for the classification and reporting of osteoarthritis. Classification of osteoarthritis of the knee. Diagnostic and Therapeutic Criteria Committee of the American Rheumatism Association. Arthritis Rheum. 1986 Aug;29(8):1039-49. doi: 10.1002/art.1780290816

8. KELLGREN JH, LAWRENCE JS. Radiological assessment of osteo-arthrosis. Ann Rheum Dis. 1957 Dec;16(4):494-502. doi:10.1136/ard.16.4.494

9. Luyten FP, Denti M, Filardo G, Kon E, Engebretsen L. Definition and classification of

early osteoarthritis of the knee. Knee Surgery, Sport Traumatol Arthrosc. 2012 Mar;20(3):401-406. doi:10.1007/s00167-011-1743-2

10. Moseley JB, O'Malley K, Petersen NJ, Menke TJ, Brody BA, Kuykendall DH, Hollingsworth JC, Ashton CM, Wray NP. A controlled trial of arthroscopic surgery for osteoarthritis of the knee. N Engl J Med. 2002 Jul 11;347(2):81-8. doi: 10.1056/NEJMoa013259

11. Lotz M, Martel-Pelletier J, Christiansen C, Brandi ML, Bruyère O, Chapurlat R, Collette J, Cooper C, Giacovelli G, Kanis JA, Karsdal MA, Kraus V, Lems WF, Meulenbelt I, Pelletier JP, Raynauld JP, Reiter-Niesert S, Rizzoli R, Sandell LJ, Van Spil WE, Reginster JY. Republished: Value of biomarkers in osteoarthritis: Current status and perspectives. Postgrad Med J. 2014 Mar;90(1061):171-178. doi:10.1136/postgradmedj-2013-203726rep

12. Prof. Dr. J. Ströve. S2k-Leitlinie Gonarthrose Version 3.0; Deutsche Gesellschaft für Orthopädie und Unfallchirurgie. Deutsche Gesellschaft für Orthopädie und Unfallchirurgie. 30.11.2017. https://register.awmf.org/de/leitlinien/detail/033-004.

13. Felson DT. Osteoarthritis as a disease of mechanics. Osteoarthritis Cartilage. 2013;21(1):10-15. doi:10.1016/j.joca.2012.09.012

14. Andriacchi TP, Mündermann A, Smith RL, Alexander EJ, Dyrby CO, Koo S. A framework for the in vivo pathomechanics of osteoarthritis at the knee. Ann Biomed Eng. 2004 Mar;32(3):447-457. doi:10.1023/B:ABME.0000017541.82498.37

15. Moore AC, Burris DL. Tribological and material properties for cartilage of and throughout the bovine stifle: Support for the altered joint kinematics hypothesis of osteoarthritis. Osteoarthritis Cartilage. 2015 Jan;23(1):161-169. doi:10.1016/j.joca.2014.09.021

16. Bevill SL, Boyer KA, Andriacchi TP. The regional sensitivity of chondrocyte gene expression to coactive mechanical load and exogenous TNF-α stimuli. J Biomech Eng. 2014 Sep;136(9):091005. doi:10.1115/1.4027937

17. Edd SN, Giori NJ, Andriacchi TP. The role of inflammation in the initiation of osteoarthritis after meniscal damage. J Biomech. 2015 Jun 1;48(8):1420-1426. doi:10.1016/j.jbiomech.2015.02.035

18. Goldring MB, Otero M. Inflammation in osteoarthritis. Curr Opin Rheumatol. 2011

Sep;23(5):471-478. doi:10.1097/BOR.0b013e328349c2b1

19. Barilla ML, Carsons SE. Fibronectin fragments and their role in inflammatory arthritis. Semin Arthritis Rheum. 2000 Feb;29(4):252-265. doi:10.1016/S0049-0172(00)80012-8

20. Loeser RF. Aging processes and the development of osteoarthritis. Curr Opin Rheumatol. 2013 Jan;25(1):108-113. doi:10.1097/BOR.0b013e32835a9428

21. Losina E, Weinstein AM, Reichmann WM, Burbine SA, Solomon DH, Daigle ME, Rome BN, Chen SP, Hunter DJ, Suter LG, Jordan JM, Katz JN. Lifetime risk and age at diagnosis of symptomatic knee osteoarthritis in the US. Arthritis Care Res (Hoboken). 2013 May;65(5):703-11. doi:10.1002/acr.21898

22. Singh T, Newman AB. Inflammatory markers in population studies of aging. Ageing Res Rev. 2011 Jul;10(3):319-329. doi:10.1016/j.arr.2010.11.002

23. Hu PF, Bao JP, Wu LD. The emerging role of adipokines in osteoarthritis: A narrative review. Mol Biol Rep. 2011 Feb;38(2):873-878. doi:10.1007/s11033-010-0179-y

24. Loeser RF. Aging and osteoarthritis: the role of chondrocyte senescence and aging changes in the cartilage matrix. Osteoarthritis Cartilage. 2009 Aug;17(8):971-979. doi:10.1016/j.joca.2009.03.002

25. Campisi J. Cellular senescence: Putting the paradoxes in perspective. Curr Opin Genet Dev. 2011 Feb;21(1):107-112. doi:10.1016/j.gde.2010.10.005

26. Delmonico MJ, Harris TB, Visser M, Park SW, Conroy MB, Velasquez-Mieyer P, Boudreau R, Manini TM, Nevitt M, Newman AB, Goodpaster BH; Health, Aging, and Body. Longitudinal study of muscle strength, quality, and adipose tissue infiltration. Am J Clin Nutr. 2009 Dec;90(6):1579-1585. doi:10.3945/ajcn.2009.28047

27. Tsezou A. Osteoarthritis year in review 2014: Genetics and genomics. Osteoarthritis Cartilage. 2014 Dec;22(12):2017-2024. doi:10.1016/j.joca.2014.07.024

28. arcOGEN Consortium; arcOGEN Collaborators; Zeggini E, Panoutsopoulou K, Southam L, Rayner NW, Day-Williams AG, Lopes MC, et al. Identification of new susceptibility loci for osteoarthritis (arcOGEN): A genome-wide association study. Lancet. 2012 Sep 1;380(9844):815-823. doi:10.1016/S0140-6736(12)60681-3

29. Zhang R, Yao J, Xu P, Ji B, Luck JV, Chin B, Lu S, Kelsoe JR, Ma J. A. A comprehensive meta-analysis of association between genetic variants of GDF5 and

osteoarthritis of the knee, hip and hand. Inflamm Res. 2015 Jun;64(6):405-414. doi:10.1007/s00011-015-0818-9

30. Southam L, Rodriguez-Lopez J, Wilkins JM, Pombo-Suarez M, Snelling S, Gomez-Reino JJ, Chapman K, Gonzalez A, Loughlin J. An SNP in the 5′-UTR of GDF5 is associated with osteoarthritis susceptibility in Europeans and with in vivo differences in allelic expression in articular cartilage. Hum Mol Genet. 2007 Sep 15;16(18):2226-2232. doi:10.1093/hmg/ddm174

31. Reynard LN, Loughlin J. Genetics and epigenetics of osteoarthritis. Maturitas. 2012 Mar;71(3):200-204. doi:10.1016/j.maturitas.2011.12.001

32. Day-Williams AG, Southam L, Panoutsopoulou K, Rayner NW, Esko T, Estrada K, et al. A variant in MCF2L is associated with osteoarthritis. Am J Hum Genet. 2011 Sep 9;89(3):446-450. doi:10.1016/j.ajhg.2011.08.001

33. Lambert C, Dubuc JE, Montell E, Vergés J, Munaut C, Noël A, Henrotin Y. Gene expression pattern of cells from inflamed and normal areas of osteoarthritis synovial membrane. Arthritis Rheumatol. 2014 Apr;66(4):960-968. doi:10.1002/art.38315

34. Panoutsopoulou K, Zeggini E. Advances in osteoarthritis genetics. J Med Genet. 2013 Nov;50(11):715-724. doi:10.1136/jmedgenet-2013-101754

35. O'Connor MI. Osteoarthritis of the Hip and Knee: Sex and Gender Differences. Orthop Clin North Am. 2006 Oct;37(4):559-568. doi:10.1016/j.ocl.2006.09.004

36. Guilak F, Alexopoulos LG, Upton ML, Youn I, Choi JB, Cao L, Setton LA, Haider MA. The pericellular matrix as a transducer of biomechanical and biochemical signals in articular cartilage. Ann N Y Acad Sci. 2006 Apr;1068:498-512. doi:10.1196/annals.1346.011

37. Wilusz RE, Sanchez-Adams J, Guilak F. The structure and function of the pericellular matrix of articular cartilage. Matrix Biol. 2014 Oct;39:25-32. doi:10.1016/j.matbio.2014.08.009

38. Asanbaeva A, Tam J, Schumacher BL, Klisch SM, Masuda K, Sah RL. Articular cartilage tensile integrity: Modulation by matrix depletion is maturation-dependent. Arch Biochem Biophys. 2008 Jun;474(1):175-182. doi:10.1016/j.abb.2008.03.012

39. Wang Y, Wei L, Zeng L, He D, Wei X. Nutrition and degeneration of articular

cartilage. Knee Surg, Sports Traumatol Arthrosc. 2013 Aug;21(8):1751-1762. doi:10.1007/s00167-012-1977-7

40. Benninghoff A. Form und Bau der Gelenkknorpel in ihren Beziehungen zur Funktion. Z.Zellforsch 2. 1925 Nov;783–862. doi: 10.1007/BF00583443

41. Ateshian GA, Lai WM, Zhu WB, Mow VC. An asymptotic solution for the contact of two biphasic cartilage layers. J Biomech. 1994 Nov;27(11):1347-1360. doi:10.1016/0021-9290(94)90044-2

42. Ricard-Blum S. The Collagen Family. Cold Spring Harb Perspect Biol. 2011 Jan 1;3(1):a004978. doi:10.1101/cshperspect.a004978

43. Eyre D. Collagen of articular cartilage. Arthritis Res. 2002;4(1):30-35. doi:10.1186/ar380

44. Izadifar Z, Chen X, Kulyk W. Strategic Design and Fabrication of Engineered Scaffolds for Articular Cartilage Repair. J Funct Biomater. 2012 Nov 14;3(4):799-838. doi:10.3390/jfb3040799

45. Knudson CB, Knudson W. Cartilage proteoglycans. Semin Cell Dev Biol. 2001 Apr;12(2):69-78. doi:10.1006/scdb.2000.0243

46. Lyon M, Rushton G, Gallagher JT. The interaction of the transforming growth factor-βs with heparin/heparan sulfate is isoform-specific. J Biol Chem. 1997 Jul 18;272(29):18000-18006. doi:10.1074/jbc.272.29.18000

47. Temenoff JS, Mikos AG. Review: Tissue engineering for regeneration of articular cartilage. Biomaterials. 2000 Mar;21(5):431-440. doi:10.1016/S0142-9612(99)00213-6

48. Nicolae C, Ko Y-P, Miosge N, Niehoff A, Studer D, Enggist L, Hunziker EB, Paulsson M, Wagener R, Aszodi A. Abnormal collagen fibrils in cartilage of matrilin-1/matrilin-3-deficient mice. J Biol Chem. 2007 Jul 27;282(30):22163-22175. doi:10.1074/jbc.M610994200

49. Chen FH, Rousche KT, Tuan RS. Technology insight: Adult stem cells in cartilage regeneration and tissue engineering. Nat Clin Pract Rheumatol. 2006 Jul;2(7):373-382. doi:10.1038/ncprheum0216

50. Sophia Fox AJ, Bedi A, Rodeo SA. The basic science of articular cartilage: Structure, composition, and function. Sports Health. 2009 Nov;1(6):461-468.

doi:10.1177/1941738109350438

51. Buckwalter JA, Mankin HJ. Articular cartilage: tissue design and chondrocyte-matrix interactions. Instr Course Lect. 1998;47:477-86

52. Saarakkala S, Julkunen P, Kiviranta P, Mäkitalo J, Jurvelin JS, Korhonen RK. Depth-wise progression of osteoarthritis in human articular cartilage: investigation of composition, structure and biomechanics. Osteoarthritis Cartilage. 2010 Jan;18(1):73-81. doi:10.1016/j.joca.2009.08.003

53. Cohen NP, Foster RJ, Mow VC. Composition and Dynamics of Articular Cartilage: Structure, Function, and Maintaining Healthy State. J Orthop Sports Phys Ther. 1998 Oct. doi:10.2519/jospt.1998.28.4.203

54. Goldring MB, Goldring SR. Articular cartilage and subchondral bone in the pathogenesis of osteoarthritis. Ann N Y Acad Sci. 2010 Mar;1192:230-7.. doi:10.1111/j.1749-6632.2009.05240.x

55. Ondrésik M, Oliveira JM, Reis RL. Knee Articular Cartilage. Oliveira, J., Reis, R. (eds) Regenerative Strategies for the Treatment of Knee Joint Disabilities. Studies in Mechanobiology, Tissue Engineering and Biomaterials, vol 21. Springer, Cham; 2017:3-20. doi:10.1007/978-3-319-44785-8_1

56. Moskalewski S, Hyc A, Jankowska-Steifer E, Osiecka-Iwan A. Formation of synovial joints and articular cartilage. Folia Morphol (Warsz). 2013 Aug.;72(3):181-187. doi:10.5603/FM.2013.0031

57. Dy P, Smits P, Silvester A, Penzo-Méndez A, Dumitriu B, Han Y, de la Motte CA, Kingsley DM, Lefebvre V. Synovial joint morphogenesis requires the chondrogenic action of Sox5 and Sox6 in growth plate and articular cartilage. Dev Biol. 2010 May;341(2):346-359. doi:10.1016/j.ydbio.2010.02.024

58. Lui JC, Nilsson O, Baron J. Growth plate senescence and catch-up growth. Endocr Dev. 2011;21:23-29. doi:10.1159/000328117

59. Burdan F, Szumiło J, Korobowicz A, Farooquee R, Patel S, Patel A, Dave A, Szumiło M, Solecki M, Klepacz R, Dudka J. Morphology and physiology of the epiphyseal growth plate. Folia Histochem Cytobiol. 2009;47(1):5-16. doi:10.2478/v10042-009-0007-1

60. Prein C, Warmbold N, Farkas Z, Schieker M, Aszodi A, Clausen-Schaumann H. Structural and mechanical properties of the proliferative zone of the developing murine growth plate cartilage assessed by atomic force microscopy. Matrix Biol. 2016 Mar;50:1-15. doi:10.1016/j.matbio.2015.10.001

61. Michigami T. Regulatory mechanisms for the development of growth plate cartilage. Cell Mol Life Sci. 2013 Nov;70(22):4213-4221. doi:10.1007/s00018-013-1346-9

62. Vanky P, Brockstedt U, Hjerpe A, Wikström B. Kinetic studies on epiphyseal growth cartilage in the normal mouse. Bone. 1998 ;22(4):331-339.April doi:10.1016/S8756-3282(97)00286-X

63. Ballock RT, O'Keefe RJ. Physiology and pathophysiology of the growth plate. Birth Defects Res Part C Embryo Today. 2003 May;69(2):123-143. doi:10.1002/bdrc.10014

64. Bland YS, Ashhurst DE. Development and ageing of the articular cartilage of the rabbit knee joint: Distribution of the fibrillar collagens. Anat Embryol (Berl). 1996 Dec;194(6):607-619. doi:10.1007/BF00187473

65. Koyama E, Shibukawa Y, Nagayama M, Sugito H, Young B, Yuasa T, Okabe T, Ochiai T, Kamiya N, Rountree RB, Kingsley DM, Iwamoto M, Enomoto-Iwamoto M, Pacifici M. A distinct cohort of progenitor cells participates in synovial joint and articular cartilage formation during mouse limb skeletogenesis. Dev Biol. 2008 Apr 1;316(1):62-73. doi:10.1016/j.ydbio.2008.01.012

66. Salazar VS, Gamer LW, Rosen V. BMP signalling in skeletal development, disease and repair. Nat Rev Endocrinol. 2016 April;12(4):203-221. doi:10.1038/nrendo.2016.12

67. Akiyama H, Lefebvre V. Unraveling the transcriptional regulatory machinery in chondrogenesis. J Bone Miner Metab. 2011 Jul;29(4):390-395. doi:10.1007/s00774-011-0273-9

68. Foster JW, Dominguez-Steglich MA, Guioli S, Kwok C, Weller PA, Stevanović M, Weissenbach J, Mansour S, Young ID, Goodfellow PN, et al. Campomelic dysplasia and autosomal sex reversal caused by mutations in an SRY-related gene. Nature. 1994 Dec 8;372(6506):525-530. doi:10.1038/372525a0

69. Hargus G, Kist R, Kramer J, Gerstel D, Neitz A, Scherer G, Rohwedel J. Loss of Sox9 function results in defective chondrocyte differentiation of mouse embryonic stem cells in vitro. Int J Dev Biol. 2008;52(4):323-332. doi:10.1387/ijdb.072490gh

70. Lefebvre V, Bhattaram P. Vertebrate skeletogenesis. Curr Top Devl Biol. 2010;90:291-317. doi:10.1016/S0070-2153(10)90008-2

71. Lefebvre V, Huang W, Harley VR, Goodfellow PN, de Crombrugghe B. SOX9 is a potent activator of the chondrocyte-specific enhancer of the pro alpha1(II) collagen gene. Mol Cell Biol. 1997 Apr;17(4):2336-2346. doi:10.1128/mcb.17.4.2336

72. Lefebvre V, Li P, De Crombrugghe B. A new long form of Sox5 (L-Sox5), Sox6 and Sox9 are coexpressed in chondrogenesis and cooperatively activate the type II collagen gene. EMBO J. 1998 Oct 1;17(19):5718-5733. doi:10.1093/emboj/17.19.5718

73. Healy C, Uwanogho D, Sharpe PT. Regulation and role of Sox9 in cartilage formation. Dev Dyn. 1999 May;215(1):69-78. doi:10.1002/(SICI)1097-0177(199905)215:1<69::AID-DVDY8>3.0.CO;2-N

74. Wagner T, Wirth J, Meyer J, Zabel B, Held M, Zimmer J, Pasantes J, Bricarelli FD, Keutel J, Hustert E, Wolf U, Tommerup N, Schempp W, Scherer G. Autosomal sex reversal and campomelic dysplasia are caused by mutations in and around the SRY-related gene SOX9. Cell. 1994 Dec;79(6):1111-1120. doi:10.1016/0092-8674(94)90041-8

75. Liu CF, Angelozzi M, Haseeb A, Lefebvre V. SOX9 is dispensable for the initiation of epigenetic remodeling and the activation of marker genes at the onset of chondrogenesis. Development. 2018 Jul;145(14). doi:10.1242/dev.164459

76. Yoshida CA, Komori T. Role of Runx proteins in chondrogenesis. Crit Rev Eukaryot Gene Expr. 2005;15(3):243-254. doi:10.1615/CritRevEukarGeneExpr.v15.i3.60

77. Zheng Q, Zhou G, Morello R, Chen Y, Garcia-Rojas X, Lee B. Type X collagen gene regulation by Runx2 contributes directly to its hypertrophic chondrocyte-specific expression in vivo. J Cell Biol. 2003 Sep 1;162(5):833-842. doi:10.1083/jcb.200211089

78. Yoshida CA, Yamamoto H, Fujita T, Furuichi T, Ito K, Inoue K, Yamana K, Zanma A, Takada K, Ito Y, Komori T. Runx2 and Runx3 are essential for chondrocyte maturation, and Runx2 regulates limb growth through induction of Indian hedgehog. Genes Dev. 2004 Apr 15;18(8):952-963. doi:10.1101/gad.1174704

79. Moffat CS, See PT, Oliver RP. Leaf yellowing of the wheat cultivar Mace in the absence of yellow spot disease. Australasian Plant Pathol. 2015;44(2):161-166.

doi:10.1007/s13313-014-0335-2

80. Buckwalter JA, Mankin HJ, Grodzinsky AJ. Articular cartilage and osteoarthritis. Instr Course Lect. 2005;54:465-480. PMID: 15952258

81. Man GS, Mologhianu G. Osteoarthritis pathogenesis - a complex process that involves the entire joint. J Med Life. 2014 Mar 15;7(1):37-41. Epub 2014 Mar 25. PMID: 24653755

82. Ernst E, Posadzki P. Complementary and alternative medicine for rheumatoid arthritis and osteoarthritis: An overview of systematic reviews. Curr Pain Headache Rep. 2011 Dec;15(6):431-437. doi:10.1007/s11916-011-0227-x

83. Esser S, Bailey A. Effects of exercise and physical activity on knee osteoarthritis. Curr Pain Headache Rep. 2011 Dec;15(6):423-430. doi:10.1007/s11916-011-0225-z

84. Zhang W, Moskowitz RW, Nuki G, Abramson S, Altman RD, Arden N, Bierma-Zeinstra S, Brandt KD, Croft P, Doherty M, Dougados M, Hochberg M, Hunter DJ, Kwoh K, Lohmander LS, Tugwell P. OARSI recommendations for the management of hip and knee osteoarthritis, Part II: OARSI evidence-based, expert consensus guidelines. Osteoarthritis Cartilage. 2008 Feb;16(2):137-162. doi:10.1016/j.joca.2007.12.013

85. Scarpignato C, Lanas A, Blandizzi C, Lems WF, Hermann M, Hunt RH; International NSAID Consensus Group. Safe prescribing of non-steroidal anti-inflammatory drugs in patients with osteoarthritis - an expert consensus addressing benefits as well as gastrointestinal and cardiovascular risks. BMC Med. 2015 Mar 19;13(1):55. doi:10.1186/s12916-015-0285-8

86. Richards MM, Maxwell JS, Weng L, Angelos MG, Golzarian J. Intra-articular treatment of knee osteoarthritis: from anti-inflammatories to products of regenerative medicine. Phys Sportsmed. 2016;44(2):101-108. doi:10.1080/00913847.2016.1168272

87. Axe JM, Snyder-Mackler L, Axe MJ. The role of viscosupplementation. Sports Med Arthrosc Rev. 2013 Mar;21(1):18-22. doi:10.1097/JSA.0b013e3182673241

88. Ayhan E, Kesmezacar H, Akgun I. Intraarticular injections (corticosteroid, hyaluronic acid, platelet rich plasma) for the knee osteoarthritis. World J Orthop. 2014 Jul;5(3):351. doi:10.5312/wjo.v5.i3.351

89. Dervin GF, Stiell IG, Rody K, Grabowski J. Effect of arthroscopic débridement for osteoarthritis of the knee on health-related quality of life. J Bone Joint Surg Am. 2003 Jan;85(1):10-19. doi:10.2106/00004623-200301000-00003

90. Rönn K, Reischl N, Gautier E, Jacobi M. Current Surgical Treatment of Knee Osteoarthritis. Arthritis. 2011;2011:1-9. doi:10.1155/2011/454873

91. Mithoefer K, Williams RJ 3rd, Warren RF, Potter HG, Spock CR, Jones EC, Wickiewicz TL, Marx RG. Chondral resurfacing of articular cartilage defects in the knee with the microfracture technique. Surgical technique. J Bone Joint Surg Am. 2006 Sep;88 Suppl 1:294-304. doi:10.2106/JBJS.F.00292

92. Mithoefer K, Mcadams T, Williams RJ, Kreuz PC, Mandelbaum BR. Clinical efficacy of the microfracture technique for articular cartilage repair in the knee: An evidence-based systematic analysis. Am J Sports Med. 2009 Oct;37(10):2053-2063. doi:10.1177/0363546508328414

93. Steadman JR, Rodkey WG, Briggs KK. Microfracture to treat full-thickness chondral defects: surgical technique, rehabilitation, and outcomes. J Knee Surg. 2002 Summer;15(3):170-176. PMID: 12152979

94. Matricali GA, Dereymaeker GPE, Luvten FP. Donor site morbidity after articular cartilage repair procedures: A review. Acta Orthop Belg. 2010 Oct;76(5):669-674. PMID: 21138224

95. Gudas R, Gudaite A, Pocius A, Gudiene A, Cekanauskas E, Monastyreckiene E, Basevicius A. Ten-year follow-up of a prospective, randomized clinical study of mosaic osteochondral autologous transplantation versus microfracture for the treatment of osteochondral defects in the knee joint of athletes. Am J Sports Med. 2012 Nov;40(11):2499-2508. doi:10.1177/0363546512458763

96. Brittberg M, Lindahl A, Nilsson A, Ohlsson C, Isaksson O, Peterson L. Treatment of Deep Cartilage Defects in the Knee with Autologous Chondrocyte Transplantation. N Engl J Med. 1994 Oct 6;331(14):889-895. doi:10.1056/nejm199410063311401

97. Hunziker EB. Articular cartilage repair: Basic science and clinical progress. A review of the current status and prospects. Osteoarthritis Cartilage. 2002 Jun;10(6):432-463. doi:10.1053/joca.2002.0801

98. Saris DBF, Vanlauwe J, Victor J, Haspl M, Bohnsack M, Fortems Y, Vandekerckhove

B, Almqvist KF, Claes T, Handelberg F, Lagae K, van der Bauwhede J, Vandenneucker H, Yang KG, Jelic M, Verdonk R, Veulemans N, Bellemans J, Luyten FP. Characterized chondrocyte implantation results in better structural repair when treating symptomatic cartilage defects of the knee in a randomized controlled trial versus microfracture. Am J Sports Med. 2008 Feb;36(2):235-246. doi:10.1177/0363546507311095

99. Zhang W, Ouyang H, Dass CR, Xu J. Current research on pharmacologic and regenerative therapies for osteoarthritis. Bone Res. 2016 Mar;4. doi:10.1038/boneres.2015.40

100. Roberts S, McCall IW, Darby AJ, Menage J, Evans H, Harrison PE, Richardson JB.. Autologous chondrocyte implantation for cartilage repair: monitoring its success by magnetic resonance imaging and histology. Arthritis Res Ther. 2003;5(1):R60-73. doi:10.1186/ar613

101. Mithoefer K, Williams RJ 3rd, Warren RF, Potter HG, Spock CR, Jones EC, Wickiewicz TL, Marx RG The microfracture technique for the treatment of articular cartilage lesions in the knee: A prospective cohort study. J Bone Jt Surg Am. 2005 Sep;87(9 I):1911-1920. doi:10.2106/JBJS.D.02846

102. Cole BJ, Pascual-Garrido C, Grumet RC. Surgical management of articular cartilage defects in the knee. Instr Course Lect. 2010;59:181-204. PMID: 20415379

103. Pestka JM, Bode G, Salzmann G, Südkamp NP, Niemeyer P. Clinical outcome of autologous chondrocyte implantation for failed microfracture treatment of full-thickness cartilage defects of the knee joint. Am J Sports Med. 2012 Feb;40(2):325-331. doi:10.1177/0363546511425651

104. Makris EA, Gomoll AH, Malizos KN, Hu JC, Athanasiou KA. Repair and tissue engineering techniques for articular cartilage. Nat Rev Rheumatol. 2015 Jan;11(1):21-34. doi:10.1038/nrrheum.2014.157

105. Buly RL, Sculco TP. Recent advances in total knee replacement surgery. Curr Opin Rheumatol. 1995 Mar;7(2):107-113. doi:10.1097/00002281-199503000-00007

106. Hodge WA, Chandler HP. Unicompartmental knee replacement: A comparison of constrained and unconstrained designs. Journal of Bone and Joint Surgery.1992 Jul;74(6):877-883. doi:10.2106/00004623-199274060-00008

107. Fehring TK, Odum S, Griffin WL, Mason JB, Nadaud M. Early failures in total knee arthroplasty. Clin Orthop Relat Res. 2001 Nov;(392):315-318. doi:10.1097/00003086-200111000-00041

108. Rau R. Adalimumab (a fully human anti-tumour necrosis factor α monoclonal antibody) in the treatment of active rheumatoid arthritis: The initial results of five trials. Ann Rheum Dis. 2002 Nov;61 Suppl 2(Suppl 2):ii70-3. doi:10.1136/ard.61.suppl_2.ii70

109. Philp AM, Davis ET, Jones SW. Developing anti-inflammatory therapeutics for patients with osteoarthritis. Rheumatology (Oxford). 2017 Jun 1;56(6):869-881. doi:10.1093/rheumatology/kew278

110. Chevalier X, Giraudeau B, Conrozier T, Marliere J, Kiefer P, Goupille P. Safety study of intraarticular injection of interleukin 1 receptor antagonist in patients with painful knee osteoarthritis: A multicenter study. J Rheumatol. 2005 Jul;32(7):1317-1323. PMID: 15996071

111. Larkin J, Lohr TA, Elefante L, Shearin J, Matico R, Su JL, Xue Y, Liu F, Genell C, Miller RE, Tran PB, Malfait AM, Maier CC, Matheny CJ. Translational development of an ADAMTS-5 antibody for osteoarthritis disease modification. Osteoarthritis Cartilage. 2015 Aug;23(8):1254-1266. doi:10.1016/j.joca.2015.02.778

112. Nagai T, Sato M, Kutsuna T, Kokubo M, Ebihara G, Ohta N, Mochida J. Intravenous administration of anti-vascular endothelial growth factor humanized monoclonal antibody bevacizumab improves articular cartilage repair. Arthritis Res Ther. 2010;12(5):R178. doi:10.1186/ar3142

113. Kan SL, Li Y, Ning GZ, Yuan ZF, Chen LX, Bi MC, Sun JC, Feng SQ. Tanezumab for Patients with Osteoarthritis of the Knee: A Meta-Analysis. Zhao C, ed. PLoS One. 2016 June 13;11(6):e0157105. doi:10.1371/journal.pone.0157105

114. Guillot P V., Gotherstrom C, Chan J, Kurata H, Fisk NM. Human First-Trimester Fetal MSC Express Pluripotency Markers and Grow Faster and Have Longer Telomeres Than Adult MSC. Stem Cells. 2007 Mar;25(3):646-654. doi:10.1634/stemcells.2006-0208

115. Friedenstein AJ, Chailakhyan RK, Latsinik N V, Panasyvk AF, Keiliss-Borok IV. Stromal cells responsible for transferring the microenvironment of the hemopoietic

tissues: Cloning in vitro and retransplantation in vivo. Transplantation. 1974 Apr;17(4):331-340. doi:10.1097/00007890-197404000-00001

116. Friedenstein AJ, Chailakhjan RK, Lalykina KS. The development of fibroblast colonies in monolayer cultures of guinea-pig bone marrow and spleen cells. Cell Tissue Kinet. 1970 Oct;3(4):393-403. doi: 10.1111/j.1365-2184.1970.tb00347.x

117. Dominici M, Le Blanc K, Mueller I, Slaper-Cortenbach I, Marini F, Krause D, Deans R, Keating A, Prockop Dj, Horwitz E. Minimal criteria for defining multipotent mesenchymal stromal cells. The International Society for Cellular Therapy position statement. Cytotherapy. 2006;8(4):315-317. doi:10.1080/14653240600855905

118. DiMarino AM, Caplan AI, Bonfield TL. Mesenchymal stem cells in tissue repair. Front Immunol. 2013 Sep4;4:201. doi:10.3389/fimmu.2013.00201

119. Docheva D, Popov C, Mutschler W, Schieker M. Human mesenchymal stem cells in contact with their environment: Surface characteristics and the integrin system. J Cell Mol Med. 2007 Jan-Feb;11(1):21-38. doi:10.1111/j.1582-4934.2007.00001.x

120. Im G, Shin YW, Lee KB. Do adipose tissue-derived mesenchymal stem cells have the same osteogenic and chondrogenic potential as bone marrow-derived cells? Osteoarthritis Cartilage. 2005 Oct;13(10):845-853. doi:10.1016/j.joca.2005.05.005

121. Kern S, Eichler H, Stoeve J, Klüter H, Bieback K. Comparative Analysis of Mesenchymal Stem Cells from Bone Marrow, Umbilical Cord Blood, or Adipose Tissue. Stem Cells. 2006 May;24(5):1294-1301. doi:10.1634/stemcells.2005-0342

122. Bonab MM, Alimoghaddam K, Talebian F, Ghaffari SH, Ghavamzadeh A, Nikbin B. Aging of mesenchymal stem cell in vitro. BMC Cell Biol. 2006 Mar 10;7(1):14. doi:10.1186/1471-2121-7-14

123. Aust L, Devlin B, Foster SJ, Halvorsen YD, Hicok K, du Laney T, Sen A, Willingmyre GD, Gimble JM. Yield of human adipose-derived adult stem cells from liposuction aspirates. Cytotherapy. 2004;6(1):7-14. doi:10.1080/14653240310004539

124. Zuk PA, Zhu M, Ashjian P, De Ugarte DA, Huang JI, Mizuno H, Alfonso ZC, Fraser JK, Benhaim P, Hedrick MH. Human adipose tissue is a source of multipotent stem cells. Mol Biol Cell. 2002 Dec;13(12):4279-4295. doi:10.1091/mbc.E02-02-0105

125. Strioga M, Viswanathan S, Darinskas A, Slaby O, Michalek J. Same or not the same?

comparison of adipose tissue-derived versus bone marrow-derived mesenchymal stem and stromal cells. Stem Cells Dev. 2012 Sep 20;21(14):2724-2752. doi:10.1089/scd.2011.0722

126. Spees JL, Lee RH, Gregory CA. Mechanisms of mesenchymal stem/stromal cell function. Stem Cell Res Ther. 2016 Aug 31;7(1):125. doi:10.1186/s13287-016-0363-7

127. Iso Y, Spees JL, Serrano C, Bakondi B, Pochampally R, Song YH, Sobel BE, Delafontaine P, Prockop DJ. Multipotent human stromal cells improve cardiac function after myocardial infarction in mice without long-term engraftment. Biochem Biophys Res Commun. 2007 Mar 16;354(3):700-706. doi:10.1016/j.bbrc.2007.01.045

128. Tille JC, Pepper MS. Mesenchymal cells potentiate vascular endothelial growth factor-induced angiogenesis in vitro. Exp Cell Res. 2002 Nov 1;280(2):179-191. doi:10.1006/excr.2002.5635

129. Glenn JD, Whartenby KA Mesenchymal stem cells: Emerging mechanisms of immunomodulation and therapy. World J Stem Cells. 2014 Nov 26;6(5):526. doi:10.4252/wjsc.v6.i5.526

130. Lyons AB, Parish CR. Determination of lymphocyte division by flow cytometry. J Immunol Methods. 1994 May 2;171(1):131-137. doi:10.1016/0022-1759(94)90236-4

131. Choi H, Lee RH, Bazhanov N, Oh JY, Prockop DJ. Anti-inflammatory protein TSG-6 secreted by activated MSCs attenuates zymosan-induced mouse peritonitis by decreasing TLR2/NF-κB signaling in resident macrophages. Blood. 2011 Jul 14;118(2):330-338. doi:10.1182/blood-2010-12-327353

132. Németh K, Leelahavanichkul A, Yuen PS, Mayer B, Parmelee A, Doi K, Robey PG, Leelahavanichkul K, Koller BH, Brown JM, Hu X, Jelinek I, Star RA, Mezey E. Bone marrow stromal cells attenuate sepsis via prostaglandin E (2)-dependent reprogramming of host macrophages to increase their interleukin-10 production. Nat Med. 2009 Jan;15(1):42-49. doi:10.1038/nm.1905

133. Caplan AI, Dennis JE. Mesenchymal stem cells as trophic mediators. J Cell Biochem. 2006 Aug 1;98(5):1076-1084. doi:10.1002/jcb.20886

134. Richter W. Mesenchymal stem cells and cartilage in situ regeneration. J Intern Med. 2009 Oct;266(4):390-405. doi:10.1111/j.1365-2796.2009.02153.x

135. Snyder TN, Madhavan K, Intrator M, Dregalla RC, Park D. A fibrin/hyaluronic acid hydrogel for the delivery of mesenchymal stem cells and potential for articular cartilage repair. J Biol Eng. 2014 May:1-11. doi: 10.1186/1754-1611-8-10

136. Seliktar D. Designing cell-compatible hydrogels for biomedical applications. Science. 2012 Jun 1;336(6085):1124-1128. doi:10.1126/science.1214804

137. Wolberg AS. Thrombin generation and fibrin clot structure. Blood Rev. 2007 May;21(3):131-142. doi:10.1016/j.blre.2006.11.001

138. Li Y, Meng H, Liu Y, Lee BP. Fibrin gel as an injectable biodegradable scaffold and cell carrier for tissue engineering. ScientificWorldJournal. 2015;2015: 685690. doi:10.1155/2015/685690

139. Malafaya PB, Silva GA, Reis RL. Natural-origin polymers as carriers and scaffolds for biomolecules and cell delivery in tissue engineering applications. Adv Drug Deliv Rev. 2007 May;59(4-5):207-233. doi:10.1016/j.addr.2007.03.012

140. Lee F, Kurisawa M. Formation and stability of interpenetrating polymer network hydrogels consisting of fibrin and hyaluronic acid for tissue engineering. Acta Biomater. 2013 Feb;9(2):5143-5152. doi:10.1016/j.actbio.2012.08.036

141. Syedain ZH, Bjork J, Sando L, Tranquillo RT. Controlled compaction with ruthenium-catalyzed photochemical cross-linking of fibrin-based engineered connective tissue. Biomaterials. 2009 Dec;30(35):6695-6701. doi:10.1016/j.biomaterials.2009.08.039

142. Mol A, van Lieshout MI, Dam-De Veen CG, Neuenschwander S, Hoerstrup SP, Baaijens FP, Bouten CV. Fibrin as a cell carrier in cardiovascular tissue engineering applications. Biomaterials. 2005 Jun;26(16):3113-3121. doi:10.1016/j.biomaterials.2004.08.007

143. Chung C, Burdick JA. Influence of three-dimensional hyaluronic acid microenvironments on mesenchymal stem cell chondrogenesis. Tissue Eng Part A. 2009 Feb;15(2):243-254. doi:10.1089/ten.tea.2008.0067

144. Nehls V, Drenckhahn D. A novel, microcarrier-based in vitro assay for rapid and reliable quantification of three-dimensional cell migration and angiogenesis. Microvasc Res. 1995 Nov;50(3):311-322. doi:10.1006/mvre.1995.1061

145. Carruthers JDA, Glogau RG, Blitzer A, Facial Aesthetics Consensus Group Faculty.

Advances in facial rejuvenation: Botulinum toxin type A, hyaluronic acid dermal fillers, and combination therapies - Consensus recommendations. Plast Reconstr Surg. 2008 May;121(5 Suppl):5S-30S. doi:10.1097/PRS.0b013e31816de8d0

146. Bian L, Hou C, Tous E, Rai R, Mauck RL, Burdick JA. The influence of hyaluronic acid hydrogel crosslinking density and macromolecular diffusivity on human MSC chondrogenesis and hypertrophy. Biomaterials. 2013 Jan;34(2):413-421. doi:10.1016/j.biomaterials.2012.09.052

147. García AJ. PEG-maleimide hydrogels for protein and cell delivery in regenerative medicine. Ann Biomed Eng. 2014 Feb;42(2):312-322 doi:10.1007/s10439-013-0870-y

148. Zhu J. Bioactive modification of poly(ethylene glycol) hydrogels for tissue engineering. Biomaterials. 2010 Jun;31(17):4639-4656. doi:10.1016/j.biomaterials.2010.02.044

149. Muhonen V, Narcisi R, Nystedt J, Korhonen M, van Osch GJ, Kiviranta I. Recombinant human type II collagen hydrogel provides a xeno-free 3D micro-environment for chondrogenesis of human bone marrow-derived mesenchymal stromal cells. J Tissue Eng Regen Med. 2017 Mar;11(3):843-854. doi:10.1002/term.1983

150. Walters BD, Stegemann JP. Strategies for directing the structure and function of three-dimensional collagen biomaterials across length scales. Acta Biomater. 2014 Apr;10(4):1488-1501. doi:10.1016/j.actbio.2013.08.038

151. Rutgers M, Saris DB, Vonk LA, van Rijen MH, Akrum V, Langeveld D, van Boxtel A, Dhert WJ, Creemers LB. Effect of collagen type I or type II on chondrogenesis by cultured human articular chondrocytes. Tissue Eng Part A. 2013 Jan;19(1-2):59-65. doi:10.1089/ten.tea.2011.0416

152. Caliari SR, Burdick JA. A practical guide to hydrogels for cell culture. Nat Methods. 2016 Apr 28;13(5):405-414. doi:10.1038/nmeth.3839

153. Kong HJ, Lee KY, Mooney DJ. Decoupling the dependence of rheological/mechanical properties of hydrogels from solids concentration. Polymer. 2002;43(23):6239-6246. doi:10.1016/S0032-3861(02)00559-1

154. LeRoux MA, Guilak F, Setton LA. Compressive and shear properties of alginate gel: Effects of sodium ions and alginate concentration. J Biomed Mater Res. 1999 Jul; 47(1):46-53. doi:10.1002/(SICI)1097-4636(199910)47:1<46::AID-JBM6>3.0.CO;2-N

155. Augst AD, Kong HJ, Mooney DJ. Alginate hydrogels as biomaterials. Macromol Biosci. 2006 Aug 7;6(8):623-633. doi:10.1002/mabi.200600069

156. Lehenkari PP, Horton MA. Single integrin molecule adhesion forces in intact cells measured by atomic force microscopy. Biochem Biophys Res Commun. 1999 Jun 16;259(3):645-650. doi:10.1006/bbrc.1999.0827

157. Tuan RS, Boland G, Tuli R. Adult mesenchymal stem cells and cell-based tissue engineering. Arthritis Res Ther. 2003;5(1):32-45. doi:10.1186/ar614

158. Lee KY, Mooney DJ. Alginate: Properties and biomedical applications. Prog Polym Sci. 2012 Jan;37(1):106-126. doi:10.1016/j.progpolymsci.2011.06.003

159. Alberts B, Johnson A, Lewis J, Raff M, Roberts K, Walter P. Molecular Biology of the Cell. 4th edition. New York: Garland Science; 2002. Available from: https://www.ncbi.nlm.nih.gov/books/NBK21054/

160. Sánchez-Mateos P, Cabañas C, Sánchez-Madrid F. Regulation of integrin function. Semin Cancer Biol. 1996 Jun;7(3):99-109. doi:10.1006/scbi.1996.0015

161. Barczyk M, Bolstad AI, Gullberg D. Role Of Integrins In The Periodontal Ligament: Organizers And Facilitators. Periodontol 2000. 2013 Oct;63(1):29-47. doi:10.1111/prd.12027

162. Takada Y, Ye X, Simon S. The integrins. Genome Biol. 2007;8(5):215. doi:10.1186/gb-2007-8-5-215

163. Ginsberg MH, Partridge A, Shattil SJ. Integrin regulation. Curr Opin Cell Biol. 2005 Oct;17(5 SPEC. ISS.):509-516. doi:10.1016/j.ceb.2005.08.010

164. Goswami S. Importance of integrin receptors in the field of pharmaceutical & medical science. Adv Biol Chem. 2013 Jan;03(02):224-252. doi:10.4236/abc.2013.32028

165. White DJ, Puranen S, Johnson MS, Heino J. The collagen receptor subfamily of the integrins. Int J Biochem Cell Biol. 2004 Aug;36(8):1405-1410. doi:10.1016/j.biocel.2003.08.016

166. Sutherland AE, Calarco PG, Damsky CH. Developmental regulation of integrin expression at the time of implantation in the mouse embryo. Development. 1993 Dec;119(4):1175-1186. doi:10.1242/dev.119.4.1175

167. Gardner H, Kreidberg J, Koteliansky V, Jaenisch R. Deletion of integrin α1 by homologous recombination permits normal murine development but gives rise to a specific deficit in cell adhesion. Dev Biol. 1996 May;175(2):301-313. doi:10.1006/dbio.1996.0116

168. Ibaragi S, Shimo T, Hassan NM, Isowa S, Kurio N, Mandai H, Kodama S, Sasaki A Induction of MMP-13 expression in bone-metastasizing cancer cells by type I collagen through integrin α1β1 and α2β1-p38 MAPK signaling. Anticancer Res. 2011;31(4):1307-1313. PMID: 21508380

169. Goessler UR, Bugert P, Bieback K, Stern-Straeter, J., Bran, G., Hörmann, K., Riedel, F. Integrin expression in stem cells from bone marrow and adipose tissue during chondrogenic differentiation. Int J Mol Med. 2008 Mar;21(3):271-279. doi:10.3892/ijmm.21.3.271

170. Gullberg D, Velling T, Sjöberg G, Sejersen T. Up-regulation of a novel integrin α-chain (αmt) on human fetal myotubes. Dev Dyn. 1995 Sep;204(1):57-65. doi:10.1002/aja.1002040108

171. Popova SN, Barczyk M, Tiger C-F, Beertsen W, Zigrino P, Aszodi A, Miosge N, Forsberg E, Gullberg D. α11β1 Integrin-Dependent Regulation of Periodontal Ligament Function in the Erupting Mouse Incisor. Mol Cell Biol. 2007 Jun;27(12):4306-4316. doi:10.1128/mcb.00041-07

172. Camper L, Hellman U, Lundgren-Åkerlund E. Isolation, cloning, and sequence analysis of the integrin subunit α10, a β1-associated collagen binding integrin expressed on chondrocytes. J Biol Chem. 1998 Aug 7;273(32):20383-20389. doi:10.1074/jbc.273.32.20383

173. Bengtsson T, Aszodi A, Nicolae C, Hunziker EB, Lundgren-Akerlund E, Fässler R. Loss of alpha10beta1 integrin expression leads to moderate dysfunction of growth plate chondrocytes. J Cell Sci. 2005 Mar 1;118(Pt 5):929-36. doi: 10.1242/jcs.01678

174. Varas L, Ohlsson LB, Honeth G, Olsson A, Bengtsson T, Wiberg C, Bockermann R, Järnum S, Richter J, Pennington D, Johnstone B, Lundgren-Akerlund E, Kjellman C. α10 Integrin expression is up-regulated on fibroblast growth factor-2-treated mesenchymal stem cells with improved chondrogenic differentiation potential. Stem Cells Dev. 2007 Dec;16(6):965-978. doi:10.1089/scd.2007.0049

175. Delco ML, Goodale M, Talts JF, Pownder SL, Koff MF, Miller AD, Nixon B, Bonassar LJ, Lundgren-Åkerlund E, Fortier LA. Integrin α10β1-Selected Mesenchymal Stem Cells Mitigate the Progression of Osteoarthritis in an Equine Talar Impact Model. Am J Sports Med. 2020 Mar;48(3):612-623. doi:10.1177/0363546519899087

176. Kyöstilä K, Lappalainen AK, Lohi H. Canine Chondrodysplasia Caused by a Truncating Mutation in Collagen-Binding Integrin Alpha Subunit 10. PLoS One. 2013 Sep;8(9). doi:10.1371/journal.pone.0075621

177. Munksgaard Thorén M, Chmielarska Masoumi K, Krona C, Huang X, Kundu S, Schmidt L, Forsberg-Nilsson K, Floyd Keep M, Englund E, Nelander S, Holmqvist B, Lundgren-Åkerlund E. Integrin α10, a Novel Therapeutic Target in Glioblastoma, Regulates Cell Migration, Proliferation, and Survival. Cancers (Basel). 2019 Apr 25;11(4):587. doi: 10.3390/cancers11040587

178. Masoumi KC, Huang X, Sime W, Mirkov A, Munksgaard Thorén M, Massoumi R, Lundgren-Åkerlund E.. Integrin α10-antibodies reduce glioblastoma tumor growth and cell migration. Cancers (Basel). 2021 Mar;13(5):1-18. doi:10.3390/cancers13051184

179. Lampropoulou-Adamidou K, Lelovas P, Karadimas E V., Liakou C, Triantafillopoulos IK, Dontas I, Papaioannou NA. Useful animal models for the research of osteoarthritis. Eur J Orthop Surg Traumatol. 2014 Apr;24(3):263-271. doi:10.1007/s00590-013-1205-2

180. Teeple E, Jay GD, Elsaid KA, Fleming BC. Animal models of osteoarthritis: Challenges of model selection and analysis. AAPS J. 2013 Apr;15(2):438-446. doi:10.1208/s12248-013-9454-x

181. Little CB, Zaki S. What constitutes an “animal model of osteoarthritis” - the need for consensus? Osteoarthritis Cartilage. 2012 Apr;20(4):261-267. doi:10.1016/j.joca.2012.01.017

182. Malfait AM, Little CB, McDougall JJ. A commentary on modelling osteoarthritis pain in small animals. Osteoarthritis Cartilage. 2013 Sep;21(9):1316-1326. doi:10.1016/j.joca.2013.06.003

183. Bendele AM. Animal models of osteoarthritis. J Musculoskelet Neuronal Interact. 2001 Jun;1(4):363-376. PMID: 15758487

184. Kamekura S, Hoshi K, Shimoaka T, Chung U, Chikuda H, Yamada T, Uchida M,

Ogata N, Seichi A, Nakamura K, Kawaguchi H. Osteoarthritis development in novel experimental mouse models induced by knee joint instability. Osteoarthritis Cartilage. 2005 Jul;13(7):632-641. doi:10.1016/j.joca.2005.03.004

185. McCoy AM. Animal Models of Osteoarthritis: Comparisons and Key Considerations. Vet Pathol. 2015 Sep;52(5):803-818. doi:10.1177/0300985815588611

186. Fang H, Beier F. Mouse models of osteoarthritis: Modelling risk factors and assessing outcomes. Nat Rev Rheumatol. 2014 Jul;10(7):413-421. doi:10.1038/nrrheum.2014.46

187. Glasson SS, Askew R, Sheppard B, Carito BA, Blanchet T, Ma HL, Flannery CR, Kanki K, Wang E, Peluso D, Yang Z, Majumdar MK, Morris EA. Characterization of and osteoarthritis susceptibility in ADAMTS-4-knockout mice. Arthritis Rheum. 2004 Aug;50(8):2547-2558. doi:10.1002/art.20558

188. Glasson SS, Blanchet TJ, Morris EA. The surgical destabilization of the medial meniscus (DMM) model of osteoarthritis in the 129/SvEv mouse. Osteoarthritis Cartilage. 2007 Sep;15(9):1061-1069. doi:10.1016/j.joca.2007.03.006

189. Gregory MH, Capito N, Kuroki K, Stoker AM, Cook JL, Sherman SL. A Review of Translational Animal Models for Knee Osteoarthritis. Arthritis. 2012;2012:1-14. doi:10.1155/2012/764621

190. Cook JL, Hung CT, Kuroki K, Stoker AM, Cook CR, Pfeiffer FM, Sherman SL, Stannard JP. Animal models of cartilage repair. Bone Joint Res. 2014 Apr;3(4):89-94. doi:10.1302/2046-3758.34.2000238

191. Arunakul M, Tochigi Y, Goetz JE, Diestelmeier BW, Heiner AD, Rudert J, Fredericks DC, Brown TD, McKinley TO. Replication of chronic abnormal cartilage loading by medial meniscus destabilization for modeling osteoarthritis in the rabbit knee in vivo. J Orthop Res. 2013 Oct;31(10):1555-1560. doi:10.1002/jor.22393

192. Pedersen DR, Goetz JE, Kurriger GL, Martin JA. Comparative digital cartilage histology for human and common osteoarthritis models. Orthop Res Rev. 2013 Feb 12;2013(5):13-20. doi: 10.2147/ORR.S38400

193. Glasson SS, Chambers MG, Van Den Berg WB, Little CB. The OARSI histopathology initiative - recommendations for histological assessments of osteoarthritis in the mouse. Osteoarthritis Cartilage. 2010 Oct;18 Suppl 3:S17-S23. doi:10.1016/j.joca.2010.05.025

194. Little CB, Meeker CT, Golub SB, Lawlor KE, Farmer PJ, Smith SM, Fosang AJBlocking aggrecanase cleavage in the aggrecan interglobular domain abrogates cartilage erosion and promotes cartilage repair. J Clin Invest. 2007 Jun;117(6):1627-1636. doi:10.1172/JCI30765

195. Cheng K, Gupta S. Quantitative tools for assessing the fate of xenotransplanted human stem/progenitor cells in chimeric mice. Xenotransplantation. 2009 May-June;16(3):145-151. doi:10.1111/j.1399-3089.2009.00526.x

196. Böcker W, Docheva D, Prall WC, Egea V, Pappou E, Rossmann O, Popov C, Mutschler W, Ries C, Schieker M. IKK-2 is required for TNF-α-induced invasion and proliferation of human mesenchymal stem cells. J Mol Med (Berl). 2008 Oct;86(10):1183-1192. doi:10.1007/s00109-008-0378-3

197. Malfait AM, Miller RJ. Emerging Targets for the Management of Osteoarthritis Pain. Curr Osteoporos Rep. 2016Dec;14(6):260-268. doi:10.1007/s11914-016-0326-z

198. Baldini A, Castellani L, Traverso F, Balatri A, Balato G, Franceschini V. The difficult primary total knee arthroplasty: a review. Bone Joint J. 2015 Oct;97-B(10 Suppl A):30-9. doi: 10.1302/0301-620X.97B10.36920

199. Chevallier N, Anagnostou F, Zilber S, Bodivit G, Maurin S, Barrault A, Bierling P, Hernigou P, Layrolle P, Rouard H. Osteoblastic differentiation of human mesenchymal stem cells with platelet lysate. Biomaterials. 2010 Jan;31(2):270-278. doi:10.1016/j.biomaterials.2009.09.043

200. Hildner F, Eder MJ, Hofer K, Aberl J, Redl H, van Griensven M, Gabriel C, Peterbauer-Scherb A. Human platelet lysate successfully promotes proliferation and subsequent chondrogenic differentiation of adipose-derived stem cells: A comparison with articular chondrocytes. J Tissue Eng Regen Med. 2015 Jul;9(7):808-818. doi:10.1002/term.1649

201. Bocelli-Tyndall C, Zajac P, Di Maggio N, Trella E, Benvenuto F, Iezzi G, Scherberich A, Barbero A, Schaeren S, Pistoia V, Spagnoli G, Vukcevic M, Martin I, Tyndall A. Fibroblast growth factor 2 and platelet-derived growth factor, but not platelet lysate, induce proliferation-dependent, functional class II major histocompatibility complex antigen in human mesenchymal stem cells. Arthritis Rheum. 2010 Dec;62(12):3815-3825. doi:10.1002/art.27736

202. Bernardo ME, Avanzini MA, Perotti C, Cometa AM, Moretta A, Lenta E, Del Fante C, Novara F, de Silvestri A, Amendola G, Zuffardi O, Maccario R, Locatelli F Optimization of in vitro expansion of human multipotent mesenchymal stromal cells for cell-therapy approaches: Further insights in the search for a fatal calf serum substitute. J Cell Physiol. 2007 Apr;211(1):121-130. doi:10.1002/jcp.20911

203. Alberton P, Popov C, Prägert M, Kohler J, Shukunami C, Schieker M, Docheva D.. Conversion of human bone marrow-derived mesenchymal stem cells into tendon progenitor cells by ectopic expression of scleraxis. Stem Cells Dev. 2012 Apr;21(6):846-858. doi:10.1089/scd.2011.0150

204. Bruderer M, Richards RG, Alini M, Stoddart MJ. Role and regulation of runx2 in osteogenesis. Eur Cells Mater. 2014 Oct;28:269-286. doi:10.22203/eCM.v028a19

205. Lin L, Shen Q, Leng H, Duan X, Fu X, Yu C. Synergistic inhibition of endochondral bone formation by silencing Hif1α and Runx2 in trauma-induced heterotopic ossification. Mol Ther. 2011 Aug;19(8):1426-1432. doi:10.1038/mt.2011.101

206. Zhang X, Yang M, Lin L, Chen P, Ma KT, Zhou CY, Ao YF. Runx2 overexpression enhances osteoblastic differentiation and mineralization in adipose - Derived stem cells in vitro and in vivo. Calcif Tissue Int. 2006 Sep;79(3):169-178. doi:10.1007/s00223-006-0083-6

207. Schoonjans K, Staels B, Auwerx J. The peroxisome proliferator activated receptors (PPARs) and their effects on lipid metabolism and adipocyte differentiation. Biochim Biophys Acta 1996 Jul 26;1302(2):93-109. doi:10.1016/0005-2760(96)00066-5

208. Tzameli I, Fang H, Ollero M, Shi H, Hamm JK, Kievit P, Hollenberg AN, Flier JS. Regulated production of a peroxisome proliferator-activated receptor-γ ligand during an early phase of adipocyte differentiation in 3T3-L1 adipocytes. J Biol Chem. 2004 Aug;279(34):36093-36102. doi:10.1074/jbc.M405346200

209. Tontonoz P, Hu E, Devine J, Beale EG, Spiegelman BM. PPAR gamma 2 regulates adipose expression of the phosphoenolpyruvate carboxykinase gene. Mol Cell Biol. 1995 Jan;15(1):351-357. doi:10.1128/mcb.15.1.351

210. Wang Y, Mu Y, Li H, Ding N, Wang Q, Wang Y, Wang S, Wang N. Peroxisome proliferator-activated receptor-γ gene: A key regulator of adipocyte differentiation in chickens. Poult Sci. 2008 Feb;87(2):226-232. doi:10.3382/ps.2007-00329

211. Lee MJ, Chen HT, Ho ML, Chen CH, Chuang SC, Huang SC, Fu YC, Wang GJ, Kang L, Chang JK. PPARγ silencing enhances osteogenic differentiation of human adipose-derived mesenchymal stem cells. J Cell Mol Med. 2013 Sep;17(9):1188-1193. doi:10.1111/jcmm.12098

212. Sitcheran R, Cogswell PC, Baldwin AS Jr. NF-κB mediates inhibition of mesenchymal cell differentiation through a posttranscriptional gene silencing mechanism. Genes Dev. 2003 Oct;17(19):2368-2373. doi:10.1101/gad.1114503

213. Xing H, Northrop JP, Russell Grove J, Kilpatrick KE, Su JL, Ringold GM. TNFα-mediated inhibition and reversal of adipocyte differentiation is accompanied by suppressed expression of PPARγ without effects on Pref-1 expression. Endocrinology. 1997 Jul;138(7):2776-2783. doi:10.1210/endo.138.7.5242

214. Gouttenoire J, Bougault C, Aubert-Foucher E, Perrier E, Ronzière MC, Sandell L, Lundgren-Akerlund E, Mallein-Gerin F. BMP-2 and TGF-β1 differentially control expression of type II procollagen and α10 and α11 integrins in mouse chondrocytes. Eur J Cell Biol. 2010 Apr;89(4):307-314. doi:10.1016/j.ejcb.2009.10.018

215. Popov C, Radic T, Haasters F, Prall WC, Aszodi A, Gullberg D, Schieker M, Docheva D. . Integrins α2β1 and α11β1 regulate the survival of mesenchymal stem cells on collagen l. Cell Death Dis. 2011 Jul;2(7):e186-e186. doi:10.1038/cddis.2011.71

216. Uvebrant K, Rasmusson L, Talts J, Alberton P, Aszodi A, Lundgren-Åkerlund E. Integrin α10β1-selected Equine MSCs have Improved Chondrogenic Differentiation, Immunomodulatory and Cartilage Adhesion Capacity. Ann Stem Cell Res. 2019;2(1):001-009

217. Girandon L, Kregar-Velikonja N, Božikov K, Barlič A. In vitro models for adipose tissue engineering with adipose-derived stem cells using different scaffolds of natural origin. Folia Biol (Praha). 2011;57(2):47-56. PMID: 21631961

218. Jockenhoevel S, Zund G, Hoerstrup SP, Chalabi K, Sachweh JS, Demircan L, Messmer BJ, Turina M. Fibrin gel -- advantages of a new scaffold in cardiovascular tissue engineering. Eur J Cardiothorac Surg. 2001 Apr;19(4):424-30. doi: 10.1016/s1010-7940(01)00624-8

219. Christman KL, Vardanian AJ, Fang Q, Sievers RE, Fok HH, Lee RJ. Injectable fibrin scaffold improves cell transplant survival, reduces infarct expansion, and induces

neovasculature formation in ischemic myocardium. J Am Coll Cardiol. 2004 Aug;44(3):654-660. doi:10.1016/j.jacc.2004.04.040

220. Dragoo JL, Carlson G, McCormick F, Khan-Farooqi H, Zhu M, Zuk PA, Benhaim P. Healing full-thickness cartilage defects using adipose-derived stem cells. Tissue Eng. 2007 Jul;13(7):1615-1621. doi:10.1089/ten.2006.0249

221. Chang J, Rasamny JJ, Park SS. Injectable tissue-engineered cartilage using a fibrin sealant. Arch Facial Plast Surg. 2007 May-June;9(3):161-166. doi:10.1001/archfaci.9.3.161

222. Catelas I, Sese N, Wu BM, Dunn JCY, Helgerson S, Tawil B. Human mesenchymal stem cell proliferation and osteogenic differentiation in fibrin gels in vitro. Tissue Eng. 2006 Aug;12(8):2385-2396. doi:10.1089/ten.2006.12.2385

223. Ho W, Tawil B, Dunn JCY, Wu BM. The behavior of human mesenchymal stem cells in 3D fibrin clots: Dependence on fibrinogen concentration and clot structure. Tissue Eng. 2006 Jun;12(6):1587-1595. doi:10.1089/ten.2006.12.1587

224. Guo HD, Wang HJ, Tan YZ, Wu JH. Transplantation of marrow-derived cardiac stem cells carried in fibrin improves cardiac function after myocardial infarction. Tissue Eng Part A. 2011 Jan;17(1-2):45-58. doi:10.1089/ten.tea.2010.0124

225. Homminga GN, Buma P, Koot HWJ, van der Kraan PM, van den Berg WB. Chondrocyte behavior in fibrin glue in vitro. Acta Orthop Scand. 1993 Aug;64(4):441-445. doi:10.3109/17453679308993663

226. van Osch GJ, van der Kraan PM, Vitters EL, Blankevoort L, van den Berg WB. Induction of osteoarthritis by intra-articular injection of collagenase in mice. Strain and sex related differences. Osteoarthritis Cartliage. 1993 Jul;1(3):171-177. doi:10.1016/S1063-4584(05)80088-3

227. Ma HL, Blanchet TJ, Peluso D, Hopkins B, Morris EA, Glasson SS. Osteoarthritis severity is sex dependent in a surgical mouse model. Osteoarthritos Cartilage. 2007 Jun;15(6):695-700. doi:10.1016/j.joca.2006.11.005

228. Fang H, Huang L, Welch I, orley C, Holdsworth DW, Beier F, Cai D. Early Changes of Articular Cartilage and Subchondral Bone in The DMM Mouse Model of Osteoarthritis. Sci Rep. 2018 Feb;8(1):2855. doi:10.1038/s41598-018-21184-5

229. Poole R, Blake S, Buschmann M, Goldring S, Laverty S, Lockwood S, Matyas J, McDougall J, Pritzker K, Rudolphi K, van den Berg W, Yaksh T. Recommendations for the use of preclinical models in the study and treatment of osteoarthritis. Osteoarthritis Cartilage. 2010 Oct;18 Suppl 3:S10-S16. doi:10.1016/j.joca.2010.05.027

230. Huang H, Skelly JD, Ayers DC, Song J. Age-dependent Changes in the Articular Cartilage and Subchondral Bone of C57BL/6 Mice after Surgical Destabilization of Medial Meniscus. Sci Rep. 2017 Feb;7(1):42294. doi:10.1038/srep42294

231. Peyron JG. Intraarticular hyaluronan injections in the treatment of osteoarthritis: State-of-the-art review. J Rheumatol Suppl. 1993 Aug;39:10-5. PMID: 8410878

232. Kobolak J, Dinnyes A, Memic A, Khademhosseini A, Mobasheri A. Mesenchymal stem cells: Identification, phenotypic characterization, biological properties and potential for regenerative medicine through biomaterial micro-engineering of their niche. Methods. 2016 Apr;99:62-68. doi:10.1016/j.ymeth.2015.09.016

233. Schelbergen RF, van Dalen S, ter Huurne M oth J, Vogl T, Noël D, Jorgensen C, van den Berg WB, van de Loo FA, Blom AB, van Lent PL.. Treatment efficacy of adipose-derived stem cells in experimental osteoarthritis is driven by high synovial activation and reflected by S100A8/A9 serum levels. Osteoarthritis Cartilage. 2014 Aug;22(8):1158-1166. doi:10.1016/j.joca.2014.05.022

234. ter Huurne M, Schelbergen R, Blattes R, Blom A, de Munter W, Grevers LC, Jeanson J, Noël D, Casteilla L, Jorgensen C, van den Berg W, van Lent PL. Antiinflammatory and chondroprotective effects of intraarticular injection of adipose-derived stem cells in experimental osteoarthritis. Arthritis Rheum. 2012 Nov;64(11):3604-13. doi: 10.1002/art.34626

235. Maumus M, Roussignol G, Toupet K, Penarier G, Bentz I, Teixeira S, Oustric D, Jung M, Lepage O, Steinberg R, Jorgensen C, Noel D. Utility of a Mouse Model of Osteoarthritis to Demonstrate Cartilage Protection by IFNγ-Primed Equine Mesenchymal Stem Cells. Front Immunol. 2016 Sep 27;7:392. doi: 10.3389/fimmu.2016.00392

236. Khatab S, van Osch GJ, Kops N, Bastiaansen-Jenniskens YM, Bos PK, Verhaar JA, Bernsen MR, van Buul GM. Mesenchymal stem cell secretome reduces pain and prevents cartilage damage in a murine osteoarthritis model. Eur Cell Mater. 2018 Nov 6;36:218-230. doi: 10.22203/eCM.v036a16

237. Ishikawa T, Nishigaki F, Christgau S, Noto T, Mo J, From N, Minoura K, Hirayama Y, Ohkubo Y, Mutoh S.. Cartilage destruction in collagen induced arthritis assessed with a new biochemical marker for collagen type II C-telopeptide fragments. J Rheumatol. 2004 Jun;31(6):1174-1179. PMID: 15170932

238. Duclos ME, Roualdes O, Cararo R, Rousseau JC, Roger T, Hartmann DJ. Significance of the serum CTX-II level in an osteoarthritis animal model: A 5-month longitudinal study. Osteoarthritis Cartilage. 2010 Nov;18(11):1467-1476. doi:10.1016/j.joca.2010.07.007

239. Andersen C, Uvebrant K, Mori Y, Aarsvold S, Jacobsen S, Berg LC, Lundgren-Åkerlund E, Lindegaard C. Human integrin α10β1-selected mesenchymal stem cells home to cartilage defects in the rabbit knee and assume a chondrocyte-like phenotype. Stem Cell Res Ther. 2022 May 16;13(1):206. doi: 10.1186/s13287-022-02884-2

240. Kehoe O, Cartwright A, Askari A, El Haj AJ, Middleton J. Intra-articular injection of mesenchymal stem cells leads to reduced inflammation and cartilage damage in murine antigen-induced arthritis. J Transl Med. 2014 Jun;12(1):157. doi:10.1186/1479-5876-12-157

241. Mak J, Jablonski CL, Leonard CA, Dunn JF, Raharjo E, Matyas JR, Biernaskie J, Krawetz RJ. Intra-articular injection of synovial mesenchymal stem cells improves cartilage repair in a mouse injury model. Sci Rep. 2016 Mar 17;6:23076. doi: 10.1038/srep23076

242. Wike MM, Nydam D V., Nixon AJ. Enhanced early chondrogenesis in articular defects following arthroscopic mesenchymal stem cell implantation in an equine model. J Orthop Res. 2007 Jul;25(7):913-925. doi:10.1002/jor.20382

243. Daadi MM, Li Z, Arac A, Grueter BA, Sofilos M, Malenka RC, Wu JC, Steinberg GK. Molecular and magnetic resonance imaging of human embryonic stem cell-derived neural stem cell grafts in ischemic rat brain. Mol Ther. 2009 Jul;17(7):1282-1291. doi:10.1038/mt.2009.104

6 APPENDIX

6.1 LIST OF ABBREVIATIONS

AAOS	American Academy of Orthopedic Surgeons
ABC	Avidin-biotin-complex
AC	Articular cartilage
ACI	Autologous chondrocyte implantation
ACR	American College of Rheumatology
ADAMTS	A disintegrin and metalloproteinase with thrombospondin motifs
ALP	Alkaline phosphatase
aP2	Adipocyte lipid binding protein
ARS	Alizarin Red staining
ASCs	Adipose-derived mesenchymal stem cells
BM-MSCs	Bone marrow-derived mesenchymal stem cells
BMP	Bone morphogenetic protein
BSA	Bovine serum albumin
C2C	Collagen type II cleavage
C2M	Collagen type II degraded by MMPs
CD	Cluster of differentiation
cDNA	Complementary DNA
CFDA-SE	Carboxyfluorescein diacetate succinimidyl ester
CMPDI	Campomelic dysplasia type I
COMP	Cartilage oligomeric matrix protein
CRP	C-reactive protein
CS	Chondroitin sulfate
CTX-II	Carboxyl-terminal end of collagen type II

DAB	3,3’ Diaminobenzidine
dH_2O	Distilled water
DMEM	Dulbecco’s modified eagle Medium
DMSO	Dimethyl sulfoxide
DNA	Deoxyribonucleic acid
dNTPs	Deoxynucleoside triphosphate
eASCs	Equine mesenchymal stem cells
ECM	Extracellular matrix
EDTA	Ethylenediaminetetraacetic acid
EO	Endochondral ossification
EtOH	Ethanol
FACS	Fluorescence-activated cell sorting
FAK	Focal adhesion kinase
FBS	Fetal bovine serum
FDA	Fluorescenindiacetat
FELASA	Federation of European Laboratory Animal Science Association
FGF	Fibroblast growth factor
GAG	Glycosaminoglycans
GAPDH	Glycerolaldehyde-3-phosphate dehydrogenase
GDF5	Growth Differentiation Factor 5
gDNA	Genomic DNA
H_2O_2	Hydrogen peroxide
HA	Hyaluronic acid
hCMT1A	Human Charcot-Marie-tooth-disease gene
HEPA	High efficiency particulate air filter

HMG	High mobility group
HPRT	Hypoxanthine-guanine phosphoribosyl-transferase
HRP	Horseradish peroxidase
IA	Intra-articular
IFN-γ	Interferon gamma
IHC	Immunohistochemistry
Ihh	Indian-hedgehog
iPSC	Induced pluripotent stem cell
IL	Interleukin
IO	Intramembranous ossification
ISCT	International Society for Cellular Therapy
IVC	Individually ventilated cages
mAB	Monoclonal antibody
MACI	Matrix-associated autologous chondrocyte implantation
MAPK	Mitogen-activated protein kinase
MMPs	Matrix-metalloproteinases
MSCs	Mesenchymal stem cells
NF-kB	Nuclear factor 'kappa-light-chain-enhancer' of activated B-cells
NGF	Nerve growth factor
NSAID	Non-steroidal anti-inflammatory drugs
OA	Osteoarthritis
OARSI	Osteoarthritis Research Society
OATS	Osteochondral autologous transfer system
OC	Osteocalcin
OSE2	Osteoblast specific element 2

PBS	Phosphate buffered saline
PCR	Polymerase chain reaction
PEG	Polyethylene-glycol
PEPCK	Phosphoenolpyruvate carboxykinase
PFA	Paraformaldehyde
PG	Proteoglycan
PGE2	Prostaglandine 2
PI	Propium iodide
PL	Platelet lysate
PPAR-γ	Peroxisome proliferator-activated receptors
PPRE	Peroxisome proliferator response element
PSI	Plexin-semaphorin-integrin
qRT-PCR	Quantitative reverse transcriptase polymerase chain reaction
RGD	Arginine-glycine-aspartate
RNA	Ribonucleotide acid
RT	Room temperature
RUNX-2	Runt-related transcription factor 2
RXR	9-cis retinoic acid receptor
SD	Standard deviation
SM	Saint-Marie
SOX-9	SRY-box9
SPF	Specific-pathogen free
SRY	Sex determining region of Y
TGF-β	Transforming growth factor beta
TKA	Total knee arthroplasty

TNF-α	Tumor necrosis factor alpha
TRIS-HCl	Tris(hydroxymethyl)aminomethane hydrochloride
TSG6	TNF-α -stimulated gene protein
UKA	Unicompartmental knee arthroplasty
VEGF	Vascular endothelial growth factor

6.2 ANIMAL PROCEEDING SHEET

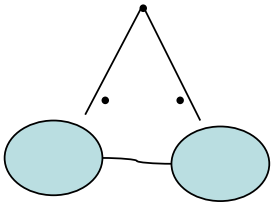

Aktenzeichen: Addendum 55.2.1.54-2532-150-13

Tier-Nummer: _____

Herkunft der Tiere: Janvier

Gewicht: _____

Lieferdatum: 05.07.2016

Geschlecht: weiblich

OP-Tag: 14.07.2016 Operateur: A. Aszodi

	Uhrzeit	Bemerkungen:
Narkose		
OP Ende		

Fibrin Gel mit hBM-MSC_____ im rechten Knie.

Datum: _____ Gewicht: _____

	Uhrzeit	Bemerkungen
Euthanasie		

Medikamente (Applikationsarten):

Narkose: Fentanyl 0,05 mg/kg + Dormicum® (Midazolam 5 mg/kg) + Cepetor® (Medetomidin 0,5 mg/kg)

Antagonisierung: Narcanti® (Naloxon 1,2 mg/kg) + Anexate® (Flumazenil 0,5 mg/kg) + Revertor® (Atipamezol 2,5 mg/kg)

postop. Analgesie: Buprenovet® 0,1 mg/kg s.c. (Buprenorphin)

6.3 SCORING SHEET

Score Sheet zum TVA Addendum 55.2.1.54-2532-150-13

Maus #		postoperativer Tag																							
Beobachtung/Score		1	2	3	6	9	12	15	18	21	24	27	30	33	36	39	42	45	48	51	54
Körpergewicht/ Flüssigkeitsauf-nahme	Kein Gewichtsverlust																				
	5-10% Gewichtsverlust																				
	>10-15% Gewichtsverlust																				
	>15-20% Gewichtsverlust																				
	>20% Gewichtsverlust																				
	Dehydratation (Hautfalte verstreicht sehr langsam, bleibt stehen)																				
Kotkonsistenz	Geformt																				
	Breiig																				
	flüssig																				
Fell	Normal, glänzend																				
	Leicht gesträubt																				
	Stumpf, struppig																				
	Haarverlust durch übermäßige Fellpflege (Barbering, Dalla Effekt)																				
Verhalten	Normal (lebhaft)																				
	Ruhig, kein exploratives Verhalten																				
	Hyperkinese																				
	Apathie																				
Atmung	Normal																				
	Leicht erhöhte Atemfrequenz																				
	Erhöhte Frequenz mit abdomineller Atmung																				
	Deutlich reduzierte Atmung																				
	Ausgeprägte abdominelle Atmung und Zyanose																				
Körperhaltung	normal																				
	Krämpfe, Lähmungen																				
	Gekrümmter Rücken																				
Verletzungen	Bisswunden (nicht infiziert, lokal begrenzt, solitär)																				
	Bisswunden (keine Wundheilung, infektiös, Selbstverstümmelung)																				

6.4 ACKNOWLEDGEMENTS

I would like to thank the people who contributed to my work, helped me to realize this thesis and supported throughout.

First and foremost, I would like to thank Dr. Paolo Alberton for his support, guidance from the first scientific steps until the final editing and reading of the present work, and his patience at all times.

Furthermore, I would like to express my gratitude to my supervisor PD Dr. Attila Aszódi for the patient supervision, encouragement and advice he gave me during my time as his student.

I would like to thank Prof. Dr. Wolfgang Böcker for making this work possible through the Department of the 'Allgemeine, Unfall- und Wiederherstellungschirurgie' of the LMU, Munich.

In addition, I would like to thank Prof. Dr. Matthias Schieker for the support in finding a suitable dissertation for me as well as the initial guidance in the laboratory.

Moreover, a special thanks to all the members of the ExperiMed laboratory for creating such a pleasant working environment and the support they provide at all times, especially Dr. Maximillian Saller and Mrs. Zsuzsanna Farkas.

Finally, I would like to thank my whole family and especially my brother Marko Schwarz who supported me through the ups and downs throughout my studies and finally in this work. They were always present and helpful and without them I would not be where I am today.

6.5 DECLARATION

Ich erkläre hiermit an Eides statt, dass ich die vorliegende Dissertation mit dem Titel

„The potential of integrin α10β1-selected mesenchymal stem cells for therapy of post-traumatic osteoarthritis in a mouse model"

selbständig verfasst, mich außer der angegebenen keiner weiteren Hilfsmittel bedient und alle Erkenntnisse, die aus dem Schrifttum ganz oder annähernd übernommen sind, als solche kenntlich gemacht und nach ihrer Herkunft unter der Bezeichnung der Fundstelle einzeln nachgewiesen habe.

Ich erkläre des Weiteren, dass die hier vorgelegte Dissertation nicht in gleicher oder ähnlicher Form bei einer anderen Stelle zur Erlangung eines akademischen Grades eingereicht wurde.

München, den 19.10.2023	Jelena Juliane Schwarz
Ort, Datum	Unterschrift Doktorandin

6.6 PUBLICATIONS

6.6.1 POSTER

- *Mesenchymal stem cells as cell therapy for osteoarthritis: a pilot study*. Jelena Schwarz, Paolo Alberton, Maximilian M. Saller, Tina Uvebrant, Jan Talts, Carl-Magnus Högerkorp, Evy Lundgren-Akerlund, Matthias Schieker and Attila Aszódi. Vll. Münchner Symposium für experimentelle Orthopädie, Unfallchirurgie und Muskuloskelettale Forschung, 2017 (July 21-22), München, Germany
- *Aggrecan is critical in maintaining the cartilage matrix biomechanics which in turn influences the correct development of the growth plate and the proper function of articular cartilage*. Paolo Alberton, Zsuzsanna Farkas, Carina Prein, Hans C Dugonitsch, Bastian Hartmann, Jelena Schwarz, Ping Li, Maximilian M Saller, Hauke Clausen-Schaumann, Toshitaka Oohashi and Attila Aszódi. OARSI World congress on osteoarthritis, 2019 (May2-5), Toronto, Canada